TECHNISCHE UNIVERSITÄT WIEN

INSTITUT FÜR ENERGIETECHNIK UND THERMODYNAMIK

DISSERTATION

Pumped-Storage Implementation in Order to Balance Volatile Renewable Energy Generation

ausgeführt zum Zwecke der Erlangung des akademischen Grades eines
Doktors der technischen Wissenschaften (Dr. techn.)

eingereicht an der TU Wien, Fakultät für Maschinenwesen und Betriebswissenschaften von

Dipl.-Ing. Leopold RUPPERT

Mat.Nr.: 0525100

unter der Leitung von

Univ.Prof. Dipl.-Ing. Dr.Ing. Christian BAUER

Institut für Energietechnik und Thermodynamik, E302

begutachtet von

Univ.Prof. Dr.-Ing. Wolfgang GAWLIK

Institut für Energiesysteme und Elektrische Antriebe, E370

und

Ao.Univ.Prof. Dipl.-Ing. Dr.techn. Reinhard WILLINGER

Institut für Energietechnik und Thermodynamik, E302

Erklärung

Ich nehme zur Kenntnis, dass ich zur Drucklegung meiner Arbeit unter der Bezeichnung **Dissertation** nur mit Bewilligung der Prüfungskommission berechtigt bin.

Eidesstattliche Erklärung

Ich erkläre an Eides statt, dass die vorliegende Arbeit nach den anerkannten Grundsätzen für wissenschaftliche Abhandlungen von mir selbstständig erstellt wurde. Alle verwendeten Hilfsmittel, insbesondere die zugrunde gelegte Literatur, sind in dieser Arbeit genannt und aufgelistet. Die aus den Quellen wörtlich entnommenen Stellen, sind als solche kenntlich gemacht.

Das Thema dieser Arbeit wurde von mir bisher weder im In- noch Ausland einer Beurteilerin/einem Beurteiler zur Begutachtung in irgendeiner Form als Prüfungsarbeit vorgelegt. Diese Arbeit stimmt mit der von den Begutachterinnen/Begutachtern beurteilten Arbeit überein.

Wien, 7. Juli 2017

Leopold RUPPERT

Danksagung

Kurzfassung

In 2015 wurde die überwiegende Mehrheit an elektrischer Energie aus fossilen Brennstoffen und Kernkraft gewonnen. Im Hinblick auf eine nachhaltige Energieversorgung müssen diese Ressourcen ersetzt werden. Seit 2000 wird vor allem Wind- und Solarenergie ausgebaut um obig genannte Energiequellen zu ersetzen. Diese Änderung in der Erzeugungsstruktur birgt jedoch Herausforderungen. Die zeitliche Balance der erzeugten und verbrauchten Leistung ist die eine und die örtliche Balance die andere. Für die örtliche Balance ist ein starkes Übertragungsnetz erforderlich, während die zeitliche Balance Speichertechnologien erfordert. In der vorliegenden Arbeit werden Speichertechnologien (vor allem gängige Pumpspeicheranlagen) untersucht und miteinander verglichen. Pumpspeicher mit fixer Drehzahl und variablen Drehzahl werden ebenso untersucht wie Pumpspeicher binärer und ternärer Bauform. Es werden genaue Verlustmodelle erarbeitet, Einsatzgrenzen bestimmt und basierend auf diesen Fahrplanoptimierungen durchgeführt. Für die Ermittlung der Erlöse aus den Fahrplanoptimierungen werden der Day-ahead Markt, Primärregelmarkt und Sekundärregelmarkt berücksichtigt. Die Erlöse werden in weiterer Folge mit den Investitionskosten gegengerechnet, um die aktuell wirtschaftlichste Bauform zu bestimmen. Aufgrund der Aktualität werden neben Pumpspeicheranlagen auch Batteriespeicher auf deren Wirtschaftlichkeit überprüft. Nach der Bestimmung der Fahrpläne werden transiente Modelle entwickelt, um transiente Vorgänge auf der hydraulischen und elektrischen Seite zu simulieren. Im Anschluss an eine Modellvalidierung, bei der ein gemessener Leistungsverlauf mit einem simulierten verglichen wird, wird das Schwingungsverhalten in den Anlagen analysiert. Des Weiteren werden im Rahmen von Eintagessimulationen die Agilitäten der Anlagen veranschaulicht. Der möglichst genaue Einhalt eines Leistungsverlaufes steht hier im Zentrum der Simulation. Schlussendlich wird die Möglichkeit untersucht mit Pumpspeicheranlagen einen Leistungsüberschuss bzw. eine Mangelversorgung schnellstmöglich zu kompensieren. Es stellt sich heraus, dass die ternäre Bauform die wirtschaftlichste ist und Anlagen mit variabler Drehzahl über einen breiten Einsatzbereich besseres transientes Verhalten zeigen als Anlagen mit fixer Drehzahl.

Abstract

In 2015, the majority of the electrical energy generated was produced by fossil fuels and nuclear power. Climate change and storage of radioactive waste are negative effects of these energy sources on the environment. So these energy sources need to be replaced by a sustainable energy sector. Since 2000, especially wind and solar power capacity is expanded rapidly in order to replace above mentioned energy sources. This change, however, comes along with two problems. On the one hand, there is the timely alignment of electrical power generation and consumption and on the other hand, there is the local alignment. For the local alignment, a robust transmission system is required, while the timely alignment requires storage technologies. The presented work investigates and compares storage technologies (especially pumped-storage). Pumped-storage plant schemes with fixed speed and variable speed as well as binary and ternary sets are considered. Detailed loss models are developed, operating ranges are determined and based on these ranges, an operation optimization is carried out. For the operation optimization, the day-ahead market as well as the primary and secondary control market are taken into account. The determined income is further collated with the costs of different plants in order to evaluate the most profitable storage types. Due to its actuality, the economic analysis also takes battery storage applications into account. Based on the operation optimization transient models are developed to simulate transient behaviour of the hydraulic as well as the electrical part. The validation of the developed model, by comparing a measured power trend with a simulated one, is followed by the analysis of the vibration characteristic of the plant. Furthermore, the agility of the different plants is demonstrated by a one-day simulation. The best possible alignment of a predefined power reference signal and the simulated power trend is the focus of this simulation. Finally, the ability to compensate a power imbalance within the power system by changing the power output of the pumped-storage plant is investigated. It turns out that the ternary set is the most profitable one and that the variable speed schemes have, within a broad operating range, a better transient behaviour than the fixed speed schemes.

Contents

Nomenclature

BEL	Best efficiency line
BEP	Best efficiency point
BEV	Battery electric vehicle
BS	Binary set
CAB	Cable
CAV	Cavern
CEPS	Central European power system
CON	Controlling
D-A	Day-ahead market
ENG	Engineering
EPS	Electrical equipment
EV	Electric vehicle
FFT	Fast Fourier transformation
FSP	Fixed speed pump
FSPT	Fixed speed pump-turbine
FSPTT	Fixed speed Pelton-turbine
FSTS	Fixed speed ternary set
GV	Guide vane
GVO	Guide vane opening
HSC	Hydraulic short circuit
HW	Head water

HYDR	Hydraulic equipment
MG	Motor-generator
P	Pump
PCM	Primary control market
PCP	Primary control power
PHEV	Plug-in hybrid electric vehicle
PI	Proportional integral controller
PID	Proportional integral differential controller
PS	Power system
PSI	Power system inertia
PSP	Pumped-storage plant
PT	Pump-turbine
SCM	Secondary control market
SCP	Secondary control power
SCW	Secondary control work
SS	Standstill
ST	Surge tank
T	Turbine
TF	Transformer
THS	Phase angle
TOT	Total costs
TS	Ternary set
TSO	Transmission system operator
TW	Tail water
VS	Voltage source
VSDFG	Variable speed doubly-fed generator
VSFSC	Variable speed full size converter

VSPT	Variable speed pump-turbine
WW	Water way

Greek Symbols

$\dot{\omega}$	Angular velocity deviation	[	$\frac{1}{\mathrm{s}^2}$	]
η	Efficiency	[	$-$	]
λ	friction coefficient	[	$-$	]
ω	Angular velocity	[	$\frac{1}{\mathrm{s}}$	]
ω_D	Damped natural frequency	[	Hz	]
ω_{UD}	Undamped natural frequency	[	Hz	]
ρ	Fluid density	[	$\frac{\mathrm{kg}}{\mathrm{m}^3}$	]
ζ	loss coefficient	[	$-$	]

Latin Letters

$\dot{E}$	Energy deviation	[	W	]
$\dot{f}$	Frequency deviation	[	$\frac{1}{\mathrm{s}^2}$	]
$\dot{m}$	Mass flow	[	$\frac{\mathrm{kg}}{\mathrm{s}}$	]
a	Wave propagation speed	[	$\frac{\mathrm{m}}{\mathrm{s}}$	]
c	Speed	[	$\frac{\mathrm{m}}{\mathrm{s}}$	]
C_I	Investment costs	[	€	]
C_m	Annual operating and maintenance costs	[	€	]
C_R	Annual repayment	[	€	]
c_T	Torsional spring constant	[	Nm	]
D	Impeller diameter	[	m	]
d	Day	[	24h	]
D_F	Damping factor	[	$-$	]

d_P	Pipe diameter	[m]
Dev	Deviation between power reference signal and actual power	[MWh]
E	Energy	[J]
E	Modulus of elasticity	[$\frac{N}{m^2}$]
f	Frequency	[Hz]
g	Acceleration of free fall	[$\frac{m}{s^2}$]
H	Head	[m]
h	Hour	[h]
H_e	Inertia constant	[s]
I	Income	[€]
I_e	Current	[A]
J	Inertia	[kgm^2]
K	Loss coefficient	[−]
k	Gradient	[−]
K_e	Synchronization power coefficient	[$\frac{W}{rad}$]
l	Length of pipe	[m]
m	Mass	[kg]
n	Number of elements	[−]
n	Speed	[$\frac{1}{s}$]
n_L	Lifetime	[a]
n_{11}	Unit speed	[$\frac{1}{s}$]
om	Operating and maintenance costs as percentage of investment costs	[%]
P	Power	[W]
p	Pressure	[$\frac{N}{m^2}$]
p_e	Number of pole pairs	[−]
Prf	Profits	[€]
Q	Flow	[$\frac{m^3}{s}$]

q	Interest rate	[	%	]
q_{11}	Unit flow	[	$\frac{\text{m}^3}{\text{s}}$	]
s	Pipe thickness	[	m	]
S_n	Rated apparent power of the generator	[	W	]
T	Torque	[	Nm	]
t	Time	[	s	]
TF	Target function	[€, Ws]
THS	Phase angle	[	rad	]
U	Voltage	[	V	]
y	Guide vane opening	[	$-$	]

Subscripts

act	Actual value
BEP	Best efficiency point
C	Consumption
CAB	Cable
$D - A$	Day-ahead market
EL	Electrical
ext	External
F	Final value
Fr	Friction
G	Generated
geo	Geodetical
$gross$	Gross value
HW	Head water
$Hydr$	Hydraulic
I	Initial value

i	i^{th} unit
imb	Imbalance
IMP	Impeller
kin	Kinetic
L	Losses
$lrms$	Root mean square value
max	Maximum
Me	Mechanical
MG	Motor-generator
n	Negative
net	Net value
nom	Nominal value
O	Offered value
Out	Outlet
P	Price
p	Positive
PCP	Primary control power
per	Period
$press$	Pressure
PS	Power system
Pu	Pump
Q	Heat
R	Required value
r	Reflection
ref	Reference value
ROT	Generator rotor
SCP	Secondary control power

SCW	Secondary control work
st	Steal
T	Turbine
t	Transit
TF	Transformer
TW	Tail water
V	Value
w	Water
WW	Water way
CP	Control power

1. Introduction

1.1. Motivation and Background

In human history the steady growth of population has led to a rising demand of energy. Population has become used to energy services such as heating, transportation, lighting and mechanical energy. These services are enabled by the use and transformation of primary energy sources. Primary energy sources occur in nature and biofuel, wind, water, coal, oil, gas or radioactive sources may be named as examples. Figure 1.1 shows the steady increasing usage of primary energy.
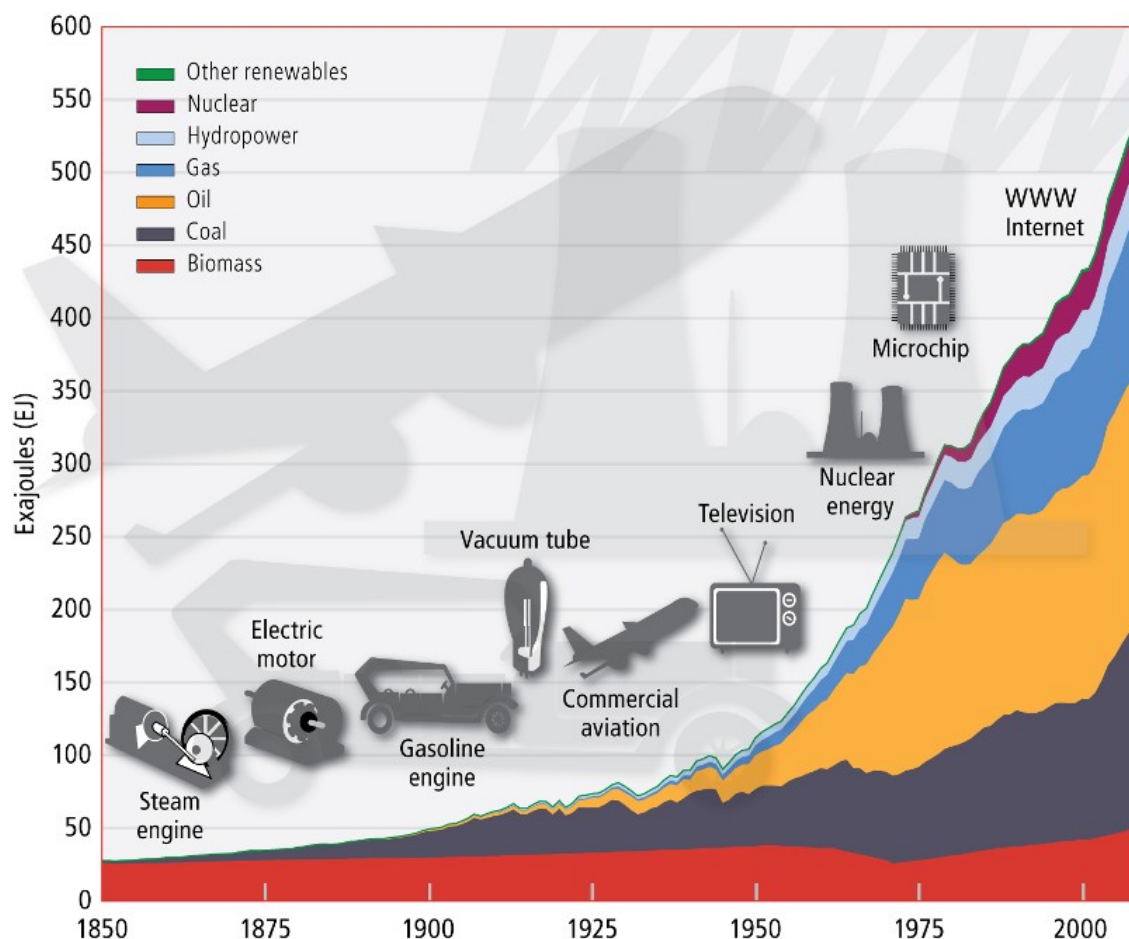

Figure 1.1.: Evolution of worldwide used primary energy sources [1] ([2], [3], [4])

Between primary energy and the desired energy service there may be intermediate steps, such as district heat, electricity, gasoline, heating oil or briquettes. The worldwide energy transformation from primary energy to the sector of final usage is illustrated in figure 1.2.
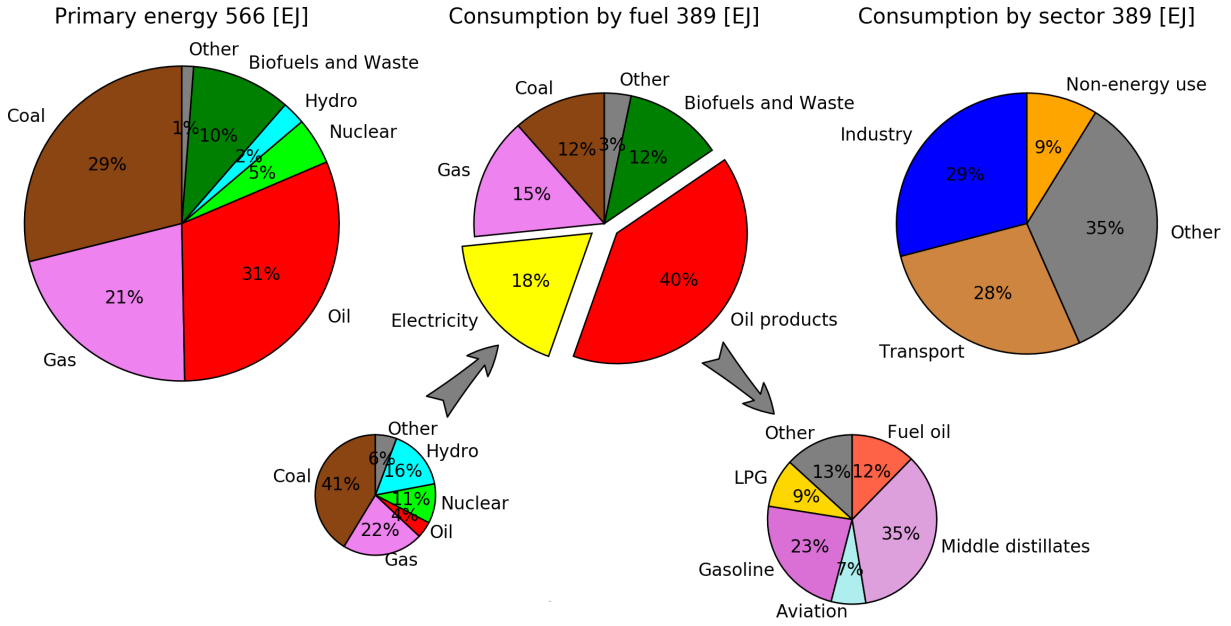
Figure 1.2.: Energy conversion from primary energy to the sector of final usage (data: [5])

The worlds primary energy is based on 81 % fossil fuels and five percent nuclear power. Only one percent of other energy sources like solar, wind and geothermal power appear. In combination with the two percent hydro power, in total about three percent of the worlds primary energy are renewable energies (biofuels and waste not taken into account). From the 566 EJ primary energy, 389 EJ reach the consumer in form of electricity, oil products and other (transformed) energy sources. The remaining 31 % are conversion losses reasoned by the generation of electrical energy and by refining oil.

Since fossil fuels and nuclear sources have negative side effects such as climate change, air pollution and long-term storage of radioactive waste, it is a worldwide concern to ensure prosperity, and thereby energy services, without the mentioned effects on the environment. Therefore, the majority of primary energy sources has to be substituted by renewable ones. As electrical energy is the common outcome of renewable energy sources such as water, wind and solar, the available type of energy changes with the primary energy towards more electrical energy. Alongside, the energy consumption (rightmost pie) has to move towards electricity, which is a current topic for the transportation sector [6], [7]. Furthermore, generation of electrical energy by solar and wind depends on the weather and is therefore not secured. This leads to challenges of balancing generation and load, which is essential for a stable power system [8].

The motivation for this research work was to use energy markets to determine the most profitable operation for storage applications and, based on this operation, investigate the transient behaviour of the storage and its interaction with the power system. On the economic side, the possible income is compared with investment costs, while on the technical side, special focus is laid on the possibility of balancing electricity generation and consumption by storage technologies. As most used storage technology ([9], [10]), pumped-storage plants are investigated in direct interaction with the power system. As battery storage prices fall by a fast rate, they become increasingly important for storage applications and are therefore investigated examined as well.

After a brief introduction to the requirements of a stable power system and current technological trends impacting the power system, it is explained why these changes require storage capabilities. Subsequently, pumped-storage schemes are investigated with regard to their capability to deliver power system services. Common plant schemes such as those equipped with a fixed speed pump-turbine, variable speed doubly-fed generator, variable speed full size converter and fixed speed ternary set are examined. For the investigation of these schemes, transient plant models have been developed. One of the developed models has been validated with measurements from a real plant. Furthermore, operating ranges of different schemes have been determined and the ability of different schemes to stabilize power system frequency has been simulated.

Since the majority of pumped-storage plants is equipped with Francis-turbines or pump-turbines, this work focuses on these types of pumped-storage plants. Nevertheless, a pumped-storage plant equipped with a Pelton-turbine is investigated in appendix A.

This work differs from existing literature in several ways:

- Extensive pumped-storage plant models have been developed including hydraulic, electrical, controlling and economic systems.

- The transient models allow for long-term simulations (one day in one go).

- Several common pumped-storage plant schemes are compared in terms of losses, profitability and transient behaviour.

1.2. Power System Stability

A stable power system (PS) requires balance between electrical power generation and consumption at any time. In addition to the timely alignment of generation and consumption, a locational alignment is required as well. The growth of additionally installed new renewable energies (wind and solar) causes problems for both kinds of alignments due to location and weather dependent generation. Locational problems can be seen in the current report of the Austrian transmission system operator [11], indicated by the massively increased redispatch costs caused by mainly wind and solar power. While the locational alignment requires a sufficient robust transmission system, the timely alignment requires flexible power plants and/or storage technologies. In case the generated power does not match with the consumed power, all rotating masses directly connected to the PS are accelerated. Directly connected rotating masses are those, connected to the PS without an interposed converter. A surplus of generation is tantamount to an acceleration while a surplus consumption leads to a deceleration. Since the rotational speed is proportional to the PS frequency, the frequency increases as well (equation 1.1). A derivation of the impact of power imbalance and PS frequency is given in appendix B.

$$f = f_{(t=0)} + \int_t \sum_i \frac{T_i(t) \cdot p_{e,i}}{2 \cdot \pi \cdot J_i} dt \tag{1.1}$$

In equation 1.1, T_i stands for the torque of one generation or load unit, J_i represents the inertia and p_i is the number of pole pairs of the unit. $f_{(t=0)}$ represents the initial frequency value.

Within the continental European power system (CEPS), the nominal frequency is 50 Hz with allowed quasi-steady-state frequency deviations of $\pm$ 200 mHz and maximum dynamic deviations of 800 mHz [12], therefore, deviations have to be kept rather low. In order to do so, transmission system operators (TSOs) predict the power consumption and adopt the generation trend so that they are balanced [13]. The generated electrical energy is purchased from the following energy markets:

1. power derivatives market: long-term contracts

2. day-ahead: contracts for the following day

3. intraday market: intra-day transactions to adapt generation to load trend

4. balancing energy market: balance of remaining deviation between generation and load

With increasing numeration of the markets, the required volatility of the power plant also increases and thus the price for the generated power. Therefore, the first attempt is to meet consumption as far as possible with long-term contracted plants. Since the consumption may vary between 50 and 100 % of its maximum value within one day [14], it is not possible to generate the whole power by inertial plant types. From the above mentioned markets, the first three are independent of PS frequency, while the balancing energy market conducts the fine adjustment of balancing generation and consumption, thus keeping the frequency within its limitations. Figure 1.3 shows the further distinction of the balancing energy market in order to deliver primary control power (PCP), secondary control power (SCP) or tertiary control power.
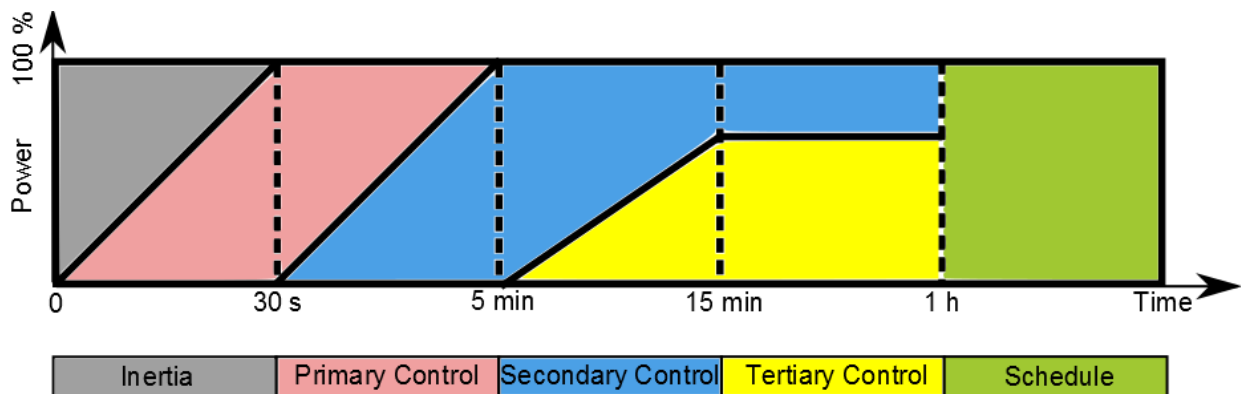
Figure 1.3.: Specifications of balancing energy

It can be seen that primary, secondary and tertiary control power are activated within different time periods. However, before control power is activated, the PS inertia (PSI) counteracts an imbalance. While there exists a market for primary, secondary and tertiary control power [15], PSI is currently not remunerated but may be in the future [16].

1.3. Technological Trends Impacting the Power System

The PS is a vital device which has always been and is currently influenced by new technologies on the consumption side as well as on the generation side. Therefore, some key technologies

which already have a great impact on the PS, or may have in the future, are introduced in this section.

The best known technologies impacting the PS are wind and solar power. Since their power generation can only be estimated roughly and they only offer low inertia values to the PS which leads to increased frequency volatility according to equation 1.1. These plants require locations with specific weather conditions which further call for sufficient transmission lines to transport generated power towards the consumers. Beside wind and photovoltaic, ground-breaking progress is made on the battery technology regarding costs and energy density [17], [18]. Sinking costs of batteries make them economically usable as storage technology which counteracts the time gap between regenerative power generation and power consumption. Furthermore, lower battery prices promote electro mobility, since the bottle neck of electric vehicles has always been the battery price and weight [19].

1.3.1. Implementation of New Renewable Energy

Since basic information about the PS stability is given, a closer look can now be taken at the current situation in the CEPS and its stability. As part of the CEPS and as example of high integration of new renewable energies, the generation situation in Germany is discussed in this subsection. To do so, the hourly averaged generated power (P_G) and the hourly averaged consumed power (P_C) for the year 2015 are plotted in figure 1.4.
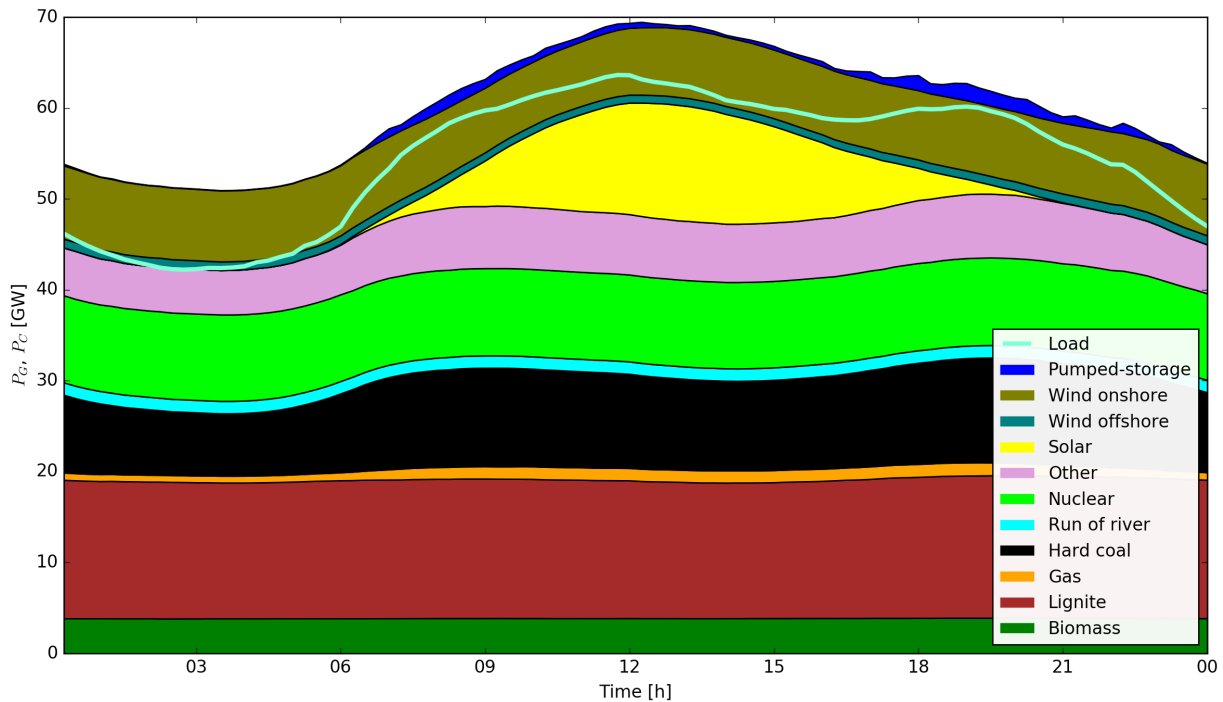
Figure 1.4.: Averaged generated and averaged consumed power of Germany in 2015 (data: [20])

For each day, quarter-hourly data are provided at [20]. After removal of incomplete day-data, 302 days for the generation and 346 days for the load were used to create the figure above. Several conclusions may be drawn:

- During 2015, 20.7 % of the electrical energy in Germany have already been produced by wind and solar power.

- The generation values indicate that only pumped-storage, hard coal and gas are operating flexible and that solar power may be named as volatile with respect to their hourly averaged values. While solar power generation depends on the day-night cycle, pumped-storage, hard coal and gas plants are used to align generation and load. Wind is a volatile energy source, but appears averaged over a year as constant.

- More energy generated than consumed indicates that Germany exports energy.

Extreme Values of New Renewable Generation

Since an average illustration can only give a rough overview of the volatile behaviour of wind and solar power, special cases within 2015 are presented in figure 1.5 (additional extreme values are presented in chapter C).
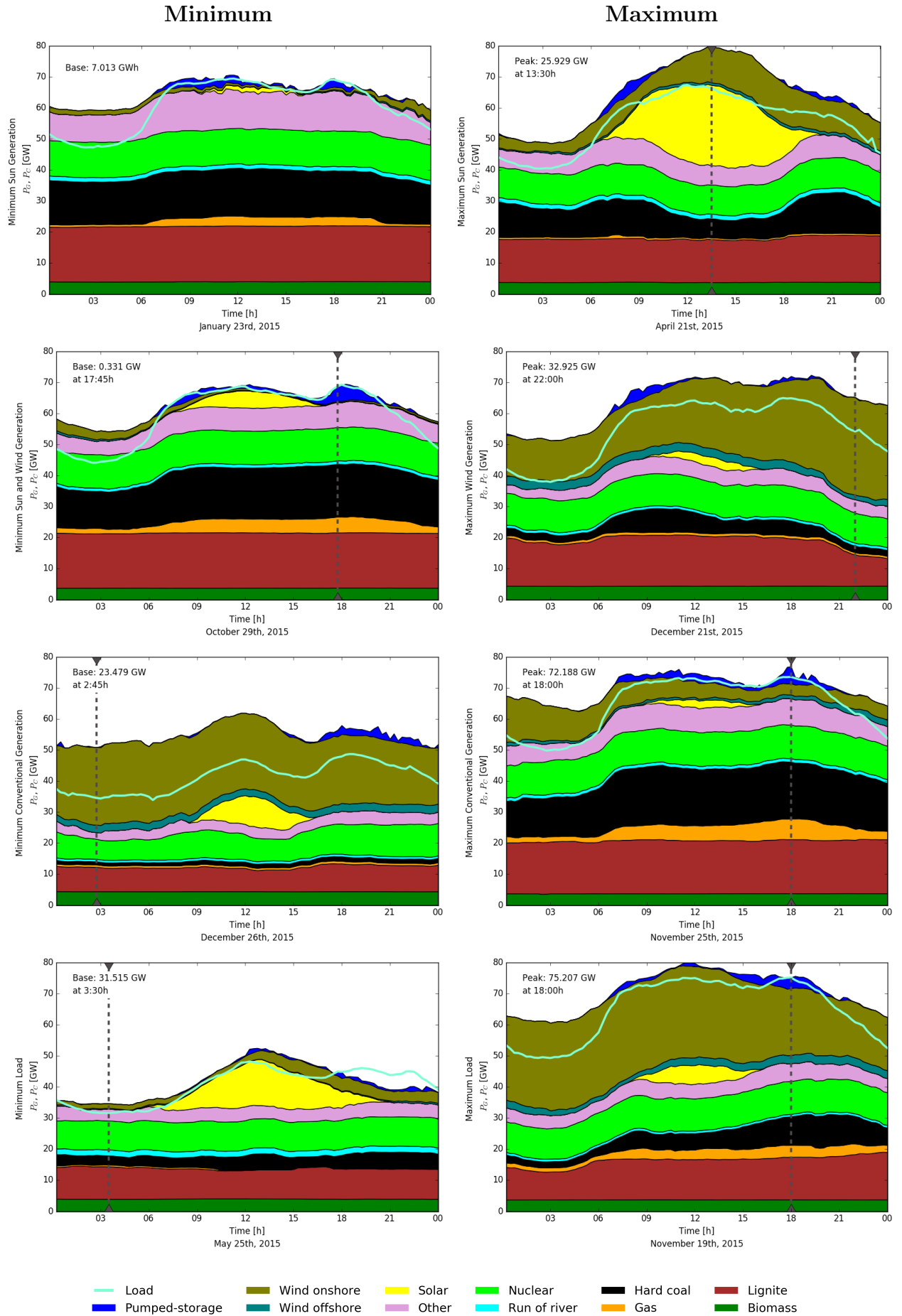
Minimum

Maximum

Figure 1.5.: Special cases of 2015 power generation in Germany

7

The figure shows extreme levels of sun, wind and conventional generation as well as minimum and maximum load. The first row shows the minimum measured solar energy within one day (7.0 GWh) and the maximum measured solar power (25.9 GW). For the minimum solar generation, the generated energy within one day is chosen instead of the power value, since night cycles are always accompanied by no solar generation. While low solar power forces gas and hard coal power plants to increase their power output, a high amount of solar power requires a reduction of the hard coal generation in order to keep the generation-consumption balance.

Considering the extrema for wind (0.3 GW and 32.9 GW), similar behaviour is recognized. The only difference is that through the high wind power value in combination with the low consumption at the same time, the lignite power also has to be reduced. As seen before, this plant type usual does not have a volatile power output since it requires drying installations which are inertial [21].

Germany's minimum generated conventional power in 2015 was 23.5 GW, while its maximum reached a value three times higher (72.2 GW). In case of minimum conventional generation, it is notable that nuclear power generation, which is the most inertial plant type of all, has been reduced in order to enable wind power feed-in.

The last row is pictured in order to estimate the load volatility. The minimum load in the German PS was 31.5 GW, while the maximum did not exceed 75.2 GW.

Reduced Inertia due to New Renewable Energies

According to equation 1.1, frequency deviations depend on the power imbalance, which is proportional to $T_i(t) \cdot p_{e,i}$, and the PSI (J_i). In terms of a low frequency volatility, low power imbalance in combination with a high PSI is desirable. Referring to power imbalance, it has already been mentioned that the weather driven generation results in more power imbalance than a demand side driven generation as in case of gas or coal power generation. In terms of the PS inertia, the inertia constant H_e (equation 1.2) is a common way to express the stability within a PS [22]. The inertia constant sets the kinetic energy ($\frac{1}{2} \cdot J \cdot \omega^2$) of rotating masses in relation to their rated power (S_n). In table 1.1, it can be seen that the inertia constant values of wind and solar power are smaller than for any other power generation.

$$H_e = \frac{1}{2} \cdot \frac{J \cdot \omega_i^2}{S_n} \tag{1.2}$$

Plant type	Inertia constant H_e [s]
Nuclear	6.3
Other thermal	4
Hydro conventional	3
Hydro small-scale	1
Wind	0
Solar	0

Table 1.1.: Inertia constant values of different plant types (data: [23])

This leads to a reduction of the PSI as visible in figure 1.6. Considering the generation mix on the left axis, it can be seen that the share of wind and solar energy is increasing and thereby the inertia constant decreases, as illustrated on the right axis.
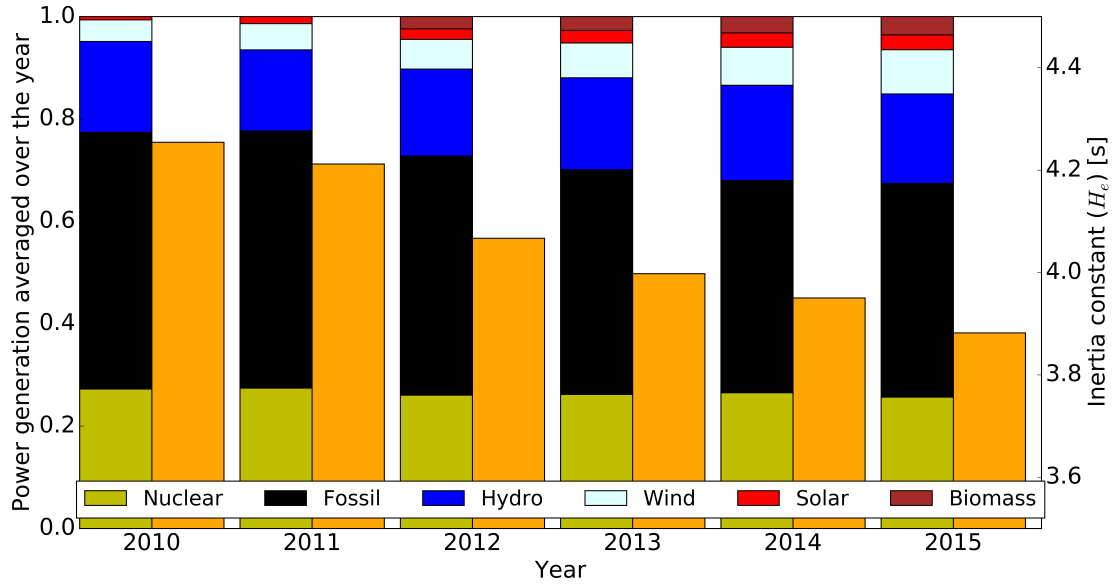
Figure 1.6.: Generation mix (left axis) and inertia constant (right axis) of the CEPS (data: [24])

1.3.2. Battery Storage

The decline of battery costs, lead to the realization of big battery storage projects such as the 52 MWh storage on Hawaii [17] or the 80 MWh, 20 MW storage in California [25]. Such storage projects have not been economic since the price for batteries has been too high. Figure 1.7 shows that the costs have declined by about 75 % from 2008 to 2015 and therefore enabled profitable battery storages. According to [26], the battery pack price will continue to fall to about $ 100/kWh in 2030 and make this form of energy storage even more attractive.
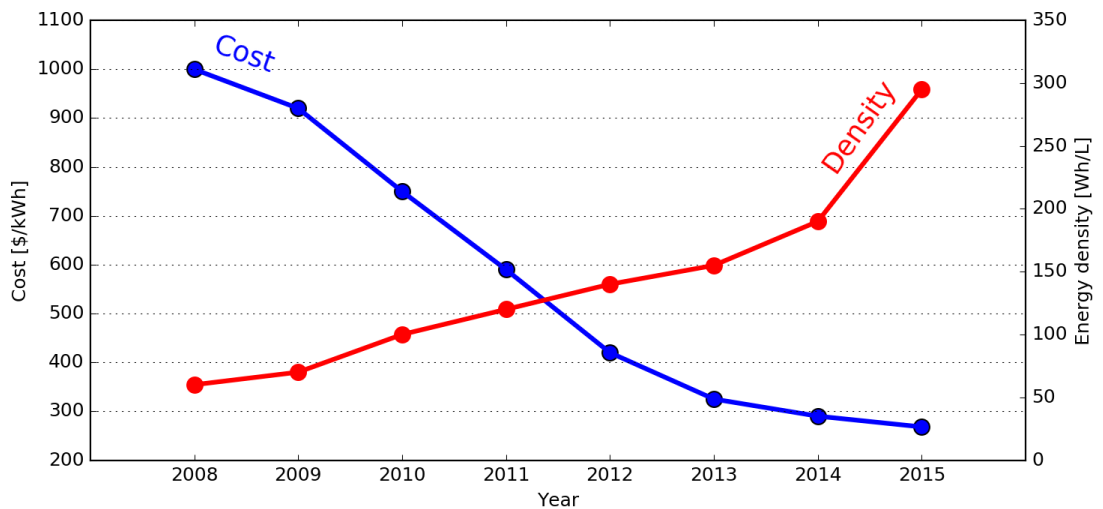
Figure 1.7.: Cost and energy density development of batteries (data: [18])

Three widespread concerns regarding batteries are the Lithium shortage, the environmental impact producing batteries and the reusability of batteries. [27] describes that the production of batteries has a relatively small environmental impact. Regarding shortage of Lithium, according to [28], there exist enough Lithium to produce enough battery capacity to replace the world wide number of internal combustion engine vehicles by battery electric vehicles ten times. Referring to the reusability of batteries, [29] shows that about 75 % of a Lithium-Ion-Battery can be recycled to a rate above 90 %. The only component that can not be recycled is the electrolyte.

1.3.3. Electro Mobility

At last, the trend towards electro mobility is considered. As shown in the rightmost pie of figure 1.2, 28 % of the consumed energy are on account of the transportation sector. This sector is further responsible for about one quarter of the global CO_2 emissions [30]. Attempts have been made to reduce those emissions through alternative drives such as combined combustion and electric drives (hybrids), fuel cells or pure electric drives. The biggest problems concerning electro mobility have always been battery costs and weight. Figure 1.7 shows that the battery costs are declining and energy density has increased almost sixfold from 2008 to 2015. Reduced costs in combination with lower weight for the same amount of storage capacity have led to an increased number of electric vehicles (EVs). EVs can be classified in battery electric vehicles (BEVs) and plug-in hybrid electric vehicles (PHEVs). Figure 1.8 shows the share of sold BEVs and PHEVs on total car sales. Sales of EVs are steadily increasing with an average growth rate of 115 % per year [18]. The amount of EVs sales is still very low (0.14 %), but considering the threshold for powering the entire transportation sector by electricity, the power generation has to increase at least twofold. The influence of EVs on PS stability is investigated in [31]. It is revealed that the EV amount acceptable for the PS depends on the charging strategy. In case of a charging if plugged in strategy 10 % of conventional vehicles can be replaced by EVs while charging if the PS can handle additional load enables a substitution of 52 % combustion vehicles by EVs.
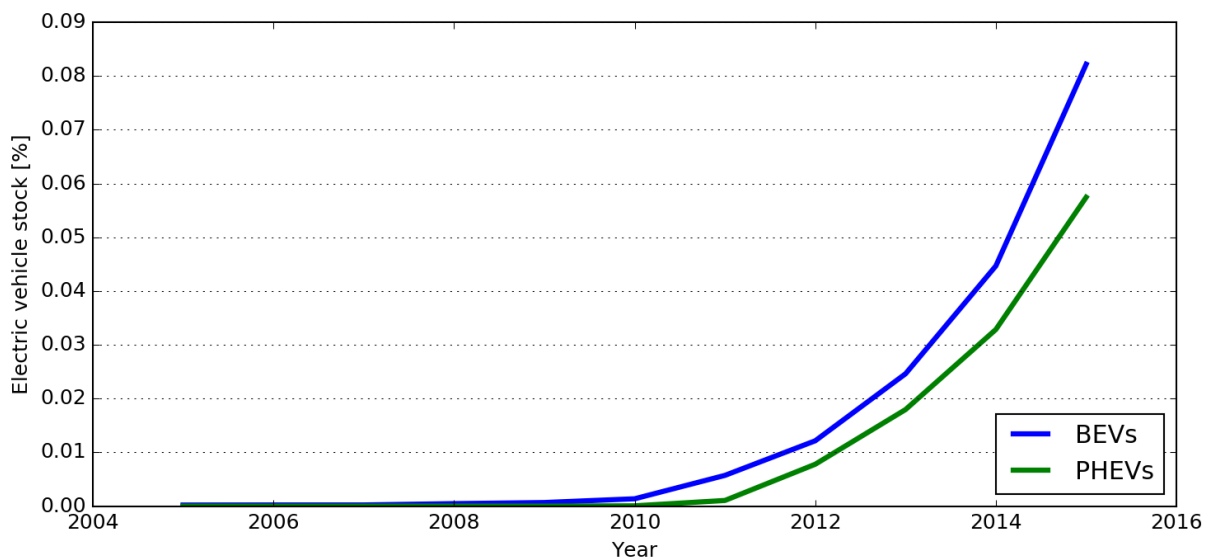

Figure 1.8.: Percentage of PHEVs and EVs on total vehicles (data: [18], [32])

1.4. Energy-Storage

According to [33] and [34], it is possible to cover the worldwide energy demand by renewable energy sources. The greater challenge is to align generation and load in terms of time and location. As explained, storage technologies are required for timely alignments. There exists a variety of storage technologies, the most common ones are:

- Compressed air
- Power to gas
- Battery
- Pumped-storage

The latter two are considered to be the most important ones as currently more than 99 % of the storage capacity are pumped-storage plants (PSPs) [35] and battery prices are declining rapidly. Storage technologies can not be compared economically by a single number since their costs depend on power, capacity, lifetime and executable storage cycles. Therefore, table 1.2 shows the most important storage parameters for different technologies. The best values are highlighted with frames.

Technology	Price $[\frac{€}{kW}]$	Price $[\frac{€}{kWh}]$	Lifetime [a]	Lifetime $[10^3$ Cycles]	Efficiency [%]
Compressed air	400 - 1000	3.5	20 - 40	8 - 12	55
Power to gas	1150 - 1650	0.2	5 - 15	>1	35
Battery	-	300	14 - 16	1 - 10	90
Pumped-storage	450 - 700	8.2	40 - 60	10 - 30	80

Table 1.2.: Parameter of different storage technologies (data: [36], [37])

As mentioned, the focus lies on pumped-storage and battery storage applications. Table 1.2 indicates that batteries have a high capacity price and PSPs a high power price. This already suggests that batteries are more profitable for high power applications while PSPs may be of advantage for high capacity applications. The views on the required ratio between storage capacity and storage power widely drift apart for a renewable energy sector. Some research assumes that a capacity-power ratio of approximately 1000 is required for a 100 % renewable power generation in Austria [38], while [39] uses a ratio of 10 to enable an 80 % renewable power generation in Germany.

1.4.1. Pumped-Storage

The PS requires energy storage. As mentioned in section 1.4, PSPs are the most used storage technology and therefore play an important role in the energy transmission towards renewable power generation. The basic approach of PSPs is to store electrical energy in form of potential energy by pumping water from a lower reservoir to a higher one and to generate electrical energy by converting potential energy to electrical energy by guiding the flow through a turbine. Basic components required for such plants are:

- Head and tail water reservoirs (HW & TW)

- Waterway that connects the head and tail water (WW)

- Pump and turbine (P & T) or pump-turbine (PT)

- Motor-generator (MG)

- Transformer (TF)

- Connection to power system (PS)

Optional are:

- Surge tank

- Frequency converter

The basic plant scheme is shown in figure 1.9.
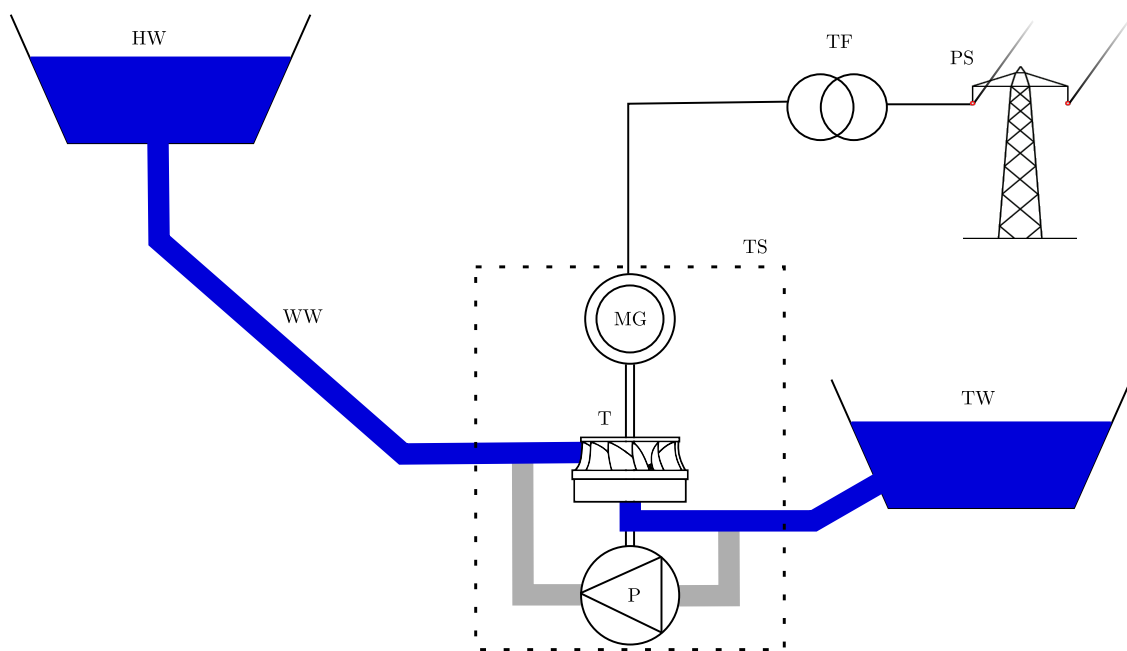
Figure 1.9.: Example of a basic ternary set plant scheme

The figure shows the classical ternary set (TS) in which the head water is connected with the tail water by a water way. Located within the water way, there is the turbine. In the water way, the potential power is converted to pressure and kinetic power, which is in turn converted to mechanical power by the turbine. The mechanical power, defined by its torque and rotational speed, drives a MG, which further converts it to electrical power. This power is transformed to high voltage power by passing the transformer before it is finally fed into the PS. In case of surplus electricity, the power flow is reversed and instead of passing the turbine, the flow passes the pump.

Several other schemes exist additionally to the outlined one. Main differences may be found in the hydraulic or electrical equipment. The hydro-electric equipment depicted in the dashed square is a ternary set, consisting of the three elements: pump, turbine and motor-generator. There exist different approaches for this part of the PSP. In terms of hydraulic equipment, the ternary set may be distinguished from the more compact binary set (BS), wherein just one hydraulic unit is used as turbine and pump by switching over the rotational direction. Referring to the electrical equipment, schemes may be distinguished by the generator type.

Common electrical equipments are for example synchronous machine, doubly fed induction machine and synchronous machine in combination with a full size converter. In figure 1.10, the most common plant schemes are pictured.

(a) FSPT   (b) FSTS   (c) VSDFG   (d) VSFSC
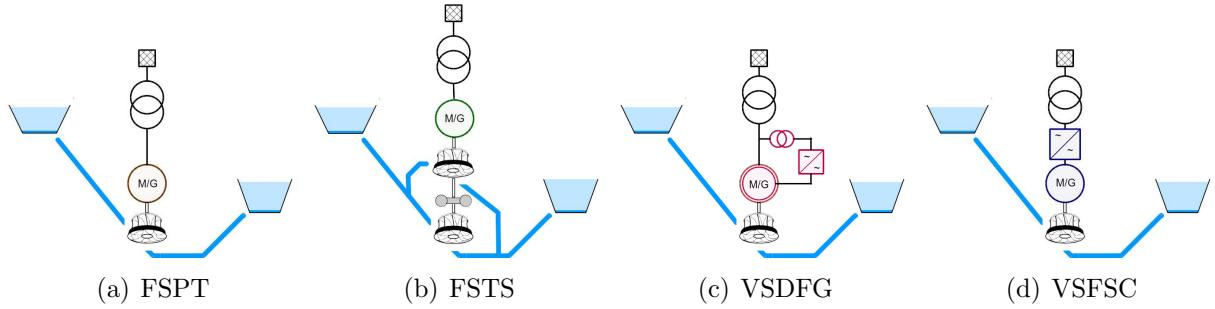
Figure 1.10.: Common schemes of PSPs (source: Andritz)

Further schemes appearing in this work are:

- FSPT (figure 1.10(a)): a fixed speed PSP scheme with a pump-turbine. This scheme is the most common one and is used e. g. in the Limberg 2 plant in Austria [40]. Turbining and pumping are permuted by the same hydraulic machine which is connected to the PS by a synchronous motor-generator.

- FSTS (figure 1.10(b)): a fixed speed PSP scheme with a separate hydraulic machine for pump and turbine mode. The connection to the PS is the same as in the FSPT scheme.

- VSDFG (figure 1.10(c)): a variable speed PSP scheme with a doubly-fed motor-generator and a pump-turbine. The speed variation is enabled by a doubly-fed asynchronous machine possessing a converter in its rotor circuit. The PSP Goldisthal in Germany can be named as an example for this scheme [41].

- VSFSC (figure 1.10(d)): a variable speed PSP scheme with a full size converter applied between the synchronous motor-generator and the PS. For this scheme, a common hydraulic unit for pump as well as for turbine operation is used. This scheme offers the highest flexibility of all schemes comprising a pump-turbine. A full size converter is used in the Grimsel 2 PSP in Switzerland [42]. Note that in the Grimsel 2 PSP, two separate units are used for pump and turbine operation which is contrary to the scheme investigated in this work.

- FSTS0 (figure 1.10(b)): the same fixed speed ternary set PSP as the FSTS scheme with the only difference that for this scheme, both hydraulic units are allowed to operate at the same time. This operation, the so called hydraulic short circuit [43], allows for regulation of the power output in pump mode by means of varying the turbine power. Such a form of operation is used in the Kops 2 PSP in Austria [44].

Switchover Times

Different schemes appear to have different switchover times and different load following abilities. A comparison of the switchover times is given in table 1.3. Since currently no

VSFSC scheme exists, there exist no example times for the switch over. The table shows combinations between standstill (SS), pump and turbine mode.

Parameter	SS $\Rightarrow$ T	SS $\Rightarrow$ P	T $\Rightarrow$ P	P $\Rightarrow$ T
FSPT	90	340	420	190
FSTS	65	85	45	60
VSDFG	90	230	470	280
VSFSC	-	-	-	-

Table 1.3.: Mode change times in seconds [45]

Hydraulic Equipment

Next to the distinction of the number of energy conversion elements and the electrical equipment, a further form of differentiation can be made by the turbine type. Depending on head (H) and flow (Q), different hydraulic equipment is used for pumped-storage applications. The binary set only consists of a pump-turbine and a motor-generator, ternary sets may consist of a Francis-turbine and a pump, or a Pelton-turbine and a pump. Pelton-turbines are used for high head values and low flow rates, while Francis-turbines are used for middle head values and middle flow rates. Kaplan turbines, used for low head values and high flow rates, are of no relevance for pumped-storage applications since they are driven by the flow of a river and do not have storage reservoirs. Explicit operating ranges are illustrated in figure 1.11.
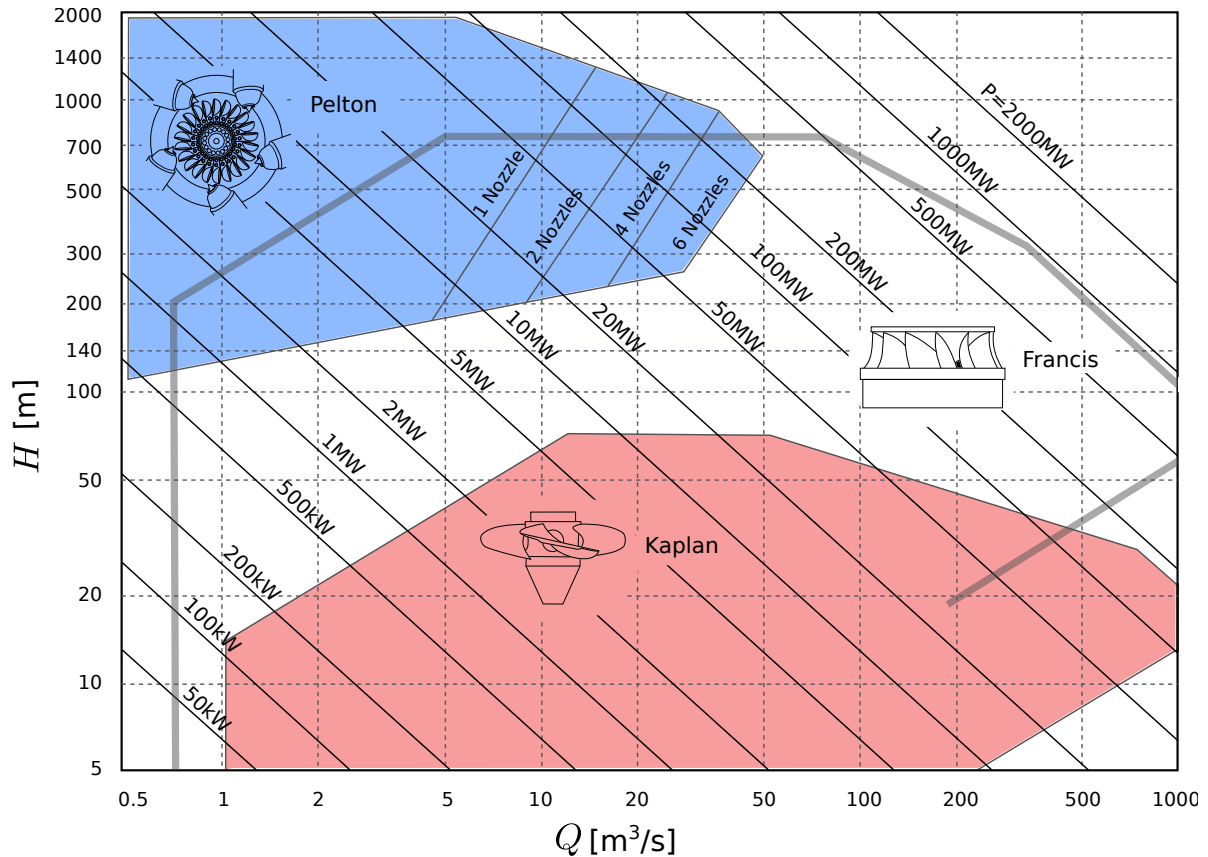
Figure 1.11.: Operating ranges of different turbine types (based on: [46])

14

Power Conversion

Basically, PSPs convert surplus electrical energy in form of potential energy by pumping water from a lower water level to a higher water level. In case of a lack of production, PSPs convert potential power to electric power by extracting power from a high water level towards low water level flow. Figure 1.12 sketches the water and power flow within a PSP in turbine operation. The three cornerstones are the head water, tail water and the PS. Considering the water path, it can be seen that the geodetic power at the head water is higher than at the tail water. The kinetic power is assumed to be constant, which is tantamount to a constant cross-sectional area along the entire water way. Furthermore, regarding the water way, the geodetic power is converted to pressure power. At the turbine, pressure power is exploited by the turbine and pump-turbine, respectively. At the head water and tail water, the pressure power is zero as, at the head water and tail water, the pressure equals the reference value, which is defined as atmospheric pressure. As last power term, losses within the water way are included. Due to the friction within the water way, losses increase with increasing water way length.

At the beginning of the indicated power path, a part of the hydraulic power, consisting of pressure, kinetic and geodetic power, is converted to mechanical power by the turbine. The mechanical power is further converted to electrical power within the motor-generator and is finally transformed to high voltage electrical power, which is fed into the PS, by the transformer. Losses at the different conversion steps are printed in red. The amount of losses is indicated by the vast of the loss vector.
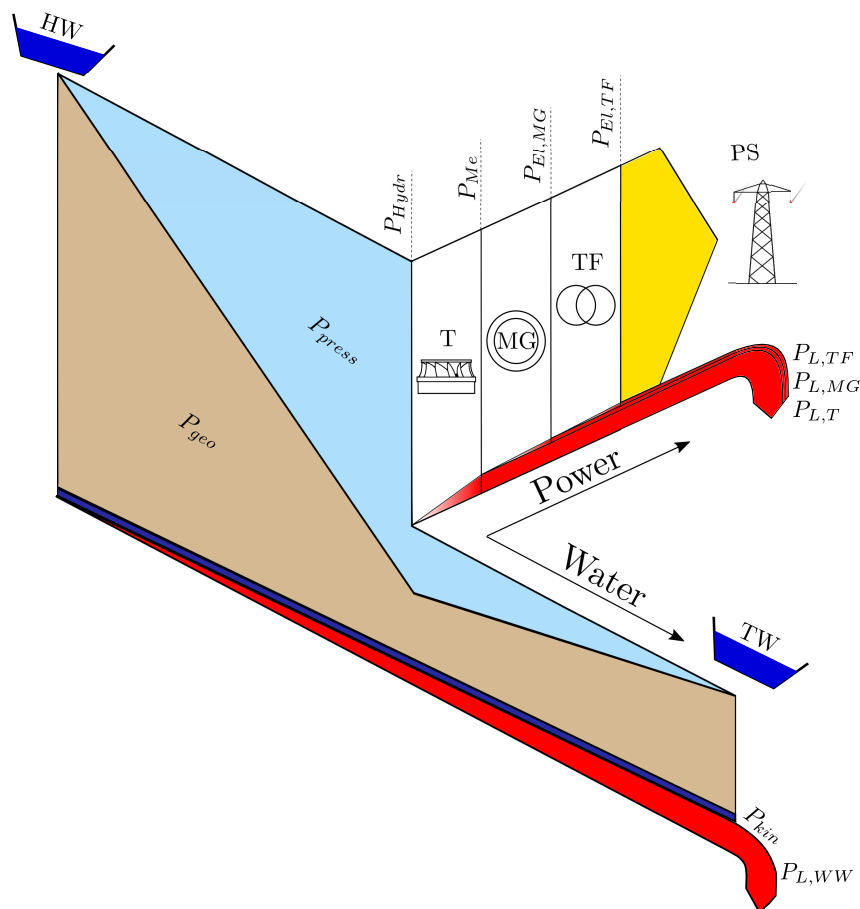
Figure 1.12.: Power conversion within a PSP in turbine mode

Assuming steady-state operation, the connection between the three cornerstones can be described by the energy conservation law differentiated with respect to time (equation 1.3).

$$P_{HW} = P_{TW} + P_{PS} + P_L \tag{1.3}$$

The power extracted from the head water equals the power fed into the tail water plus power fed into the PS and losses in the water way, turbine, motor-generator and transformer. The energy change in the head water and tail water can be expressed by the Bernoulli-equation [47] as given in equations 1.4 and 1.5. Herein, the energy change equals the integral of the power over time. The power term may be divided further into pressure (p), speed (c) and head term. $\dot{m}$ stands for the mass flow, ρ represents the density and g means the gravity constant. The change of the energy in the PS can be described by equation 1.6 and is proportional to voltage (U) and current (I_e).

$$\Delta E_{HW} = \int (P_{HW}) dt = \int (\dot{m} \cdot \frac{p_{HW}}{\rho} + \dot{m} \cdot \frac{c_{HW}^2}{2} + \dot{m} \cdot g \cdot H_{HW}) dt \tag{1.4}$$

$$\Delta E_{TW} = \int (P_{TW}) dt = \int (\dot{m} \cdot \frac{p_{TW}}{\rho} + \dot{m} \cdot \frac{c_{TW}^2}{2} + \dot{m} \cdot g \cdot H_{TW}) dt \tag{1.5}$$

$$\Delta E_{PS} = \int (P_{PS}) dt \tag{1.6}$$

In equation 1.7, the losses are further classified in friction losses in the water way ($P_{L,WW,Fr}$), outlet losses at the entrance to the tail water ($P_{L,Out}$), thermal losses in the water way ($P_{L,WW,Q}$), turbine losses ($P_{L,T}$), motor-generator losses ($P_{L,MG}$), losses of the transformer ($P_{L,TF}$) and cable losses ($P_{L,CAB}$). Thermal losses within the water way and power plant cable losses may be neglected as they are relatively small.

$$P_L = P_{L,WW,Fr} + \underbrace{P_{L,Out}}_{\sim 0} + \underbrace{P_{L,WW,Q}}_{\sim 0} + P_{L,T} + P_{L,MG} + P_{L,TF} + \underbrace{P_{L,CAB}}_{\sim 0} \tag{1.7}$$

The friction losses within a pipe may be calculated by equation 1.8. They are directly proportional to the mass flow, length (l), friction coefficient (λ) and squared speed, and inversely proportional to the pipe diameter (d_P). The total friction losses are the sum of all i pipe elements. The loss coefficient (ζ) is required for armatures and cornered parts of the pipe.

$$P_{L,WW,F} = \sum_i \dot{m}_i \cdot \frac{c_i^2}{2} \cdot (\zeta_i + \lambda_i \cdot \frac{l_i}{d_{P,i}}) \tag{1.8}$$

Turbine, generator and transformer losses cannot be expressed by a single equation and will be further examined separately in chapter 2.

Advantages and Disadvantages of different Pumped-Storage Schemes

Generally, there exist PSPs operating at fixed or variable speed. The traditional way of operation is at fixed speed, but recently planned plants or plant extensions such as Limberg

3, Le Cheylas and Kruonis are intended to operate at variable speed [48]. For fixed speed PSPs, both asynchronous and synchronous motor-generators may be used. Asynchronous motor-generators are generally used for small hydro plants due to their low efficiency, but easier structure, lower cost and better dynamic behaviour [47]. In the case of variable speed PSPs, the one used most is a doubly-fed asynchronous motor generator; alternatively, there is the more sophisticated form which uses a full size converter in combination with a synchronous motor-generator. Advantages and disadvantages are summed up in table 1.4.

It is shown that the installation costs of the FSPT scheme are lowest followed by the VSDFG scheme; the FSTS, VSFSC and FSTS0 scheme are the most expensive ones. Reasons why the FSTS/FSTS0 scheme is expensive are higher costs due to additional hydraulic equipment and a bigger cavern. The high cost of the VSFSC scheme is a result of the high costs for the full size converter.

The controllability in pump mode is the worst, as it is non-existent, in the FSPT and FSTS schemes. For these schemes, one power value is assigned to each head value. Changes of the guide vane opening (GVO) have either little effect on the power output or cause cavitation [49]. The FSTS0 scheme allows for power controlling by the hydraulic short circuit (HSC), where the pump power output is varied by the simultaneous turbine operation. The variable speed schemes enable power control due to speed variations.

In turbine mode, the unrestricted speed range of the VSFSC scheme enables the adjustment of the speed to its optimal value. Speed restrictions of the VSDFG scheme and no possibility of speed variation for the FSPT scheme result in lower efficiency values. The FSTS and FSTS0 scheme consist of two separate hydraulic units and the turbine can therefore be designed solely for the turbine operation, which results in higher feasible efficiency values.

Starting a pump-turbine in pump mode requires high amount of power [49]. The FSTS scheme is able to deliver this power with the help of a hydraulic torque converter [50], while the VSFSC scheme is able to provide this power since this scheme's power output is not restricted by any speed limits. Nevertheless, the FSPT and VSDFG scheme are not able to provide high power values beyond their speed limits. This is why the pump-turbine is blown out, so that it runs in air instead of water which reduces the power crucially to accelerate the runner [49].

The lower power can be delivered by an auxiliary motor or directly by the converter. The main reasons for long switchover times are blow out, the change of direction of rotation and the thereby required synchronization to the PS. This is why the FSPT and VSDFG schemes are the slowest ones. The FSTS and FSTS0 schemes are the fastest as the rotating mass does not have to change the direction of rotation. The VSFSC scheme does not require a blow out, but the change of the direction of rotation requires more time than the connection of the pump as it is the case for the FSTS scheme.

	FSPT	FSTS	VSDFG	VSFSC	FSTS0
installation costs	+	-	o	-	-
controllability in pump mode	-	-	+	+	+
efficiency in turbine mode	-	o	o	+	o
blow out (pump mode)	-	+	-	+	+
switchover time	-	+	-	o	+

Table 1.4.: Advantages and disadvantages of different PSP schemes

Water Hammer

As limiting phenomena for hydraulic power changes, the water hammer deserves special attention. The water hammer may cause extremely high as well as extremely low pressure. Both may lead to damage on the facility. While high pressure could cause an explosion of the penstock, low pressure could cause the appearance of cavitation or implosion of the penstock [51]. The maximum possible pressure values can be estimated by the Joukowsky-equation [52]. Joukowsky assumes that the flow through a pipe is instantaneously set zero, simulates an immediate closure of a valve. The propagation of the pressure and speed waves is illustrated in figure 1.13. Due to the abrupt closure of the valve, the flow changes to zero at the valve, while at the pipe inlet the flow is still at its steady value. In order to estimate the maximum possible pressure, the initial flow is set equal to its maximum. The deceleration energy at the valve initiates a rise of the pressure value to its maximum. The increased pressure propagates towards the pipe inlet. Together with the pressure, the changed flow also propagates in form of a wave from the valve towards the pipe inlet. Reaching the inlet, where the pressure value equals the atmospheric pressure, the pressure wave is reflected with a changed sign of its amplitude. This leads the pressure value back to its initial value. This means that a negative pressure wave propagates towards the valve and the flow direction is towards the inlet (indicated by -max). Reaching the valve, the pressure wave is reflected in a similar way to the pipe inlet with the difference that at this point, the sign of the amplitude does not change. As a result, the pressure is reduced further (indicated by -max). Once the pressure and speed waves have passed the inlet a second time and again reaches the valve, one full period has passed. Significant time points are the time the waves require to reach the other end of the pipe (t_t), the time the waves require to reach their initial point (t_r) and the time required for an entire period (t_{per}). In case the initial steady state flow is realized by losses only occurring at the valve (frictionless pipe), the pressure and speed waves would continue infinitely as illustrated in figure 1.13.
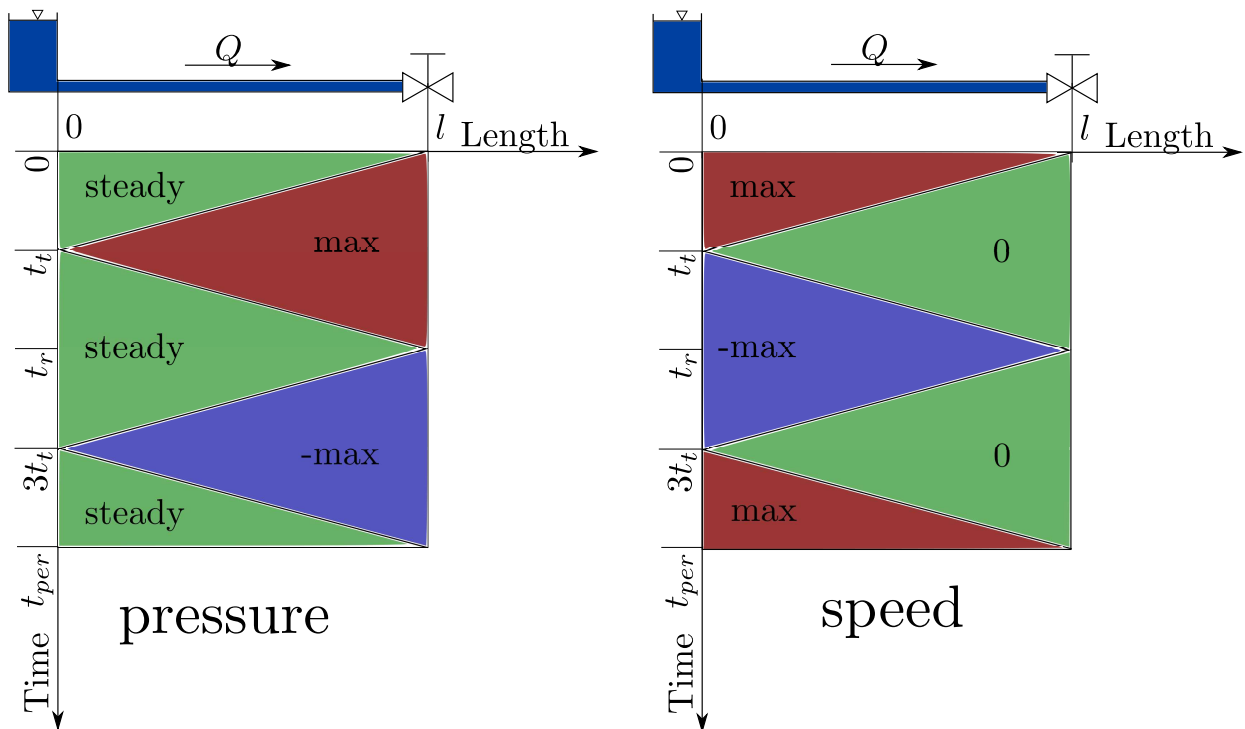
Figure 1.13.: Propagation of pressure and speed waves caused by an abrupt closure of a valve

The wave propagation speed within a thin-walled pipe is presented in equation 1.9. For pure water, the second additive term in the denominator has to be neglected and for the case of pipes installed in rock, the elasticity of the rock has to be taken into account as well. A complete collection of all types of pipes is given in [47]. The wave propagation speed depends on the modulus of elasticity of water and pipe material ($E_{M,w}$, $E_{M,st}$), the pipe diameter, the pipes thickness (s) and the density of the water (ρ_w).

$$a = \sqrt{\frac{1}{\rho_w} \cdot \frac{1}{\frac{1}{E_{M,w}} + \frac{d_P}{s} \cdot \frac{1}{E_{M,st}}}} \tag{1.9}$$

The characteristic time points of figure 1.13 are defined in equation 1.10.

$$t_per = 2 \cdot t_r = 4 \cdot t_t = 4 \cdot \frac{l}{a} \tag{1.10}$$

The maximum possible pressure variation occurring due to an abrupt closure can be approximated by equation 1.11. Therein, the maximum possible pressure variation depends on the density, wave propagation speed and deceleration of the flow. The equation is just an approximation since no friction effects are not considered.

$$\Delta p_{max} \approx \rho \cdot a \cdot \Delta c_{max} \tag{1.11}$$

So far, an abruptly closing of the valve is assumed, but the same maximum pressure occurs for a closing time of the valve smaller than the reflection time (t_r). In case the valve is closed exactly within the reflection time, the pressure at the valve would increase steadily within the reflection time, until it reaches its maximum. If the valve closure takes more time, the negatively reflected pressure wave arrives at its point of departure before the maximum pressure value is reached and decreases the pressure value.

2. Losses within the different Sections of the Power Plant

As mentioned in subsection 1.4.1, there are losses in the different sections of a PSP. While the calculation of the WW losses has already been presented, losses in other sections of the power plant are more sophisticated to calculate. In this chapter, the hydraulic and electrical losses, including generator, converter and transformer, are examined with respect to power and head value.

2.1. Losses in the Hydraulic Unit at Constant Gross Head

The losses in the hydraulic unit depend on the flow conditions within the hydraulic unit. These conditions vary widely depending on speed, flow and head value at the hydraulic unit. By introducing unit speed and unit flow (equations 2.1 (n_{11}) and 2.2 (q_{11})), the loss dependence of three parameters can be reduced to a dependence of two parameters and may further be plotted in form of a characteristic.

$$n_{11} = n \cdot \frac{D}{\sqrt{H_{net}}} \tag{2.1}$$

$$q_{11} = \frac{Q}{D^2 \cdot \sqrt{H_{net}}} \tag{2.2}$$

The unit speed depends on speed, impeller diameter (D) and net head (H_{net}), while the unit flow depends on flow, diameter and net head. The subscript $_{11}$ stands for the head value of one meter and the impeller diameter of one meter. This means that wherever a diameter or head appears in one of the detailed equations, the value is divided by the head respectively diameter value of one meter. Thereby, the units of unit speed and unit flow become congruent to those of speed and flow. The dependency on the diameter has the advantage that a unit speed - unit flow characteristic is valid for all diameters of the same specific impeller design. The net head equals the gross head reduced about the head losses appearing in the WW.

Such an unit speed - unit flow characteristic is shown in figure 2.1. The lower graph represents the behaviour of a pump-turbine. The graph is divided in the four quadrants: turbine, pump brake, pump and reverse pumping. For steady operation, only the first and the third quadrant are important. These quadrants represent the turbine and pump mode. The second and fourth quadrant are of minor importance, since they are just passed in transient operation but do not host steady operating points. While the second quadrant has to be passed for

switchover from pump to turbine mode and vice versa, the fourth quarter must be avoided and only occurs due to instabilities [53]. The colour coded area represents the efficiency of the pump-turbine in turbine and pump mode. In the first quadrant, the right hand side lower corner is not colour coded, as the flow in this area is too low to power the impeller at this speed and therefore, power has to be extracted from the PS, in order to operate in this corner. Due to the required power extraction from the PS, this area can not be considered as turbine operation. Magenta lines have been added in order to indicate constant GVO of the pump-turbine. In case of closed guide vanes (GVs) ($y = 0$), the flow and thereby the unit flow equals zero. Operating points regarding entirely opened GVs are given by the magenta line where y equals 1. Black lines connect operating points with the same mechanical power. According to equations 2.3 and 2.4, the mechanical power is proportional to the hydraulic power multiplied by the turbine efficiency (η_T) or divided by the pump efficiency (η_{Pu}). The hydraulic power depends on net head and flow. Considering a constant gross head, the net head does not vary widely. Only WW losses change the net head value and these are usually lower than five percent, e.g. [54]. Therefore, the hydraulic power mainly depends on the flow, which means that the mechanical power reaches its maximum around the maximum flow even if the turbine efficiency is distorting this behaviour. According to equation 2.2, the flow is proportional to the unit flow, if it is assumed that net head variations are relatively small. This explains why the maximum mechanical power appears close to the maximum unit flow.

$$P_{Me,T} = \underbrace{\rho \cdot g \cdot H_{net} \cdot Q}_{P_{Hydr}} \cdot \eta_T \tag{2.3}$$

$$P_{Me,P} = \frac{\rho \cdot g \cdot H_{net} \cdot Q}{\eta_{Pu}} \tag{2.4}$$

Finally, the best efficiency lines (BELs) of different plant schemes are attached. BELs are lines connecting operating points with highest efficiency regarding one specific power output. They are the result of several optimization tasks, whose goal it is to minimize the required flow for specific power values taking into account the PSP schemes restrictions. The operating range is limited downwards by unfavourable flow conditions leading to cavitation or formation of vortices [55], [56]. Since these conditions vary with design and plant structure, a general limitation of 80 % minimum hydraulic efficiency is set and restricts a further power decrease. On the upper end, completely opened GVs limit the power output in turbine mode, while for the pump mode, the maximum generator power limits a further increase of the pump power. It is mentioned that the term "pump power" refers to the absolute value of the pump power in this work. This means a higher pump power is tantamount to a higher value of the negative power.

Turbine operation BELs are pictured for the FSPT, VSDFG and VSFSC schemes in the first quadrant. Different BELs are caused by different speed limits. The VSFSC scheme enables arbitrary speed settings. It is possible to reduce the speed towards low values which are required for high efficient power generation at low load. The BEL of the VSDFG scheme is congruent with the BEL of the VSFSC scheme for high power output values, but since the VSDFG scheme just enables a reduction of the speed to a certain speed value, the BELs of these schemes diverge for low power output values. Lower speed values required for the

most efficient operation at lower power output values can not be reached by the VSDFG scheme and highest possible efficiency is realized by an operation at the minimum possible speed. The BEL of the FSPT scheme is placed at higher unit speed values than those of the variable speed schemes. The BEL is an almost vertical line, only curved by changes of the net head value due to different WW losses. It is placed on the right hand side of the BEP since pump-turbines are designed for the more critical pump mode, which leads to a suboptimal turbine operation. This design strategy is due to the higher cavitation risk in pump mode than in turbine mode [57], [58].

Considering the pump mode, it has to be clarified first that in this operation case, no regulation by GVs is possible as flow conditions are highly sensitive with respect to cavitation [49], [59]. By means of this, the only way of pump power regulation is by changes of the speed. BELs of VSFSC and VSDFG schemes are thereby again congruent with exception of low pump power values where the operating range of the VSFSC scheme exceeds the one of the VSDFG scheme since no lower speed limitation exists. Nevertheless, the VSFSC schem's operating range is limited by the pump instability, where several operating points may occur for one speed and one GVO. Since no pump power regulation is possible due to GVs, the BEL of the FSPT scheme appears as operating point.
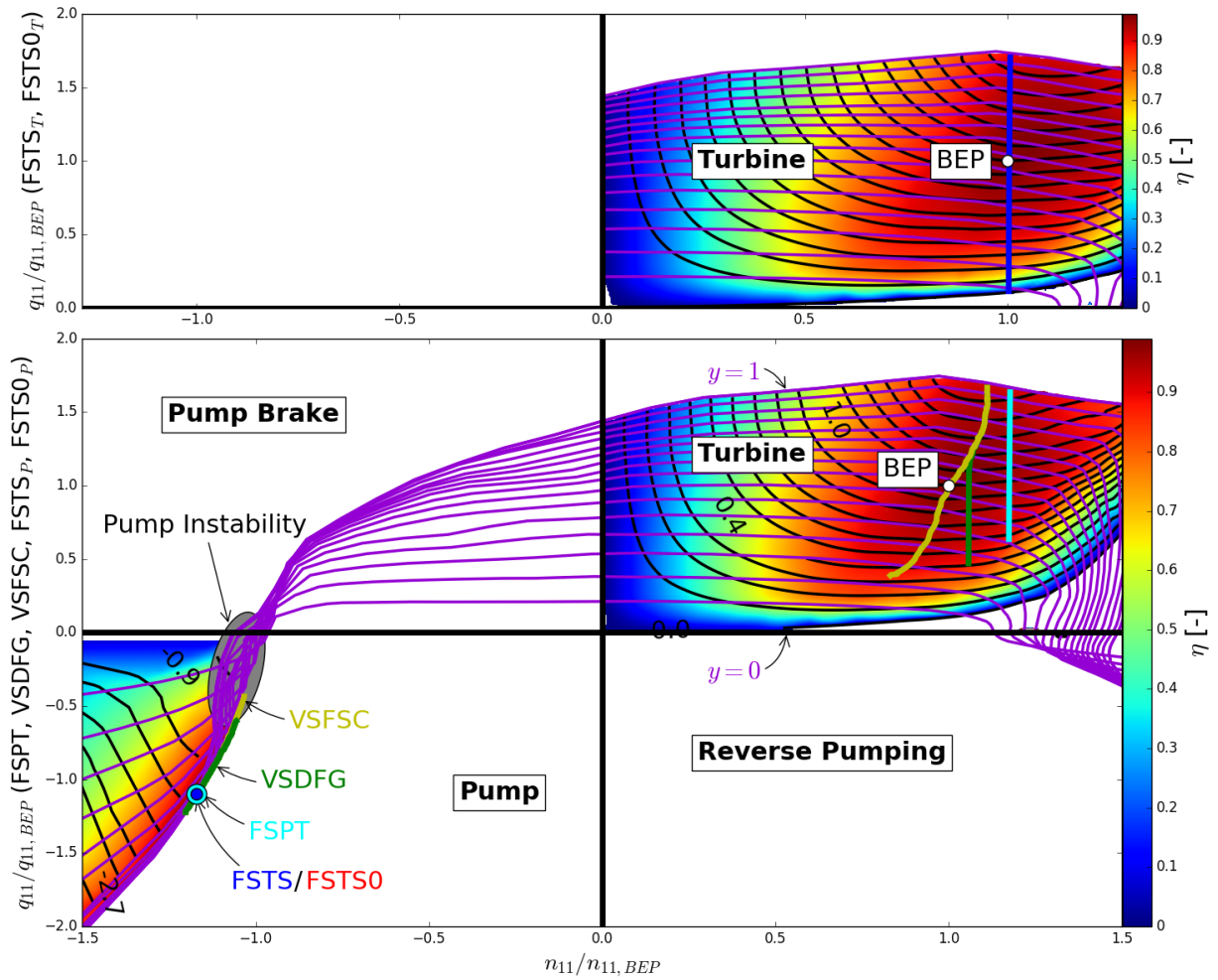

Figure 2.1.: Hydraulic efficiency including lines of constant mechanical power (black), constant GVO (magenta) and BELs of all considered schemes

The FSTS scheme is a special case. As pump and turbine are different hydraulic units, both units can be designed for their respective proper operation mode. The different unit used for the turbine case also changes the characteristic. The appropriate characteristic is shown in the upper graph of figure 2.1. The FSTS scheme has further been subdivided into the FSTS scheme and the FSTS0 scheme for its practical significance. While in case of the FSTS scheme, the hydraulic efficiency limit is set to 80 % (as in all above mentioned schemes), the FSTS0 scheme efficiency limitation is set to zero percent. Thereby, the turbine can be regulated within the entire power band and, more importantly, the pump power output can be regulated from zero to maximum power output as well by operating the turbine and pump unit at the same time (HSC). It has to be mentioned that a turbine operated to an efficiency value of zero percent requires a special hydraulic design [60], [61]. In pump mode, the BELs of the FSTS and FSTS0 schemes appear, as in case of the FSPT scheme, as points. These points correspond with the operating point of the FSPT scheme in pump mode. This congruence appears as the impeller of the FSPT scheme is designed for the pump mode and it is thereby assumed that its behaviour equals the one of a pump impeller.

Similar to the turbine mode of the FSPT scheme, the turbine mode BELs of the FSTS and FSTS0 schemes appear as almost vertical lines as well. Only the BEL of the FSTS0 scheme is pictured, as the BEL of the FSTS scheme is part of it.

2.2. Electrical Losses at Constant Gross Head

In addition to losses in the WW and the hydraulic unit, losses also occur in the electrical equipment. Power output and speed depending losses of the generator, converter and transformer are plotted in figure 2.2. The upper five graphs show the power losses of the hydraulic unit as well as the sum of the entire electrical losses depending on the plant scheme and power output. The spread along the abscissa of the different schemes is in accordance with the length of the BELs of figure 2.1. On the right hand side, losses in turbine mode are illustrated while the left side presents losses in pump mode. Regarding the PSP power output, losses are only pictured for power output values within their operating range. Turbine losses are pictured in blue, pump losses are presented in green and electrical losses are depicted in red. When referring to electrical losses, it can be seen that they are relatively small compared to the losses of the hydraulic unit and that schemes containing frequency converters have higher electrical losses than those without. Hydraulic losses show that turbine losses only occur in turbine operation and pump losses in case of pump mode, with the exception of the FSTS0 scheme. In this scheme, turbine losses also occur in pump mode due to the HSC. It can be seen that the operating range in pump mode is extended compared to the FSTS scheme but at the cost of higher losses.

An overview of the plant efficiency for different schemes is presented in the lowermost row. As the 80 % efficiency is no fixed limitation, the plant efficiency trend is also illustrated for hydraulic efficiency values lower than 80 %. In turbine mode, the VSFSC scheme operates at highest overall efficiency. Only the FSTS and FSTS0 schemes exceed the maximum efficiency value, since the FSTS, FSTS0 and VSFSC schemes are able to pass the BEP (see figure 2.1), the ternary set, however, operates with lower electrical losses due to the absence of a converter. The VSDFG scheme has the same behaviour as the VSFSC scheme for high turbine power values. However, due to the speed limitation, the efficiency at lower power output values is smaller than in the case of the VSFSC scheme. The FSPT scheme has a

poor efficiency behaviour at low turbine power values, but the trend converges to the variable speed schemes for higher power output values, since in this case, the FSPT scheme's BEL converges to the variable speed ones, as can be seen in figure 2.1.

The efficiency trends in pump mode diverge more than in turbine mode. While variable speed schemes operate at high efficiency within a wide range, the efficiency trend of the FSTS0 scheme shows lower efficiency values. This behaviour is a result of the synchronous operation of pump and turbine. Two active hydraulic units mean two times hydraulic losses. The difference between the two variable speed schemes is caused by speed limitations. While for low pump power values, the VSFSC scheme is able to operate at the associated speed, the VSDFG scheme is not able to do so. The power output related to the minimum speed value can be further reduced by closing the GVs. As mentioned, such a variation would cause cavitation, but considering only the pump-turbine characteristic, such a regulation would be possible. The same holds true for the FSPT scheme. A power regulation by the GVs causes a steep gradient of the plant efficiency. Since the FSTS scheme neither has GVs nor the possibility of speed variation, its efficiency trend shrinks to one operating point, which efficiency value is higher than those of variable speed schemes as electric losses are less.
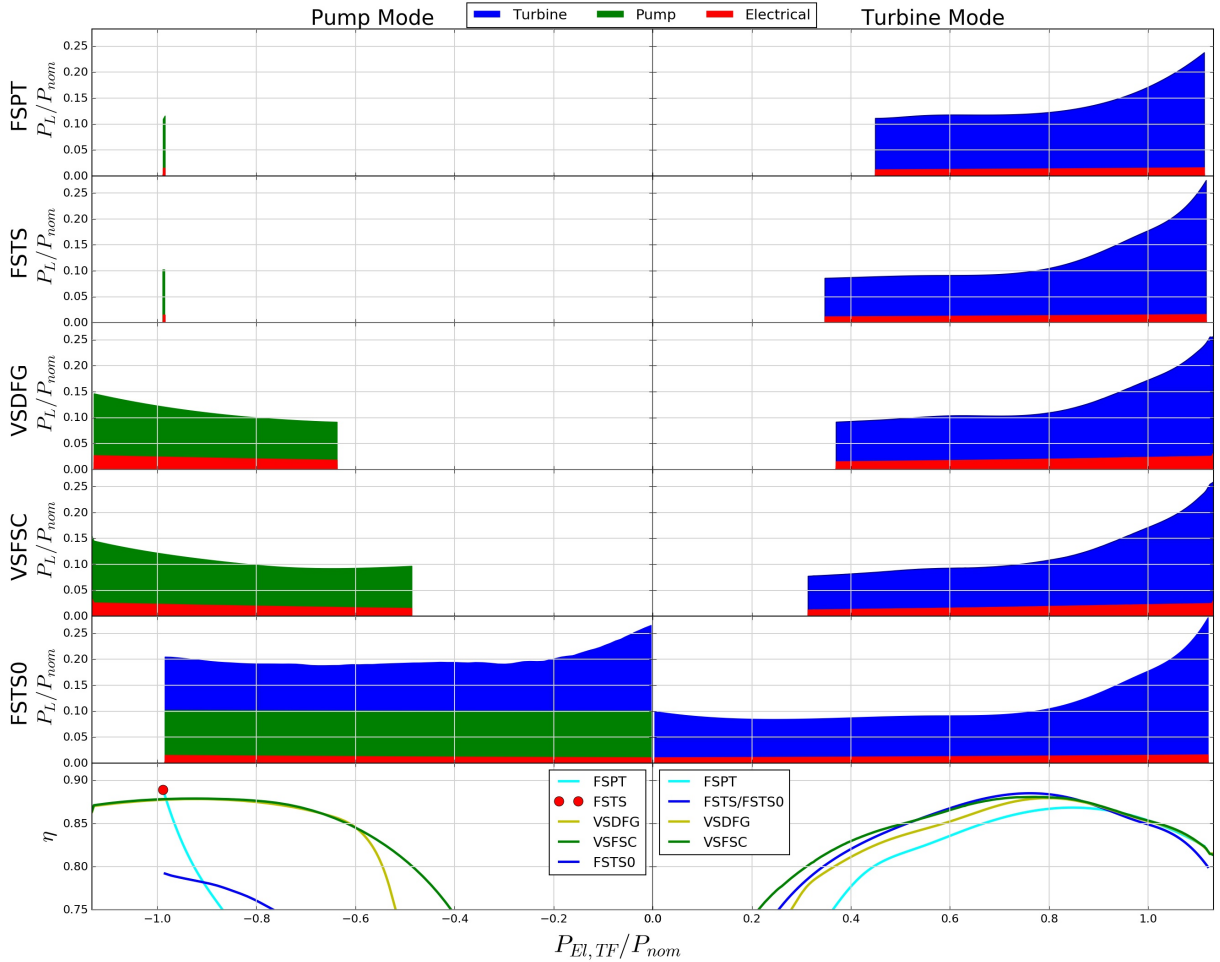

Figure 2.2.: Electrical losses, pump losses, turbine losses and plant efficiency trends for all investigated schemes

2.3. Influence of Gross Head Variation on Losses

Previous outlined losses were related to a constant gross head. Nevertheless, the gross head of PSPs varies. Therefore, the efficiency (lowermost row of figure 2.2) is evaluated for several values between the minimum and maximum gross head. As a result, an efficiency dependence on power output and gross head value is pictured in figure 2.3. Colour coded areas represent operating ranges for the different PSPs in pump and turbine mode. As mentioned in section 2.1, the operating range is limited by a minimum hydraulic efficiency of 80 %. The red area indicates high efficiency values, while low values are depicted in blue. Magenta areas are operating ranges with hydraulic efficiency values below 80 %. This area is permitted only for the FSTS0 scheme.

Considering the turbine mode, a similar behaviour for all schemes can be seen. An operation with rather high efficiency is possible within a wide range of head and power. The FSPT scheme is operating with its highest possible efficiency at high head values. A high head value reduce the unit speed value (equation: 2.1) and thereby moves the operating line closer towards the BEP (figure 2.1). Variable speed schemes such as the VSDFG and VSFSC schemes are able to compensate the design trade off, causing lower efficiency values for the FSPT scheme, by varying the speed. Due to the speed variation, the efficiency values regarding head and power values increase and thus widen the operating range. According to equation 2.1, these two schemes resemble one another concerning high head values, since relatively high speed values are required to operate close to the highest possible efficiency. For high efficient power generation at declining head values, declining speed values are required as well. The VSDFG scheme is able to follow this request only in a restricted manner since at some point it reaches its lower speed limit. As there are no speed limits, the VSFSC scheme is able to offer high efficiency values and a wide operating range also at low head values. The FSTS and FSTS0 schemes have, as mentioned in section 2.2, no design trade offs and no converter. This results in the highest efficiency values at nominal head and power. The efficiency gradient is higher than in the case of the VSFSC scheme since no speed adjustment is possible. The advantage of higher peak efficiency in combination with the disadvantage of the steeper efficiency gradient make the 80 % limited operating range of the FSTS appear almost the same size as one of the VSFSC scheme. The low head - high power areas are outside the operating range for all schemes, because the hydraulic power is too weak to generate the required electrical power. Even with fully opened GVs and optimal speed, the turbine is not able to generate a high power output.

Considering the pump mode, the most obvious feature is that one head value only offers one power value for the FSPT and FSTS schemes, while several power values are possible for the other schemes. Considering the FSPT and FSTS schemes, a linear relation between power and head would appear in case the hydraulic power would be printed on the ordinate. However, the power output also takes into account the plant efficiency and thereby distorts the relation. The VSDFG and VSFSC schemes' characteristics are both in pump mode and turbine mode very similar. It can be seen that the minimum pump power for the VSFSC scheme increases with growing head values. Bearing in mind figure 2.1, it is seen that an increasing head, which causes a decreasing absolute unit speed, moves the entire operating line towards pump instability and thereby lowers the efficiency values. The same holds true for the VSDFG scheme, except that for lower head values, the limitation is not the 80 % efficiency boundary, but the speed limit. Therefore, a small piece of the operating range, compared to the VSFSC scheme, is forfeited at lower head values. With respect to the upper

pump power limit, it is seen that the speed variability allows the variable speed schemes to reach their maximum pump power output along the entire head range, which is different to the turbine mode. In this case, the limiting factors are the power limit of the generator and transformer, respectively. The FSTS0 scheme has the same characteristic as the FSTS scheme, but the characteristic can be moved seamlessly towards lower pump power values by applying the HSC. It has to be mentioned that for the case of the HSC, even plant efficiency values lower than zero percent may appear. Low pump power output in HSC operation requires high pump and high turbine power output and thereby causes high losses in the turbine as well as in the pump. This means that for low pump power output values, the flow direction in the common WW is towards the TW even if little power is extracted from the PS. The edge between flow towards HW and flow towards TW is indicated by the line of zero efficiency in the FSTS0 scheme pump mode graph.

In terms of a round-trip, consisting of pumping at low energy prices during the night and turbining at high energy prices during the day [62], a round-trip efficiency of up to 80 % is reachable [63]. This value strongly depends on the chosen operating points. An off-design operation, as in the case of the FSTS0 scheme, can reduce this value dramatically.
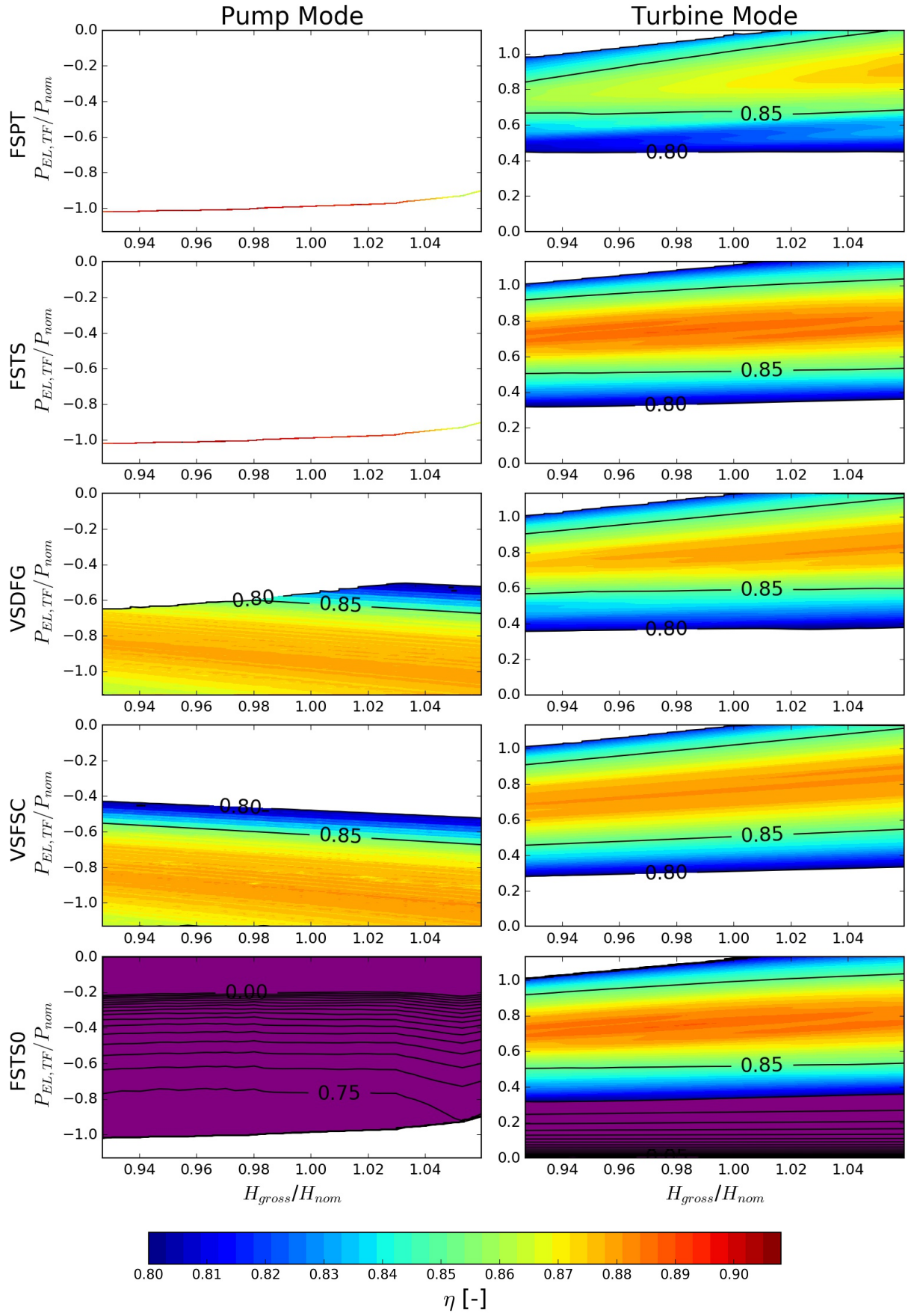
Figure 2.3.: Plant efficiency in dependence of power output and gross head

3. Economics

In this chapter, the form of operation of PSP schemes which generates the highest income is determined. By comparing the income with the installation and maintenance costs, the profitability of PSPs can be estimated. This kind of investigation does not only cover PSPs, but also Lithium-Ion-Batteries, since it is currently a hot topic if batteries will either replace or supplement PSPs. The economic examination is also of major importance for the subsequent investigation of the PSP's transient behaviour. The transient behaviour of PSPs depends strongly on the power reference signal which, in turn, depends on the kind of operation which is assumed to gain maximum income. Round-trip operation, for example, requires few operating point chances, while delivering balancing energy requires the plant to react on unpredictable power reference signals.

3.1. Energy Market Situation

So far, the third millennium is characterized by an expansion of new renewable electricity generation such as wind and solar [64], [65]. Beside the impact on PS stability, as mentioned in subsection 1.3.1, new renewable energies further change the situation on the energy market. In this section, the energy markets of section 1.2 are looked at in a more detailed manner.

3.1.1. Power Derivatives Market

The power derivatives market contracts plants to generate energy for time frames between one week and six years. Typically, it is used for base load plants [66]. Since the energy price is relatively low at the power derivatives market, and since storage technologies are not used for base load purposes, this market is irrelevant for further investigations.

3.1.2. Day-Ahead Market

On the day-ahead market, the energy for the next day is traded. Due to the relatively high prices compared to the power derivatives market and the high price volatility on the day-ahead market, this market is optimal for storage technologies. Storage technologies thrive on the volatility of the energy price [67]. Figure 3.1 shows the yearly and hourly averaged day-ahead market price spread on the combined Austrian and German market for the years 2002 to 2016. The hourly averaged day-ahead market price spread for one year is defined as hourly averaged day-ahead market price spread, reduced by its minimum value. A clearly declining trend of the spread can be observed since 2008. Furthermore, two local minima regarding to the year 2015 can be observed - one during the early morning hours and one approximately at noon. The early morning minima is caused by the low consumption of

energy, while the high noon local minima is caused due to the high penetration of the PS by solar generation. During the years 2002 to 2008, the price was highest at noon, but this price maxima has reduced in the following years. Due to the rapid growth of solar energy, more power is now available at noon and therefore the price is reduced. This effect is called peak shaving [68], [69]. According to [70], the current penetration of around five percent solar power is the worst in terms of price spread. A further increase of the installed solar capacity will increase the price spread and thereby the profitability of storages.
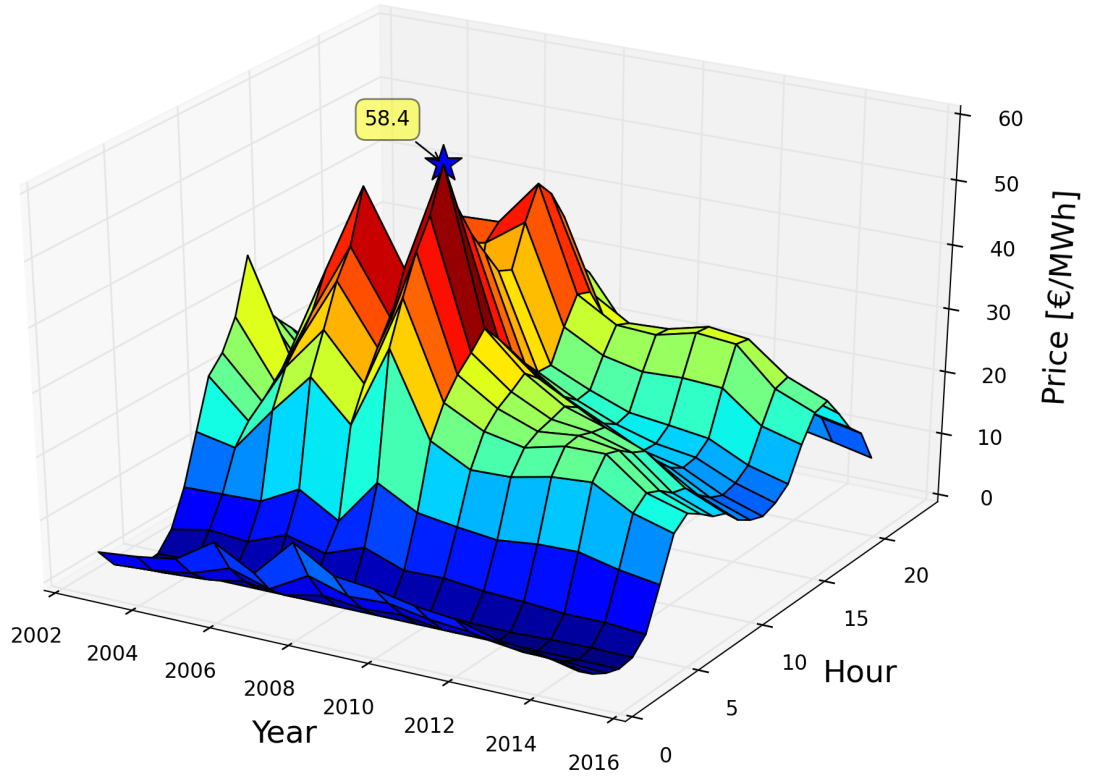
Figure 3.1.: Electricity price spread on the day-ahead market (data: [71])

Beside the essential energy price spread for storage technologies, the price has also declined ([72], [73]), as visible in figure 3.2. The sharp decline of price and consumption from 2008 to 2009 is caused by the economic crisis. The general downward trend in consumption is due to increasing efficiency of lightning, heating and household applications. The general downward trend in the price is due to the reduced consumption and increased installed capacity [74], [75]. Furthermore, the installed capacity of solar and wind power is increasing, leading to excess supply which reduces the electricity price as well [65].
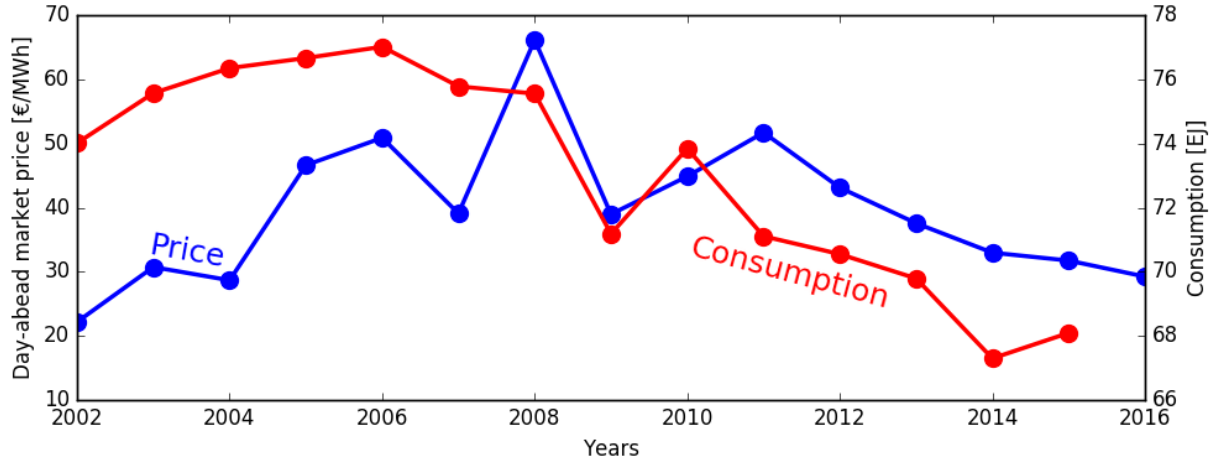
Figure 3.2.: Declining trend of Austrian-German day-ahead market price and declining energy consumption within the European Union (data: [71], [75])

The influence of increasing new renewable energy generation on the electricity price is shown in figure 3.3. On the x-axis, the increasing new renewable power generation is plotted, the y-axis presents offered and demanded power, and the z-axis shows the resulting price. The offered power trend (bidding) accrues by stringing together the offered generation power in an ascending order. In case no new renewables are installed, the cheapest type of plants is the nuclear power plant, followed by lignite, hard coal, natural gas and fuel oil plants. The point of intersection of demand and bidding defines the in fact market price. If there was no renewable energy generation the market price would be about 87 €/MWh.

In case 15 GW new renewable energy is installed, the offered price trend moves 15 GW towards higher power values. The fixed feed-in tariffs of wind and solar power allow them to offer power at no additional cost. This means that wind and solar power are placed on the lower end of the y-axis. Assuming the same amount for demand, the demand intersects the bidding curve at a lower price (72 €/MWh).

This price is further reduced if 35 GW instead of 15 GW new renewables are installed. The higher amount of new renewables moves the conventional plants further towards higher power values. Thereby, the intersection point of demand and bidding declines to lower prices. The conventional plants are pushed so far towards higher power values that all natural gas plants fall out of the generation mix. Thereby, the price also falls to a value of 41 €/MWh.
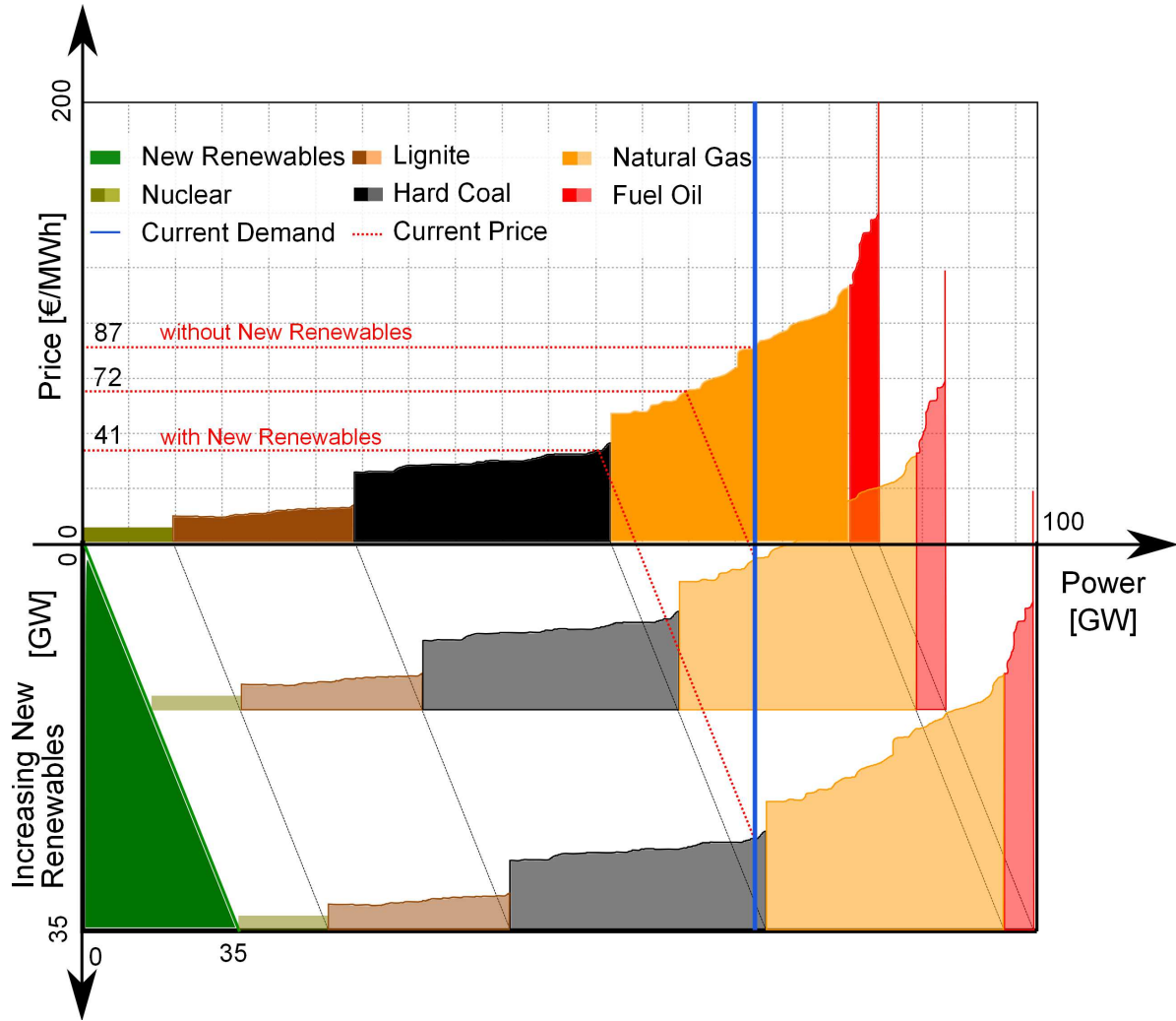
Figure 3.3.: Influence of new renewable energy on the day-ahead market price (based on: [76])

3.1.3. Intraday Market

The intraday market allows the trading of energy on the same day it is delivered. The price is higher than at the day-ahead market, but the volume is relatively small [77]. Due to the small volume, this market is also not taken into account for further investigations.

3.1.4. Balancing Energy Market

Beside the day-ahead market, the balancing energy market is an opportunity for PSPs to generate income. Data for the balancing energy market are provided by [78]. As explained in section 1.2, three different balancing energy types exist. While the primary control market (PCM) is easily designed as there is a single price for providing a power range, the so called primary control power (PCP), the secondary control market (SCM), is subdivided into 12 sections. While in the case of the PCM, the offered power range has to be provided in positive as well as in negative directions, a positive and negative band are tendered separately as positive secondary control power (SCP_p) and negative secondary control power (SCP_n) in

case of the SCM. Positive control power means that the generated power is increased and negative control power is tantamount to a reduction of the generated power. Beside payment for a provided power range, the SCM offers payment for effectively delivered positive or negative secondary control work (SCW_p, SCW_n). Apart from this, power and work are further subdivided into peak, off peak and weekend prices. Peak hours are from Monday to Friday from 8 am to 8 pm, off peak hours are from Monday to Friday between 8 pm and 8 am and the entire Saturday and Sunday are covered by weekend prices. The economic situation at the balancing energy market is shown in figure 3.4. Beside the prices of PCP, SCP_p, SCP_n, SCW_p and SCW_n, indicated by the additional subscript $_P$, the in fact value of the requested PCP and SCP is pictured. Requested power values are indicated by the additional subscript $_V$.

Considering the PCP_P, a slowly declining trend is seen. There are also peaks at the end of each year notable. A possible explanation is that, at the end of the year, the consumption is low, therefore the generating units are few as well. This causes less competition and is therefore accompanied by higher prices. The PCP_V shows a fairly continuous behaviour. The increase of the delivered amount of PCP during July 2013 is caused by the addition of the Switzerland control area to the combined Austrian- German area [79]. It should also be mentioned that the delivered PCP within Austria exceeds the tendered amount of about 67 MW at some points. On May 28th 2015, 2 pm, for example, the quarter hourly averaged PCP reached a value of 115 MW (this peak appears in the figure strongly reduced due to the hourly averaging). Referring to the SCP_P, it can be seen that off peak, peak and weekend are widely congruent for the positive power as well as for the negative. Both trends show a declining behaviour and peaks at the end of the year, which is similar to the PCP_P. The SCW_P trends are very similar for off peak, peak and weekend. The SCW_P price trends show a general tendency towards higher prices, but become quite volatile after mid 2015.

The SCP_V does not show any noteworthy behaviour. The requested amount of delivered SCP is widely homogeneous.
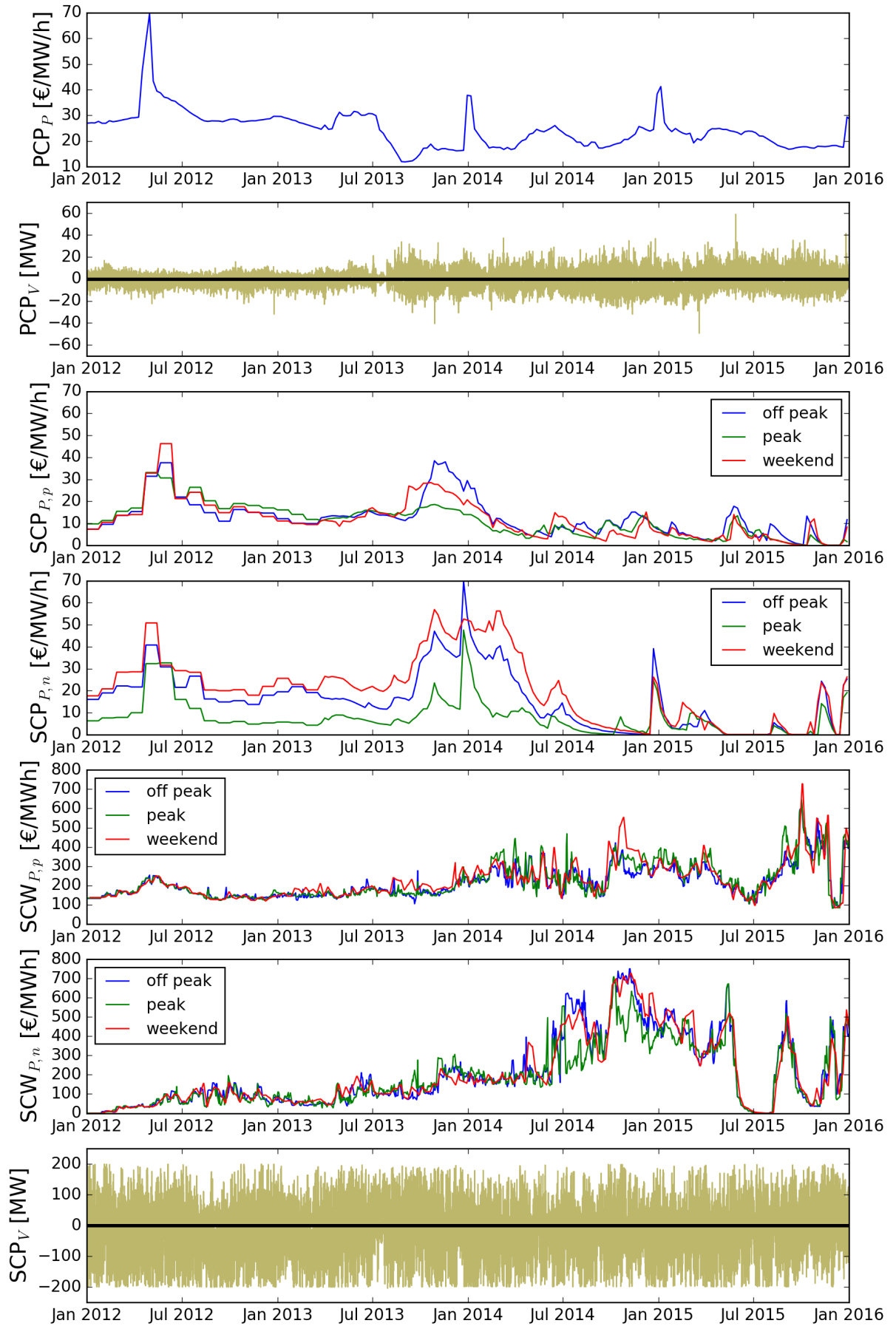
Figure 3.4.: Prices and retrieval of balancing energy

3.2. Income Maximization

Based on electricity market prices and the operating ranges and loss models of chapter 2, an optimization problem is developed in order to maximize the income of the different PSP schemes within a time range of four years. It has been decided to use the time range of 2012 to 2016, since sufficient data is provided for this time period (figures 3.1, 3.2 and 3.4). The following model simplifications and restrictions are made in order to enable an economical investigation:

- A pre-qualification is required in order to deliver balancing energy. It is assumed, that all schemes are able to fulfil the requirements.

- The inertial regulation by GVs causes differences between the power reference signal and actual power output. These deviations reduces the income. This income reduction is neglected initially, nevertheless, an estimation of the deviations follows in subsection 4.3.4.

- Deviations of the power reference signal and the actual power output due to switchover between pump and turbine mode, and vice versa, are neglected.

- Time ranges of day-ahead market and balancing energy markets diverge. For the following investigation, it is assumed that day-ahead power and balancing power are tendered for the same time range of one day.

- According to [12], one generating unit is allowed to deliver not more than 90 MW primary control power.

- The usage of the PS amounts to 5 €/MWh for generated as well as consumed energy ([80],[81]).

- Balancing power is delivered by merit order ranking. In the optimization case, it is assumed that all bidders offer at the same price and thereby share the delivered power and income proportionally.

- In order to be able to offer balancing power in a sufficient amount of time, all units delivering balancing power have to operate in pump or turbine mode. The rapid provision of balancing power makes a standstill impossible since the start-up time would exceed the time frame in which the balancing power has to be provided.

3.2.1. Optimization Model

The scheme of the optimization process is illustrated in figure 3.5. Since it is assumed that each market announces daily and the prices for the following days are unknown, the optimization case considers each day separately and passes the four years in one-day loops. For the initial day ($d = 0$), the head value can be chosen arbitrarily. Depending on the initial head value of one day ($H_I(d)$), the minimum and maximum reachable power values ($P_{min}(d)$, $P_{max}(d)$) on the considered day are determined in the *Operating range* block. The initial head value and power extrema are passed on to the *Optimization* block.

The optimization of the income for one day is enabled by given limitations of the power and the initial head value which is combined with the hourly resolved energy prices of the considered day. As a result the hourly resolved offered power ($P_O(d, h)$) can be determined.

The offered power and the initial head value are passed on to the *Determination* block.

The power range offered to the balancing energy market in combination with the actually required power ($P_R(d, h)$) allows the calculation of the actual generated power in dependence on time ($P_{act}(d, h)$), the actual head ($H(d, h)$) and the actual income ($I(d, h)$). The head value at the end of one day is set as the head value at the beginning of the next day and the calculation of the next day starts.
The three blocks *Operating range*, *Optimization* and *Determination* will be explained separately in the following subsections.
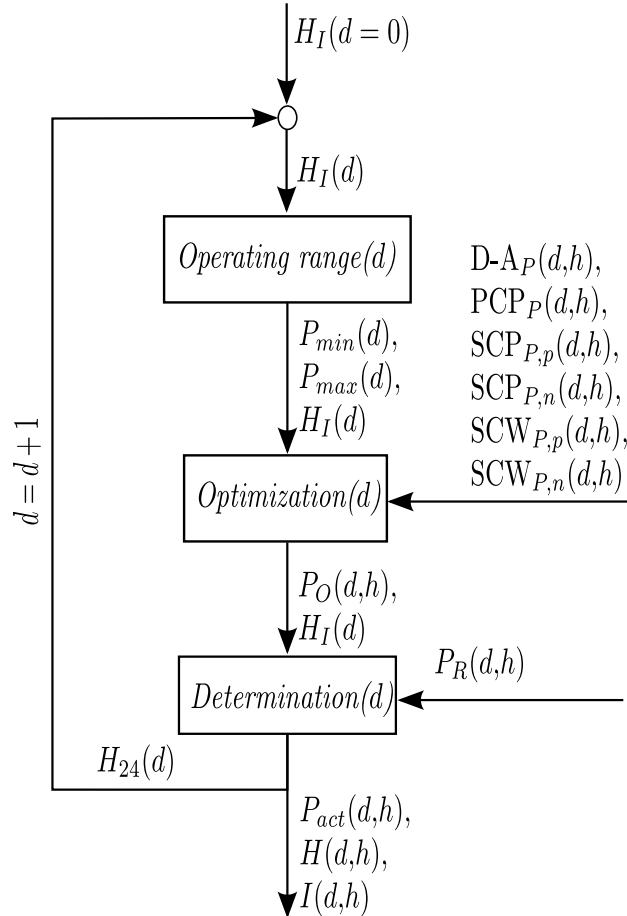
Figure 3.5.: Income maximization scheme for PSPs

3.2.2. Operating Range Block

The determination of the operating range for the VSDFG scheme is illustrated in figure 3.6. The red lines indicate the initial head value at one day. Additional red lines show the minimum possible head value during one day as result of one day turbining and the maximum possible head value during one day as reached in case of an entire day of pumping. Knowing the entire possible head range, the related power range can be determined. The maximum possible power range is defined by the rectangle between minimum and maximum head with the widest spread in power direction without breaching the operating range (colour coded surface in the figure).
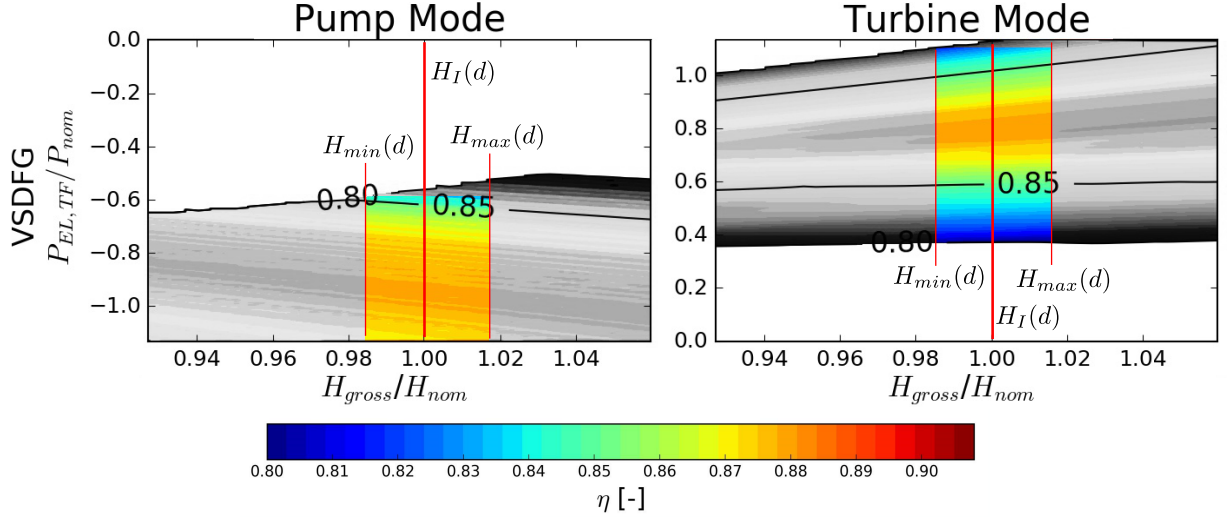
Figure 3.6.: Determination of widest possible power band

3.2.3. Optimization Block

The operational planning for one day takes place in the *Optimization* block of figure 3.5. Based on power limitations, initial head value and market prices, the power trend $(P_O(d,h))$ to be offered for one day is determined. It is necessary to couple individual days, as otherwise, the maximum possible turbine power would be offered each day until the HW is drained. In order to do so, the daily income has to be extended by about a gross head proportional additive penalty term. The applied target function (TF) for one day is given by equation 3.1. It represents the sum of the income, the PS fee (I_{PS}) and the head penalty $(I_{H_{gross}})$ in order to prevent HW draining. The income is separated into income from the day-ahead market (I_{D-A}), the primary control market (I_{PCP}) and the summed up income of the secondary control market (I_{SCP}) including $I_{SCP_{P,p}}$, $I_{SCP_{P,n}}$, $I_{SCW_{P,p}}$, $I_{SCW_{P,n}}$. In order to maximize the income, the optimization's target has to be to maximize the TF.

$$TF = I_{D-A} + I_{PCP} + I_{SCP} - I_{PS} + I_{H_{gross}} \tag{3.1}$$

The income within the entire time range is the sum of all daily TFs minus the sum of all head penalties (equation 3.2).

$$I = \sum_{i=1}^{n} TF - \sum_{i=1}^{n} I_{H_{gross}} \tag{3.2}$$

Equation 3.3 shows the structure of the gross head penalty term. The term is designed in such a way, that a deviation of the actual gross head $(H_{gross}(h))$ from a gross head reference value $(H_{gross,ref})$ results in an additional penalty term. In the case of high day-ahead prices, the possible income from the day-ahead market exceeds the head penalty and the storage is depleted. In the case of low day-ahead prices, the head penalty outnumbers the day-ahead market income and the storage is filled. The power term consists of the power offered on the day-ahead market and an estimated balancing power. For optimization, the balancing power is gauged by the ratio of tendered and delivered balancing power between 2012 and 2016. This factor is calculated for each type of balancing power. Within the four years considered,

five percent primary control power, 11 % positive secondary control power and 19 % negative secondary control power have been retrieved.

$$I_{H_{gross}} = \sum_h ((H_{gross}(h) - H_{gross,ref}) \cdot k \cdot P(h)) \tag{3.3}$$

Gradients (k) and gross head reference values ($H_{gross,ref}$) have been estimated empirically and are presented in table 3.1.

	FSPT	FSTS	VSDFG	VSFSC	FSTS0
k	0.5	0.5	0.25	0.25	2.2
$H_{gross,ref}$	1.25	1.25	1.5	1.5	1.05

Table 3.1.: Parameter of gross head penalty

3.2.4. Determination Block

Based on the offered power ($P_O(d,h)$) in combination with the control power which is in fact required ($P_R(d,h)$), the actual power output ($P_{act}(d,h)$), head ($H(d,h)$) and income ($I(d,h)$) can be determined. The actual income diverges from the optimized one since the income of SCW depends on the actually delivered energy, which is unknown at the time of optimization. A similar effect occurs for the head value. The actual head value at the end of one day depends on the in fact delivered power. As the actual head is determined at the end of one day, the loop switches to the next day, wherein the calculated head value at the end of the previous day is used as initial head value for the following day.

3.3. Income Orientated Operation of Different Pumped-Storage Plant Schemes

3.3.1. Operating Points

Once the optimization model is developed, simulations can be carried out in order to maximize the income of the PSPs. Income investigation results of one of the four example years are shown in figure 3.7. The figure shows the results of the year 2012. While the first row indicates the trend of the gross head values, the bottom rows depict operating points in a quarter-hourly resolution for each scheme, respectively. As usual, turbine operation is indicated by positive values, while negative values represent pump mode. The following conclusions are drawn from figure 3.7:

- All schemes make extensive use of the gross head range (minimum ratio between gross head and nominal head: 0.928, maximum ratio between gross head and nominal head: 1.06).

- Since the FSTS0 scheme anticipates on the day-ahead market only because of storage management, its gross head trend varies from those of the other schemes.

- In the head trends of the FSPT, FSTS, VSDFG and VSFSC schemes, weekends and holidays may be spotted. Due to lower day-ahead market prices, the plant operates in pump mode and thereby increases the gross head value.

- The power trends generally have three different forms:

  - The FSPT and FSTS schemes do not have an operating range in pump mode, and therefore do not offer balancing energy, which enables them to operate at standstill since no rapid changes of the operating point are required.

  - The VSDFG and VSFSC schemes do have an operating range in pump as well as in turbine mode. Therefore, they may offer balancing energy what further permits operation in standstill since fast changes of the operation point are required.

  - The FSTS0 scheme has an continuous operating range from maximum pump to maximum turbine operation. This makes it possible to offer the whole operating range to the balancing energy market and therefore, the day-ahead market has the minor role of storage management.

- Power trends of the FSPT and FSTS schemes indicate that the influence of day-ahead market price volatility outdo the influence of efficiency volatility. This is visible from the marked operating points in turbine operation. They are either at the minimum or at maximum turbine power output, but rarely centred within the turbine operating range, except when the minimum gross head value is reached and no higher turbine power is permitted. This means, the operating point with highest efficiency is omitted in favour of points with lower efficiency, because the day-ahead market price spread is much higher than the efficiency span.

- In contrast to the other schemes, the FSTS0 scheme shows an operation around zero power output. As shown in the lowermost graph of figure 2.2, the efficiency is lowest for little pump and turbine power respectively. Deviations from zero power output are caused by delivering balancing energy or storage management actions.

- The round-trip efficiency values can be calculated by forming the ratio between turbine and pump energy. Strictly speaking this calculation is only applicable for the same initial and final gross head value. Nevertheless, the influence of different gross head values diminishes with increasing time and is therefore neglected for the considered year. The round-trip efficiency of the FSPT, FSTS, VSDFG, VSFSC and FSTS0 schemes are thus 75 %, 75 %, 76 %, 74 % and 42 %, respectively. While the schemes with the lower efficiency limit of 80 % have a relatively high round-trip efficiency of about 75 %, the FSTS0 scheme's round-trip efficiency is much lower. The operating point concentration around the zero power output area, where the efficiency is lowest, causes this small round-trip efficiency value.
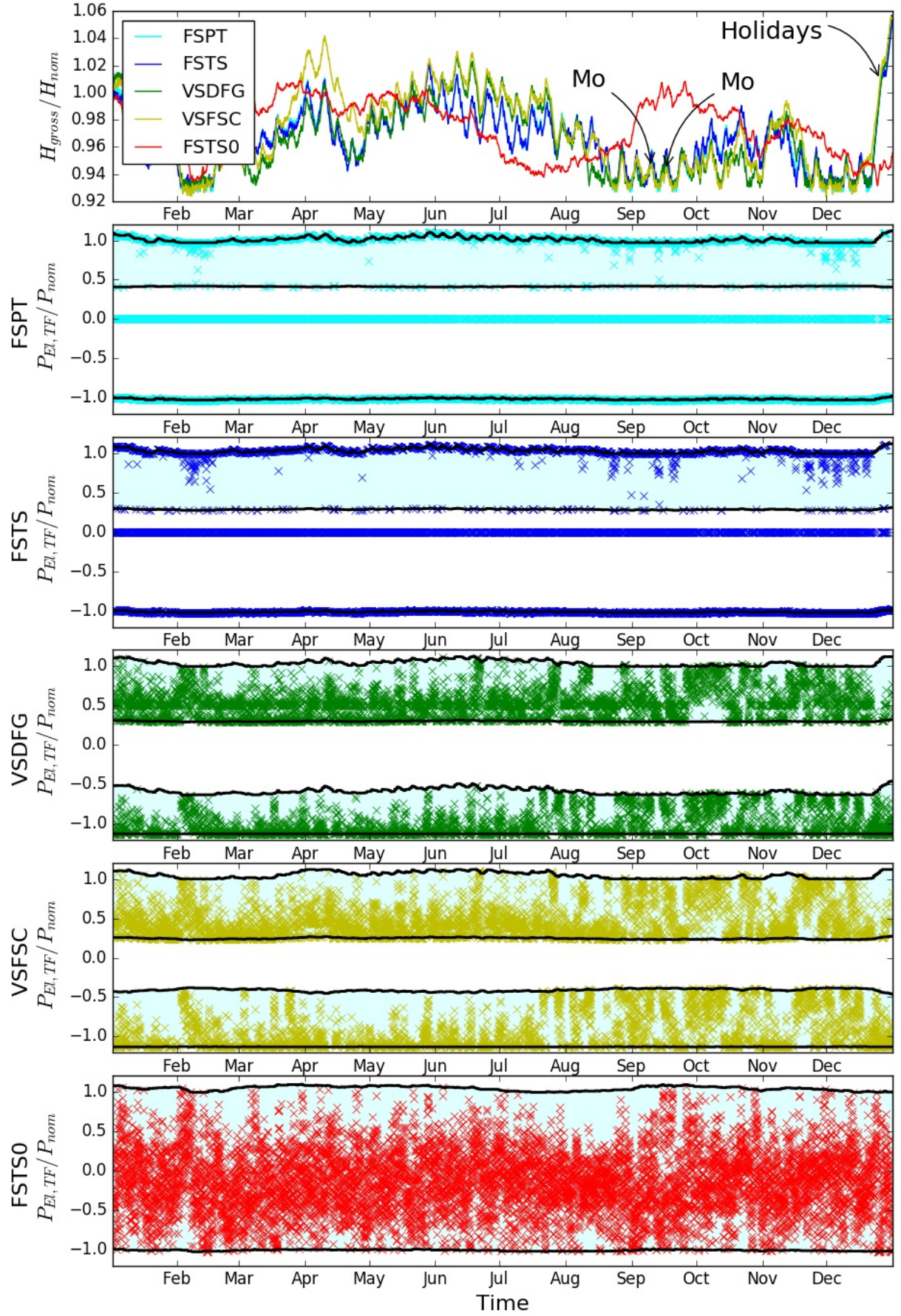
Figure 3.7.: Storage level and power output values with respect to time for the year 2012

3.3.2. Income of One-Week Storage Schemes

Economic results belonging to operation as presented in figure 3.7, are pictured in figure 3.8. The figure shows income dependent on the plant scheme, separated in sections as described in section 3.1 including the PS fee and total income. As can be seen, income is only generated on the day-ahead and secondary control market. The PCM delivers zero income since the payment is higher on the SCM. It is further visible that income from the SCM is much higher than from the day-ahead market.
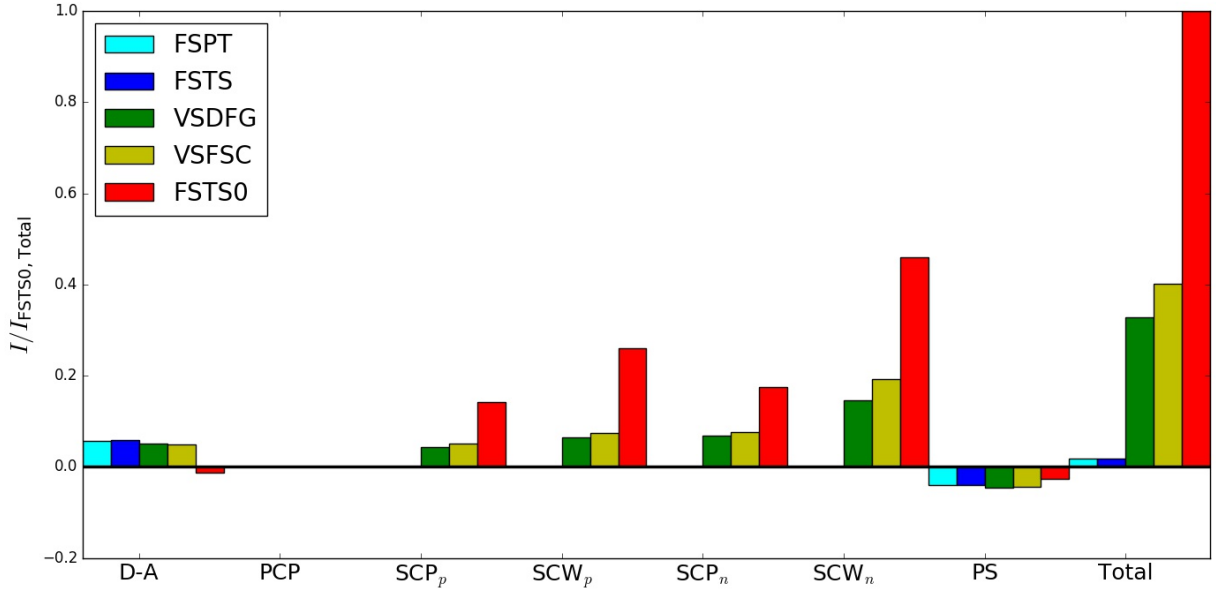
Figure 3.8.: Income of one-week storage PSPs depending on type and energy market including PS fee and total income

Noteworthy aspects of figure 3.8 are:

- Total income is proportional to the smallest continuous operating range (pump or turbine mode).

- On the day-ahead market, the FSPT and FSTS schemes have the best performance, followed by the VSDFG and VSFSC schemes. The FSTS0 scheme possesses the worst behaviour with respect to the day-ahead market. This is because the FSPT and FSTS schemes only participate on the day-ahead market and therefore, the operation optimization equals the maximization of the day-ahead market income. The VSDFG and VSFSC schemes participate on the SCM as well. Disadvantageous day-ahead market prices have to be dealt with since no control power can be generated during a standstill, and therefore, standstill is forbidden. Negative income has to be accepted since the main share of income results from the SCM and the day-ahead market is only used to fill up the HW in case of low gross head values.

- Income from the SCM increases with the potential offered operating range. Therefore, income of the FSTS0 scheme outperforms those of the VSDFG and VSFSC schemes by a factor of approximately 2.5.

- Comparing SCP and SCW, it is shown that income from SCW is higher than from SCP.

- Total income indicates that an economic plant operation without participation on the balancing energy market is currently not possible.

- Income gained on the day-ahead market is almost entirely compensated by PS fee as visible for the FSPT and FSTS schemes.

3.4. Investment Costs

The investment costs for different storage schemes are pictured in figure 3.9. As can be seen, the costs for PSP schemes diverge only by approximately 10 %. The small difference between the PSP schemes can be explained by the similar prices for the majority of the project (HW, WW, cavern (CAV) and engineering (ENG)). Different schemes only require a different hydraulic equipment (HYDR), MG, electrical equipment (EPS) and controlling (CON). Since these parts only cause about 25% of the project costs, a variation of these costs does not cause crucial differences in the entire project costs. The battery for the considered two - days storage costs approximately five times more in 2020 and more than ten times more in 2017 than the PSPs. The main difference between battery and PSPs in terms of investment costs is that power and capacity costs are decoupled in case of the PSPs and coupled for battery storages. This means that for a different storage capacity of a PSP, only the price of the HW varies, but the other sections cost the same. Vice versa, in case of a different power, the price of all other sections vary while the price of the HW stays the same. For battery storage applications, there is a fairly fixed ratio between capacity and power and just little variation is possible indicated by the little range of specific power and specific energy in [82]. Therefore, a change in power or capacity influences each one another and the entire storage costs (TOT) change.

(a) FSPT   (b) FSTS   (c) VSDFG

(d) VSFSC   (e) FSTS0   (f) Battery
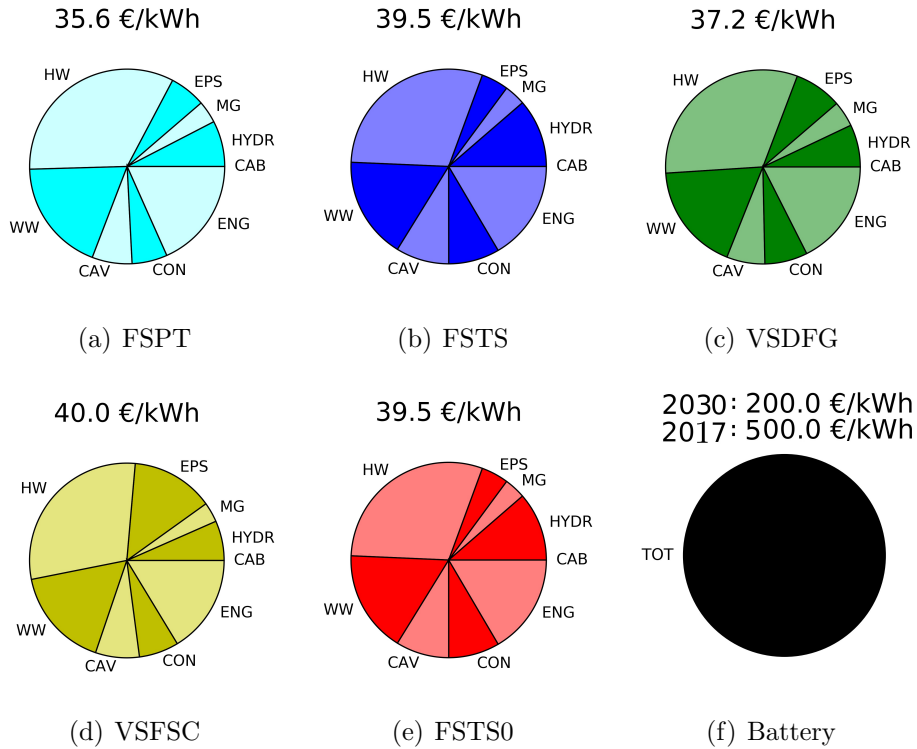
Figure 3.9.: Investment costs of different storage technologies

3.5. Profitability

Up to this point, the losses in combination with the energy markets were used in order to investigate the threshold of the income. A profitable plant requires a sufficient high ratio between income and costs. Within this section, income, investment costs and operating and maintenance costs are investigated for PSPs and battery storage. Since battery storages are more competitive in low capacity applications, a smaller storage (two-days storage) is chosen [83].

3.5.1. Comparison of One-Week and Two-Days Storage

As mentioned in section 3.5, the storage size is changed from a one-week storage to a two-days storage in order to generate operating conditions closer to those of battery storage applications. In this subsection, the influence of the storage capacity is investigated. Due to the high computational cost, only the income maximization of the two-days storage for the FSTS0 scheme and the VSFSC scheme are carried out. Both uppermost graphs of figure 3.10 show the head trends of the same scheme with different storage capacity. It can be seen that the general trend is the same, but the two-days storages show a much higher volatility. With respect to the addressed operating points, it is visible that the storage capacity has almost no influence. The operating points mostly coincide. The influence of the higher volatility of the smaller storage capacity is also visible in form of the shape of the operating range limiting lines consisting in minimum and maximum of pump and turbine power (black). Since the operating range varies with the head value, smaller storage capacities vary with the head trend, resulting in a more stepped form of the operating range limiting lines.
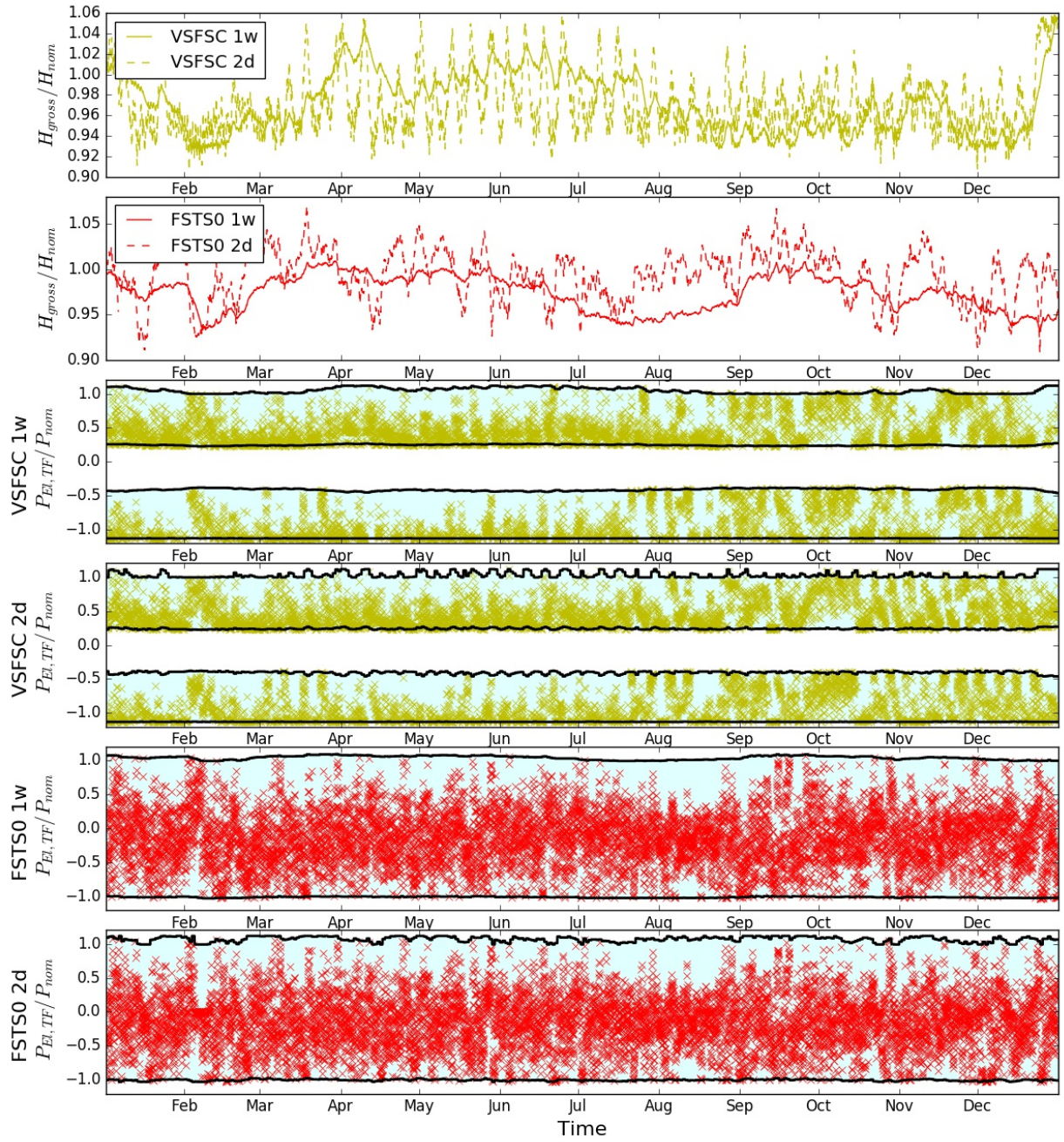
Figure 3.10.: Comparison of storage management of the year 2012 for one-week and two-days storages

It is assumed that a changed storage capacity influences the income since smaller storage capacities require more effort to maintain operation within head limitations. The influence of the storage capacity on the income is illustrated in figure 3.11. Except for the negative SCW of the VSFSC scheme, no significant difference between the two different storage capacities can be seen.
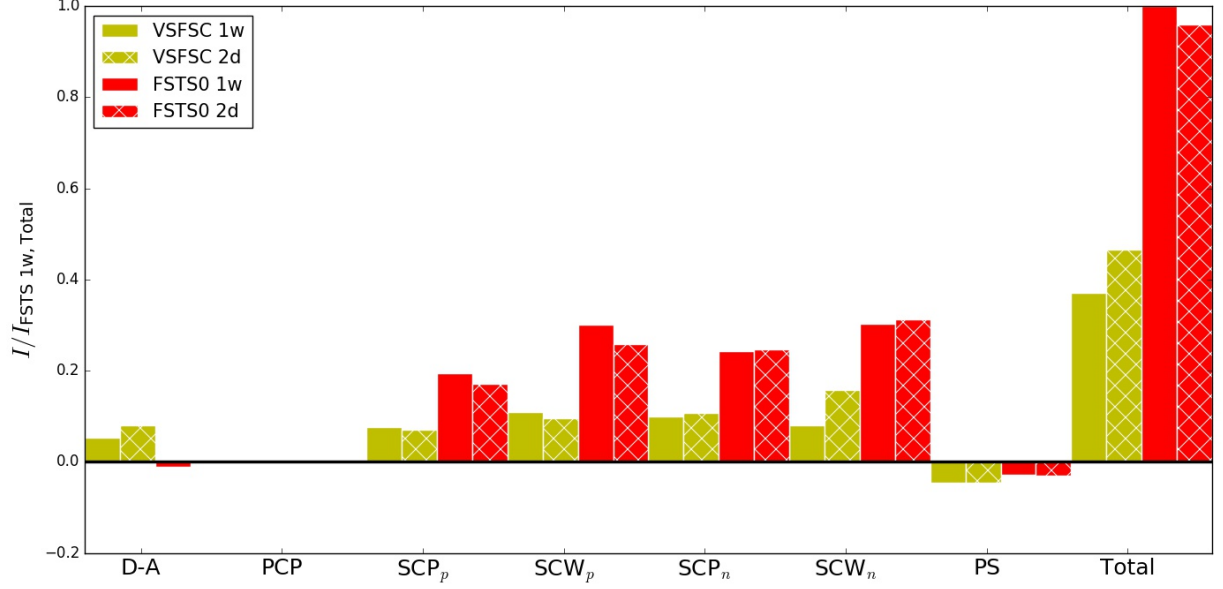
Figure 3.11.: Comparison of one-week and two-days storage capacity income

3.5.2. Income of Two-Days Storage

Since the reduction from a one-week to a two-days storage capacity does not show changes on the income side of the VSFSC and FSTS0 schemes, the income of the one-week storage is used for the two-days storage from now on. The income of the battery storage is calculated analogous to the FSTS0 scheme with the difference of a head and power independent efficiency value of 93 %. As result of the higher and constant efficiency value, additional income of 43 % for the battery storage is gained in comparison to the FSTS0 scheme.

3.5.3. Profits

For the calculation of profits, the annuity method is used [84]. The lifetime is assumed to be 60 years for PSPs and 20 years for batteries. The difference to the values given in table 3.2 is caused by the fact that future battery prices and lifetimes (year 2030) are investigated in this work. An interest rate of five percent and taxes on the income of 25 % are applied. For the yearly operating and maintenance, 2.25 % of the investment costs are assumed for PSPs [85] and zero percent for batteries. As mentioned in subsection 3.5.2, the efficiency of PSPs depends on power and head (figure 2.3), while for batteries, an efficiency of 93 % is chosen [86]. Additionally, a yearly availability of 90 % is assumed for PSPs, while battery storage applications are expect to operate at 100 % of the time. All parameters are summed up in table 1.2.

	FSPT	FSTS	VSDFG	VSFSC	FSTS0	Battery
Availability [%/a]	90	90	90	90	90	100
Lifetime [a]	60	60	60	60	60	20
Interest rate [%]	5	5	5	5	5	5
Taxes [%]	25	25	25	25	25	25
Maintenance [% of Invest.]	2.25	2.25	2.25	2.25	2.25	0
Efficiency [%]	80-91	80-91	80-91	80-91	0-91	93

Table 3.2.: Profitability parameters

The annual repayment is calculated by equation 3.4.

$$C_R = C_I \frac{q^{n_L} \cdot (q - 1)}{q^{n_L} - 1} \tag{3.4}$$

Therein, C_R is the annual repayment, C_I are the investment costs, q is the interest rate and n_L the lifetime. Operating and maintenance costs are calculated according to equation 3.5

$$C_m = C_I \cdot om \tag{3.5}$$

Therein, C_m are the absolute annual operating and maintenance costs and om are the operating and maintenance costs in percent of the investment costs. By subtracting the annual repayment (C_R) and the operating and maintenance costs (C_m) from the annual income reduced by 25 % taxes, the annual profit is calculated (see figure 3.12). It is hard to predict energy prices for 60 years, nevertheless, it is assumed that the income stays constant, presuming that the inflation and the declining energy price trend repeal each other.

Figure 3.12.: Profits of different PSP schemes including the battery storage

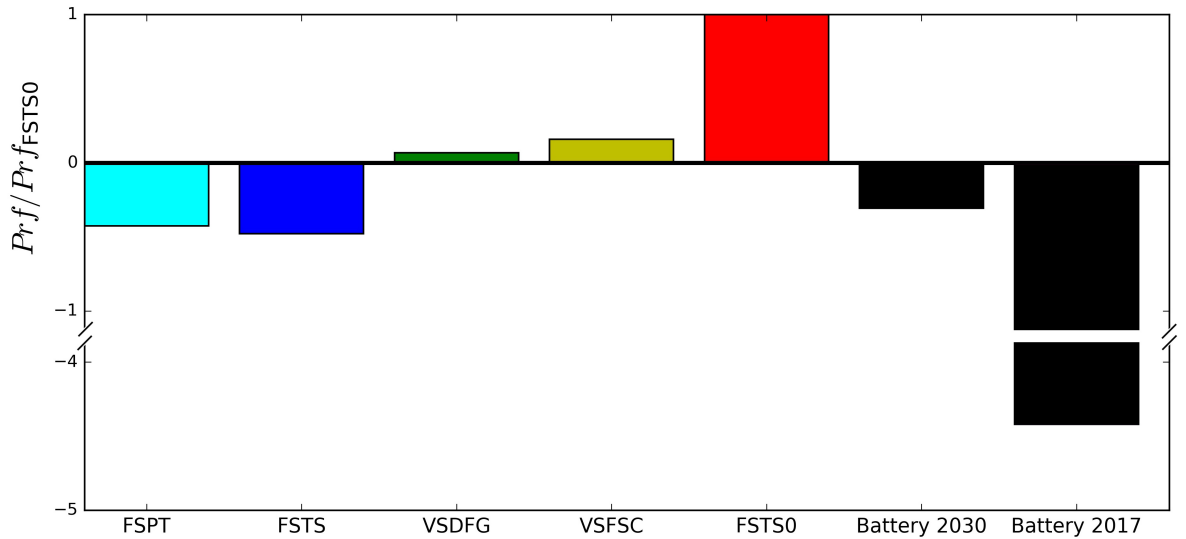It turns out that the FSTS0 scheme allows for the most lucrative operation. The VSDFG and VSFSC schemes also gain a small profit, while the FSPT scheme, the FSTS scheme and the battery generate losses. The FSPT scheme, even if it is the cheapest in construction, is victim

of its little income, since it does not participate on the balancing energy market. Something similar applies for the FSTS scheme, only that its economic losses are a little higher due to higher investment costs. The VSFSC scheme profit exceeds the VSDFG scheme profit, since its available operating range is slightly bigger. The FSTS0 scheme costs approximately the same as the other PSPs, its profit exceeds those of the other PSPs by far due to its operating range which is more than twice as big. The battery generates losses. Its income is higher than of all PSPs, but this is more than compensated by its high investment costs and low lifetime.

One further important factor for storage technologies, which has not been considered, is the construction time. For large scale PSPs, a construction time of about seven years is required, while battery storage applications can be built within a few hundred days. In addition to the construction time, an environmental impact assessment, which takes several years, is necessary for PSPs.

3.5.4. Parameter Study

In subsection 3.5.3, it is shown that, under the prevailing conditions, the FSTS0 scheme is the most profitable one. In this subsection, it is attempted to change parameters in such a way that battery storage becomes more profitable than PSPs. There are three parameters with a large impact on the profitability and which are widely variable: the ratio between capacity and power, lifetime and the investment costs.

Capacity-Power Ratio:

The specific power and specific energy of Lithium-Ion batteris call for short storage times [82]. Assuming that the income stays the same if the capacity is further reduced, batteries become more profitable than the FSTS0 scheme (point of intersection) when reducing the storage time from two days to 22 hours. For lower time spans, batteries are more profitable, for higher time spans the FSTS0 scheme.

Lifetime:

Lifetime is another uncertain parameter. Currently, the lifetime of batteries is approximated between 14 to 16 years. An improvement of up to 30 years is predicted for the year 2030 [87]. For the investigated case, even an increased lifetime of 60 years for batteries only leads to 60 % of the FSTS0 scheme's profitability. High annual repayment along with the interest rate restrict the positive effect of a longevity.

Price:

Currently, the price for battery storage systems is about €400 to 500 for one kWh [88]. A price of 200 €/kWh is assumed, since the battery prices are predicted to fall to 150 to 300 €/kWh until 2030 [89]. In order to exceed the profits of the FSTS0 scheme, the battery price has to fall to 97 €/kWh, which is lower than the possible production costs according to [89].

4. Transients

Declining day-ahead market price spreads force plant operators to participate on balancing energy markets. Participating on balancing energy markets is more challenging than participating on the day-ahead market in terms of flexibility. In contrast to the day-ahead market, where the operating point can be chosen and held at least for a quarter of an hour [90], the operating point in the case of balancing energy generation is not known previously. The operating point results from the PS frequency, schedule deviations, faults and electricity exchange with neighbouring countries [91]. As discussed in section 1.2, the time to reach an operating point is much shorter than in the case of the day-ahead market. Additionally, a good transient behaviour is required for the SCW income, since deviations between a power reference signal and the actual power output reduce the income of the plant operator.

The above mentioned challenges to generate balancing energy are reasons for investigating the transient behaviour and flexibility limits of PSPs. In this chapter, transient models are developed and validated with measurements, critical frequencies are determined, the start-up behaviour is examined, accuracy of following a power reference signal is investigated and PS faults are simulated and compensated by the different PSP schemes.

4.1. Transient Model

In order to investigate the transient behaviour of a PSP and the interaction with the PS, a sufficient accurate model has to be developed. This means, all systems required for a PSP operation have to be developed within one model. This model contains hydraulics, mechanics, electrics, control engineering and the PS itself. At this point, it has to be mentioned that the electrical model of the variable speed schemes has been developed mainly by a separate project at the Institute of Energy Systems and Electrical Drives ([92], [93]).

4.1.1. Systems effecting the transient Behaviour of the Power Plant

Hydraulic Equipment

The hydraulic equipment is of importance, as the inertia of the water column in the water way limits the flexibility of the power plant. A rapid change of the GVO causes a water hammer which may lead to damage on the plant or at least complicates the controlling of the power and speed, respectively. The connection between flow change and accompanied pressure change is explained in subsection 1.4.1. As example, an abrupt deceleration of a flow from five m/s to zero m/s within the reflection time would lead to an increase of the pressure about 50 bar.

Mechanical Equipment

The mechanical system and especially the inertia of its rotating assembly (impeller, shaft and generator rotor) are important as the inertia counteracts any kind of speed variation.

Electrical Equipment

The electrical equipment, in particular the application of converters, influences speed limits and the associated operating ranges. As mentioned above, a speed variation is counteract by the inertia of the rotating assembly. This means that a change of the speed value allows for the decoupling of the generated power and the power output. Generated power refers to the power generated by the impeller (P_{Me}), while power output refers to the power the motor-generator feeds into the PS ($P_{El,TF}$).

Control Strategy

As variable speed schemes have one more degree of freedom than fixed speed schemes, it is possible to apply different control strategies. Fast speed and fast power control are the two options used [94]. The two control variables are speed and power output, respectively. Whichever value is to be controlled within the shorter time frame, it is adjusted from the electrical side, while the slow controlled value is governed by the GVO.

Characteristics of the Power System

The characteristic of the PS is given by its inertia constant and its total generated power. With these two factors, the inertia of the entire PS can be determined and thereby, the damping behaviour with respect to power imbalances is given.

4.1.2. Fixed Speed Model

The model used for transient simulations of a fixed speed unit in turbine mode is shown in figure 4.1. The model consists of four blocks:

- **BEL:** Within this block, the optimal operating point in dependence on the gross head and the power output is determined as described in chapter 2.

- **Power Reference Signal:** This block optimizes the power reference signal in order to generate the highest income as described in chapter 3.

- **Transient:** Within this block, the transient simulation is carried out. The software used for transient simulations is SIMSEN ([95], [96]). In SIMSEN, all above mentioned properties (hydraulic, mechanical, electrical, control behaviour and PS) are modelled.

- **Automation:** It includes the *BEL*, *Power Reference Signal* and *Transient* block. This block allows for parameter change and the automated expiry of several optimizations and transient simulations.

The explained model structure makes transient simulations possible which only require basic input values such as energy market prices, stage of storage charge and PS frequency. These values are prepared by the *Automation* block for a chosen time range. After the input values have been used to generate a power reference signal in the *Power Reference Signal* block and the transient simulation has finished, the simulation may be ended or continued with the subsequent time range. Since the *BEL* block is independent of energy prices and the PS frequency, it has to be run only once for each gross head before the transient simulation. The structure is designed in such a way, that each block can be used independently, but also in any combination with other blocks. By deactivating one block, the absence of its output (e.g. P_{ref}, y_{ref}) has to be compensated manually. Furthermore, the power imbalance (P_{imb}) caused by a frequency control operation is not required. The transient block only requires a power reference signal to follow and, depending on the power output, optional GVO values. The value of the GVO is used for feed-forward controlling [97]. If not available, the model works as well, but the control behaviour is impaired. The controlling adjusts the GVO with the help of a proportional integral controller (PI) in order to equate the power output value to the currently required power value of the power reference signal. The task of the proportional integral differential controller (PID) is to set the operating point of the unit.

Figure 4.1.: Block diagram of fixed speed binary set PSP in turbine mode

The different pump mode can be seen in figure 4.2. As mentioned in section 2.1, a power regulation due to the GVs is not possible. This means that the GVs are placed at the position of maximum efficiency in order to minimize cavitation and, therefore, the power output results. It can be seen that no power output is delivered from the *Power Reference Signal* block to the transient model. The only use of this block is to indicate when the operation mode has to be changed in order to initiate the switchover process.
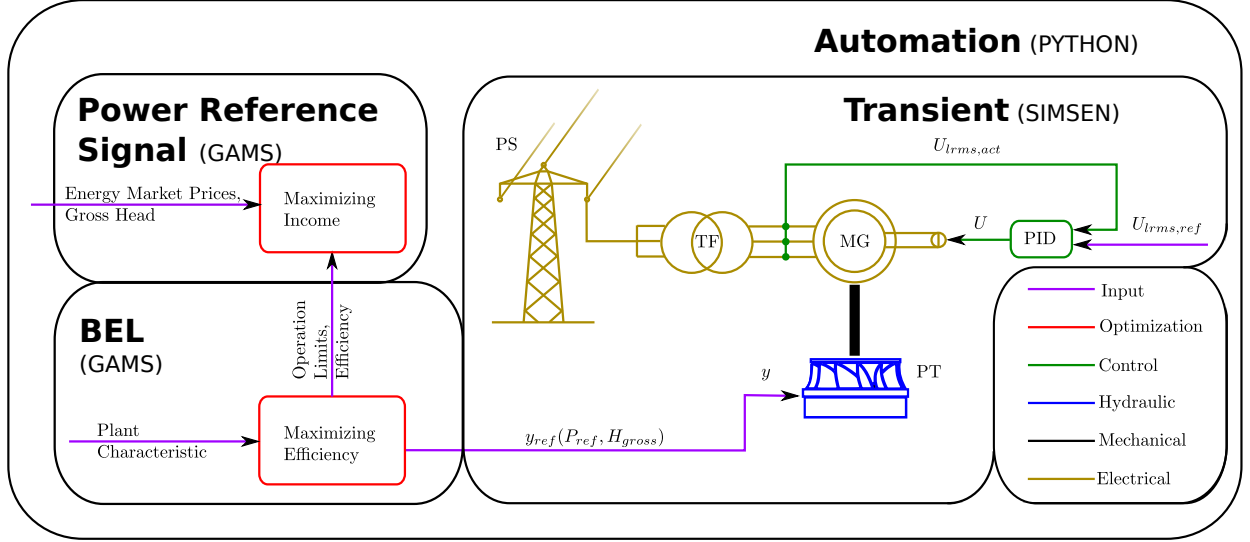
Figure 4.2.: Block diagram of fixed speed binary set PSP in pump mode

4.1.3. Variable Speed Model

The variable speed model in turbine mode (figure 4.3) matches the fixed speed model in turbine mode in many ways. One difference with respect to the *BEL* block is that the optimization process does not only find the related GVO, as in the fixed speed model case, but also the related speed value. In the *Transient* block, a different generator type appears. While a common synchronous motor-generator is chosen for the fixed speed model, the variable speed model uses a voltage source (VS). The advantage of not exactly modelling the motor-generator is that this element allows the simulation of both variable speed schemes (VSDFG and VSFSC) within one model. Other advantages are that no power electronics have to be explicitly modelled and that a relatively large time step of one millisecond (ms) can be used. Therefore, the simulation time is moderated which means that one real time day requires 16 hours of simulation time. The last difference is the control strategy. As mentioned in subsection 1.4.1, speed variability also delivers the possibility of fast power control. In the SIMSEN model, the fast power control is realized by controlling the power with the help of the phase angle (THS) and the root mean square value of the voltage (U_{lrms}), while the speed is controlled by the GVO.

Analogous to the fixed speed scheme, the variable speed scheme does not allow for controlling by the GVs in pump mode either. Figure 4.4 shows that there is no feedback loop for the GVO. Therefore, the GVO with the highest efficiency value belonging to one power output is applied to the pump-turbine. Nonetheless, the feedback loop for the power output value on the generator side is still available. The speed variability in combination with no feedback control of the speed means that the speed value is a result of the steady operating point where the power output equals the hydraulic power including the losses. In case the power output increases, the speed increases and, thereby, the hydraulic power. The acceleration continues until a new steady operating point is reached.
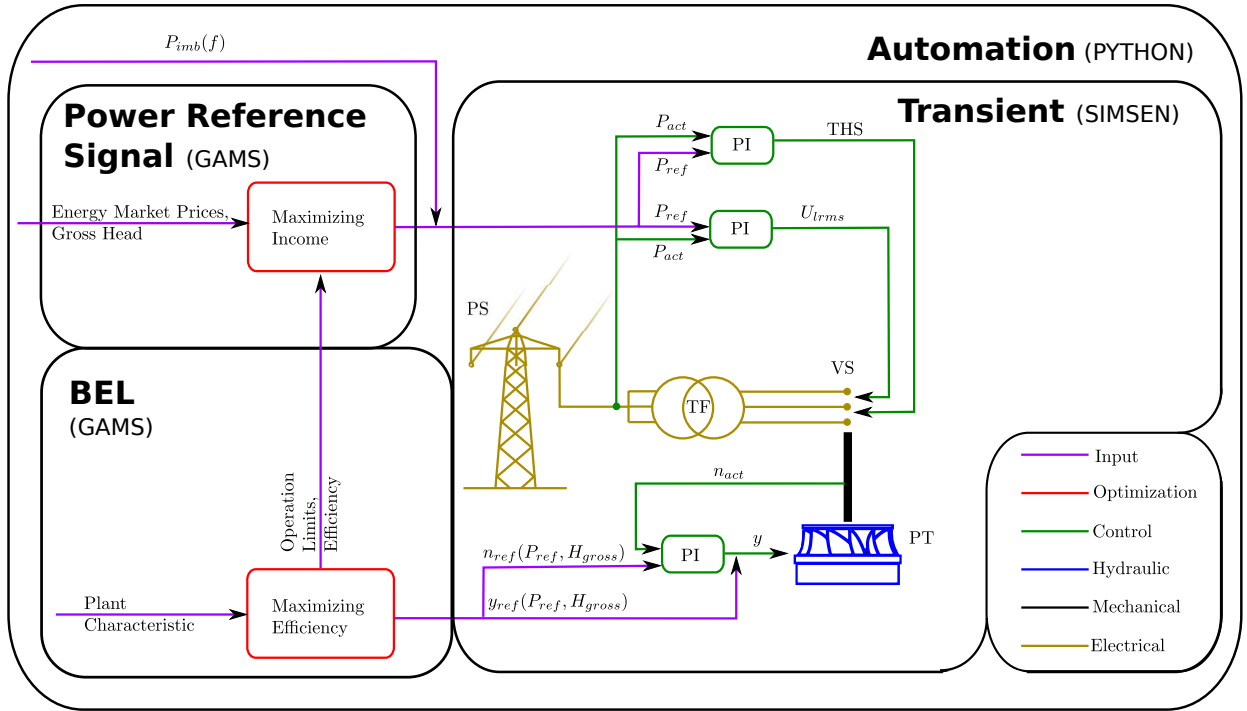
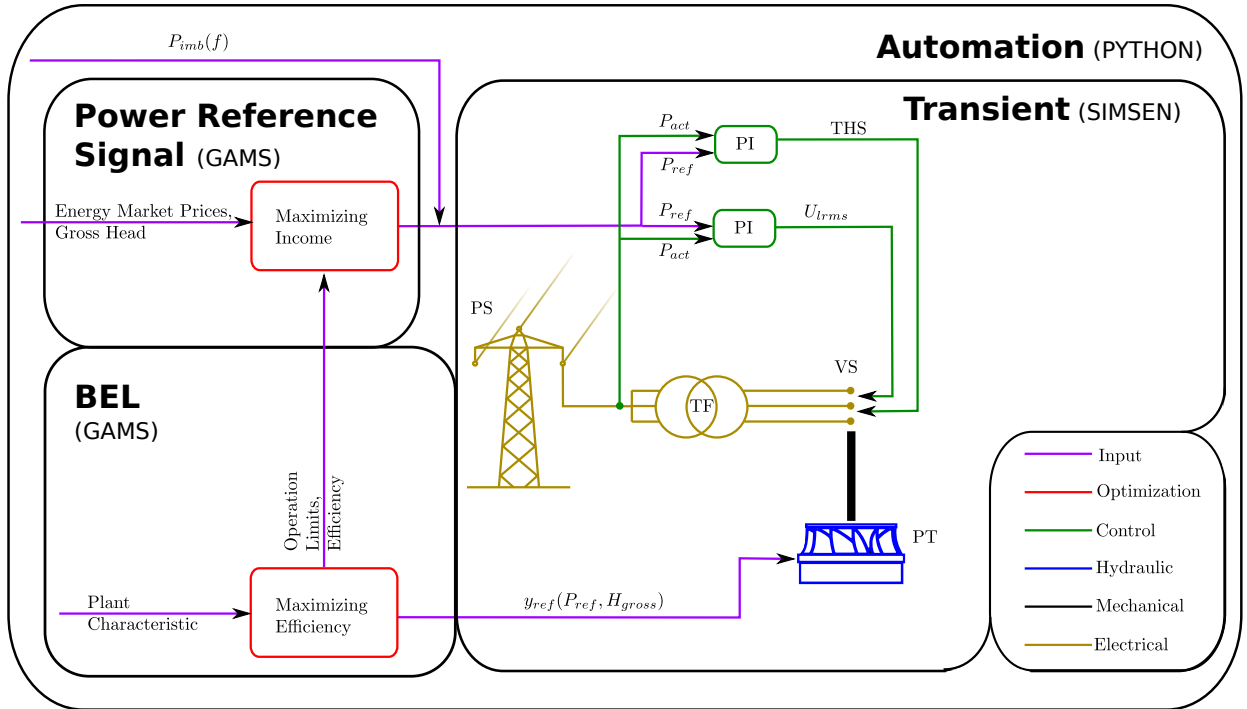Figure 4.3.: Block diagram of variable speed binary set PSP in turbine mode

Figure 4.4.: Block diagram of variable speed binary set PSP in pump mode

4.1.4. Combined SIMSEN Model

The models of subsections 4.1.2 and 4.1.3 are combined to form one overall model, since a combined model allows for the investigation of the units interaction on the hydraulic side

as well as on the electrical side. The SIMSEN model, containing one fixed and one variable speed scheme, is pictured in figure 4.5. The head water and the tail water are connected by a water way which divides and each path is intermitted by a FSPT and a variable speed pump-turbine (VSPT), respectively. The FSPT and the VSPT represent hydraulic elements and are each connected with one mass representing the impeller mass and one mass representing the mass of the generator rotor. The impeller is connected with the motor-generator and voltage source (VS), respectively, which is followed by two switches. In the case of the FSPT, the two switches are required for pump and turbine mode, respectively, since different phases are connected in pump mode and in turbine mode. In contrast, the VSPT would require only one switch, but for the sake of symmetry to the FSPT, one switch for pump and one for turbine mode are chosen. The switch is followed by a transformer, after the transformer, the electric lines of FSPT and VSPT are merged, an element of electric losses is applied and the connection to the PS is made. The red elements are controlling the plant. The model contains the following control and controlled elements, respectively:

- **Input:** The two input elements read in the power reference signal and the optimized operating point regarding to each power output value.

- **Status inquiry:** Three elements check the status of the plant, the FSPT and the VSPT, respectively. Depending on their states, other elements react (e.g. GVs are closed, switches are opened). The plant states are:

  - pump mode

  - turbine mode

  - standstill mode

  - pump to standstill mode

  - turbine to standstill mode

  - standstill or pump mode to turbine mode

  - standstill or turbine mode to pump mode

- **Variable Frequency:** For variable frequency simulations, the frequency trend has to be calculated. Therefore, one element calculates the power imbalance in the PS, the other element calculates the resulting PS frequency and applies it to the PS.

- **HW:** The control element acting on the head water element calculates the actual gross head in dependence on the flow and storage size and applies it to the head water reservoir.

- **Switch related control elements:** Programs pick off the phase and voltage. If phase, voltage and speed match sufficiently, the switch can be closed.

- **MG:** Depending on the reactive power and the actual voltage on the MG, the excitation voltage is adapted.

- **MG mass (FSPT):** In order to start-up the FSPT in pump mode, an auxiliary motor is required. This motor is simulated by an external torque (T_{ext}).

- **FSPT:** In turbine mode, the FSPT's power output can be regulated by the GVO. These programs check the FSPT's state and in case of turbine mode, they feed-forward control the power output in turbine mode. Alternatively, they close the GVs in case

of switchover processes or open the GVs to a predefined value in case of pump mode.

- **VSPT:** Different to the FSPT in the VSPT case, the speed instead of the power output is regulated by the GVO.

- **MG mass (VSPT):** This element is connected to the VS. Thereby, the controlled power on the VS is applied to this element during pump or turbine mode by an external torque (T_{ext}). The external torque is further used for the pump start-up, similar to the FSPT.

- **VS:** Depending on the active and reactive power reference signal as well as actual power, a multi-variable controller calculates the required phase and voltage root mean square value. In two additional elements, the controller results are combined and applied to the VS.

Figure 4.5 shows the changed transient model for the case of two hydraulic units sharing one water way. It has to be mentioned that the *BEL* and *Power Reference Signal* blocks of figures 4.1 to 4.4 also have to be adapted for a two hydraulic unit configuration.

Figure 4.5.: Composed fixed and variable speed model

4.2. Validation of Transient Model

In order to verify if the simulation results are realistic, a validation is exercised. A complete validation requires comparison of the simulation and the real plant main parameters within a transient operation. The plant parameters required for a sufficient accurate validation are:

- geometric data of turbine, surge tank and water way

- gross head

- net head

- speed

- flow rate

- generated power

- power output

Of the above mentioned data, only the trend of the power output and the power reference signal have been available. These data do not allow for an exact comparison of all parameters, but at least it is possible to calculate the divergence once between a power reference signal and the measure power output of the real plant and the other time between a power reference signal and the simulated power output. Since the limitations were unknown, they have been estimated by typical values for this kind of PSPs (table 4.1).

Parameter	lower limit	upper limit
steady head	0.93	1.06
dynamic head	0.8	1.2
speed	0.9	1.04

Table 4.1.: Limitations of main parameters [47]

Figure 4.6 shows plant parameters within one hour. The power reference signal, the simulated power output and the measured power output have a resolution of one second. Considering the uppermost graph, the trend of the power reference signal (red), the real plant power output (green) and the simulated power output (blue) can be seen. In this graph, differences are hard to detect. Therefore, in the second graph, the integrated, absolute value of the divergence between power reference signal and the real plant power output as well as between power reference signal and simulated power output is plotted. It can be seen that the simulated case has a much smaller deviation to the power reference signal than the real plant. In order to make sure that no critical limitations have been breached, significant parameters are shown in the four lowermost graphs. The dynamic head variation of approximately $\pm$ 6 % is not critical and within the $\pm$ 20 % dynamic head range. The speed varies within a range of about two percent. It is the lower speed limit which is problematic, since a compromise between efficiency and kinetic energy buffer has to be found. In order to generate power with highest possible efficiency, low power output values require minimum speed. For the purpose of rapid operating point changes, kinetic energy extraction is required, which calls for a speed buffer between actual and minimum speed value. In the simulated case, a speed offset of 0.6 % towards higher speed is sufficient in order not to breach the lower speed limitation. The required offset depends on the power reference signal's volatility in terms of amplitude

and frequency. The investigated case is assumed to be a moderate case and therefore, a higher tolerance is recommended. Considering the GVO and the efficiency, it can be seen that small GVO values are accompanied by low efficiency values. As mentioned in section 2.1, an efficiency value of 80 % is a common guideline. Nevertheless, the investigated plant operates at lower efficiency values (65 %) as well.
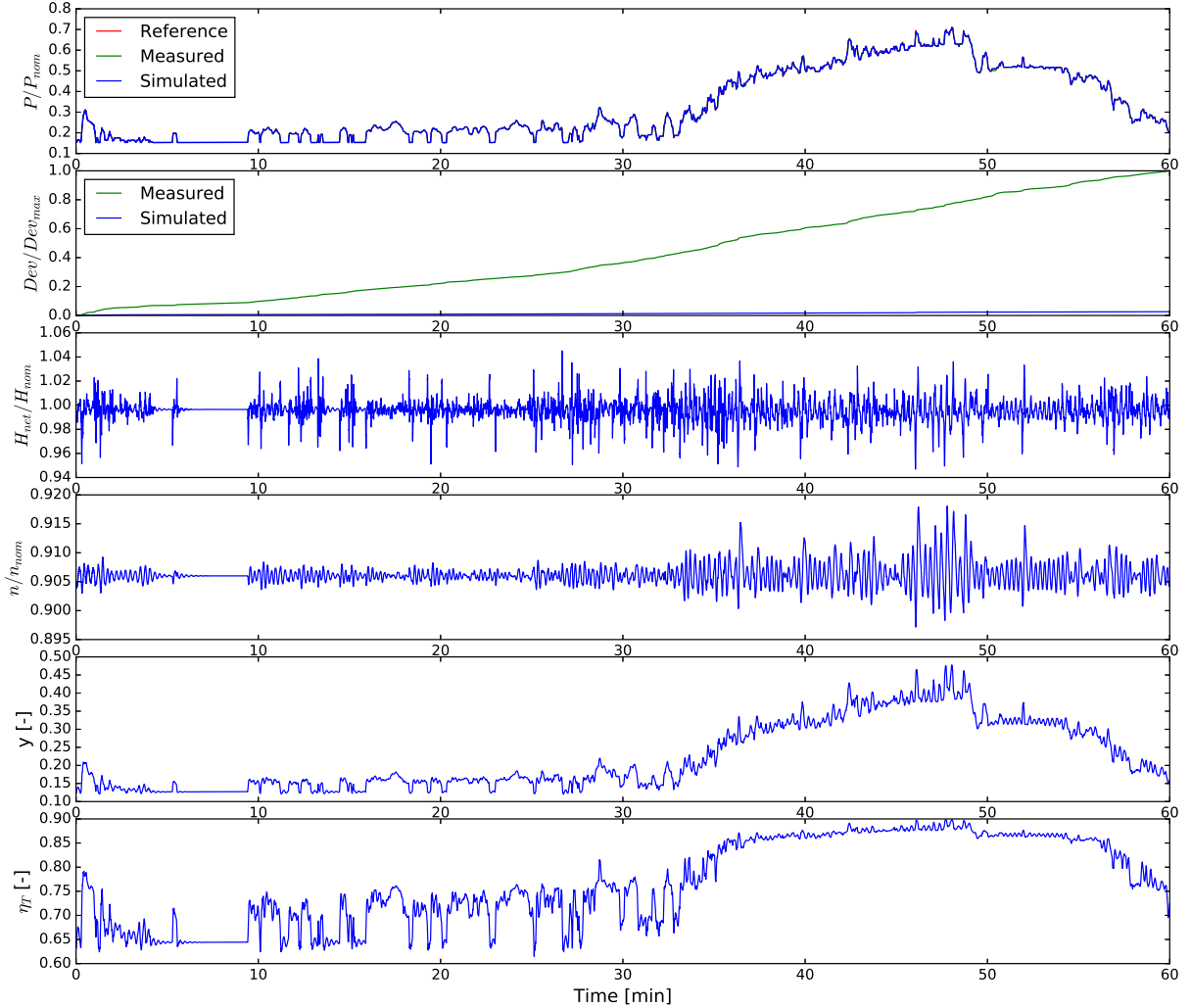
Figure 4.6.: Validation of the capability to follow a power reference signal

4.3. Transient Simulations

In the following section, the transient investigations are described. Based on the introduced models, natural frequencies are determined, start-ups of different schemes are investigated, the interaction between two units is examined, the accuracy of the different models is investigated, the ability to compensate a power leap is simulated and an optimization task in order to improve the transient behaviour of the VSFSC scheme is introduced.

4.3.1. Vibrations

Vibrations are a critical topic regarding power plant operation. Vibrations of flow, torque or speed can harm the plant. Therefore, natural frequencies of different parts of the plant are investigated in order to avoid excitation close to these frequencies during the operation. Natural frequencies are frequencies a system tends to oscillate with. A preloaded bar, for example, oscillates with its natural frequencies if it is released. For the determination of those frequencies, the plant is excited once and released without any further impact. Due to the excitation, the plant does not operate at stable operation and thereby, plant parameters vary with respect to time. This form of parameter variation is a form of vibration. Since vibrations may be difficult to detect within the time domain, the trends of the investigated plant parameters are transformed into the frequency domain. The transformation from time to the frequency domain is carried out by a fast Fourier transformation (FFT). In order to estimate the maximum amplitudes of the vibrations, undamped vibrations are required. This means that damping of the friction coefficient, shaft and the generator damping winding have to be set zero in the simulation. Nevertheless, the damping effect of the pump-turbine rotating in water can not be removed in the simulation. Therefore, in order to avoid the damping effects of the pump-turbine running in water, the vibration in the water way were investigated separately from the vibrations in the electromechanical equipment.

At the beginning of the simulation, the pump-turbine operates steadily at maximum flow, which is changed to a flow rate of zero at the first time step by a sudden closure of the GVs. This causes a water hammer which can propagate through the water way. Since the hydraulic part of the plant is separated from the electromechanical system, the closure of the GVs does not excite the electromechanical system of the plant. A torque trend, which corresponds to the sudden valve closure, is applied for the transmission of the excitation on the electromechanical system.

A sufficient resolution is a crucial point to determine natural frequencies. The hydraulic vibrations require an enhanced local discretisation of the water way, while for the determination of the generator's natural frequency a reduced time step is necessary. The higher the local discretisation of the water way, the better the accuracy of the frequency value, since thereby, the numerical solution approximates to the analytical solution. A time step of one ms leads to subsiding of the vibration (non-physical damping) in the case of generator frequency.

Hydraulic Equipment

At first, vibrations on the hydraulic side are investigated. Therefore, a basic model is used and expanded stepwise. In the first column, figure 4.7 shows the model configuration, in the second column, the natural frequencies are presented in the frequency domain and in the third column, equations for the analytical estimation of the frequency are depicted. The first row shows the most simplified model, just consisting of head water, tail water, one pump-turbine (PT1) and a water way composed of a single pipe. The analytical column shows that the natural frequency of a single pipe is the inverse of its period (see equation 1.10). The vertical gray lines in the frequency domain plots present the analytical calculated natural frequencies of this configuration and its multiples (a=1000 m/s, l=600 m). It can be seen that the lowest simulated natural frequency (blue peak) corresponds with the lowest calculated natural frequency. Considering the simulated natural frequencies, only each odd

multiple of the first natural frequency appears. Even multiples of the first natural frequency are multiples of the frequency corresponding to the reflection time and thereby cause a decay of the vibration.

For the second row, the model is expanded by a pipe leading to another pump-turbine (PT2). The GVs of the PT2 are closed during the entire simulation. Due to the closure of the GVs of PT1, the pipe configuration becomes the same as in the first row case, with the difference of having a longer water way. The longer water way, and thereby increased period, causes a decrease of the first natural frequency.

In the third row, a pipe is pre-connected to PT1. Thereby, the water hammer can be reflected at the head water as well as at PT2. This leads to two natural frequencies instead of one as there are two possible ways for the wave to propagate. The closeness of the pump-turbines is accompanied by a low reflection time and thereby high natural frequency as visible by the second natural frequency of about 5 Hz. Furthermore, due to the same conditions at both pump-turbines ($c = 0$), the pressure and speed wave are reflected the same way at both pump-turbines. This leads to a period equal the reflection time instead of half the reflection time as in the case of the wave reflection on the water surface.

In the fourth row, the distance between pump-turbines and head water is extended in order to simulate a pressure tunnel. Thereby, the model stays the same, but the longer distance causes a higher period of the wave between the PT1 and the head water, which is tantamount to a lower first natural frequency.

Finally, a surge tank (ST) is applied. The advantage of a surge tank is that the water hammer is reflected already at the surge tank instead of the head water. This reduces the reflection time and, thereby, according to subsection 1.4.1, the required closure time. The additional element allows for a further natural frequency due to the wave between head water and surge tank. The same boundary condition at the surge tank and head water ($p =$ constant, $v =$ variable) causes in this case a period equal to the reflection time.

In the illustrated cases, the reflection between PT2 and head water, respectively surge tank, are not listed, as they are congruent to those of PT1 due to same distance to head water, respectively surge tank.
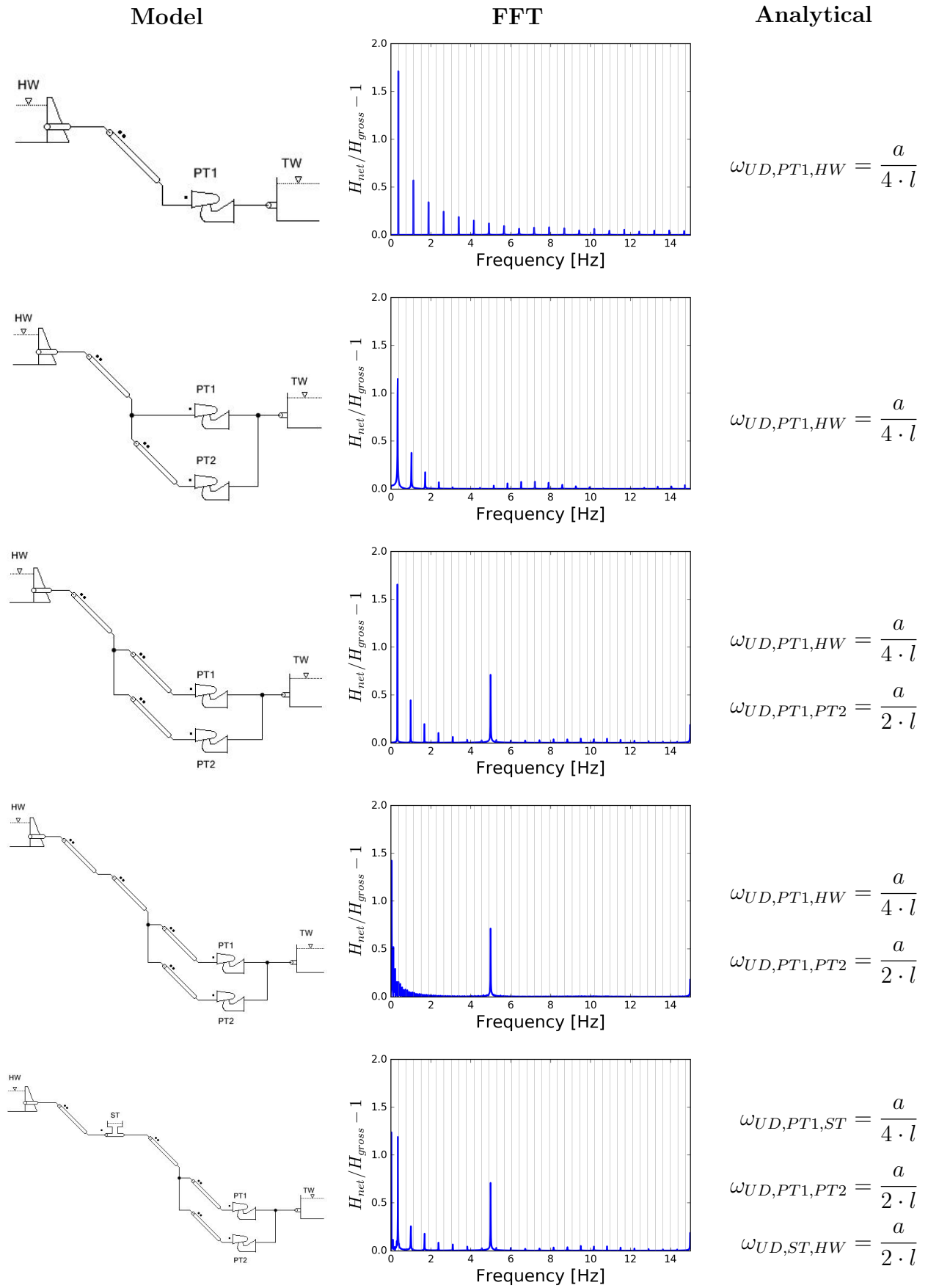
Figure 4.7.: Vibrations in the hydraulic system

Reflection at Tail Water: It has to be noted that in the case of a partial closure of the GVs, the water hammer is reflected on the tail water instead of the closed pump-turbine. Due to the different boundary conditions on the tail water (p = constant, v = variable) compared with the closed pump-turbine (p = variable, $v = 0$), the periodicity changes from two times the reflection time to the reflection time. Thereby, all multiple natural frequencies occur instead of only the odd ones.

Electromechanical Equipment

Beside the hydraulic vibrations, the natural frequencies in the electromechanical equipment are investigated. The mechanical oscillation between the impeller and the generator runner may be estimated by an unrestrained two mass oscillation [98]. The natural frequency depends on the torsional spring constant (c_T) and the inertia constants of the impeller (J_{IMP}) and rotor (J_{ROT}). The resulting frequency is plotted in the second column of the first row of figure 4.8. The natural frequency appearing is about 15 Hz, which is close to the third multiple of the water hammer's natural frequency between PT1 and PT2.

In case the model is extended by the electrical system, the generator's natural frequency [99] of 1.21 Hz appears additionally. The natural frequency of the generator varies with speed, the synchronization power coefficient (K_e) and the inertia constant (H_e). This natural frequency is close to a multiple of the water hammer's natural frequency between PT1 and surge tank.
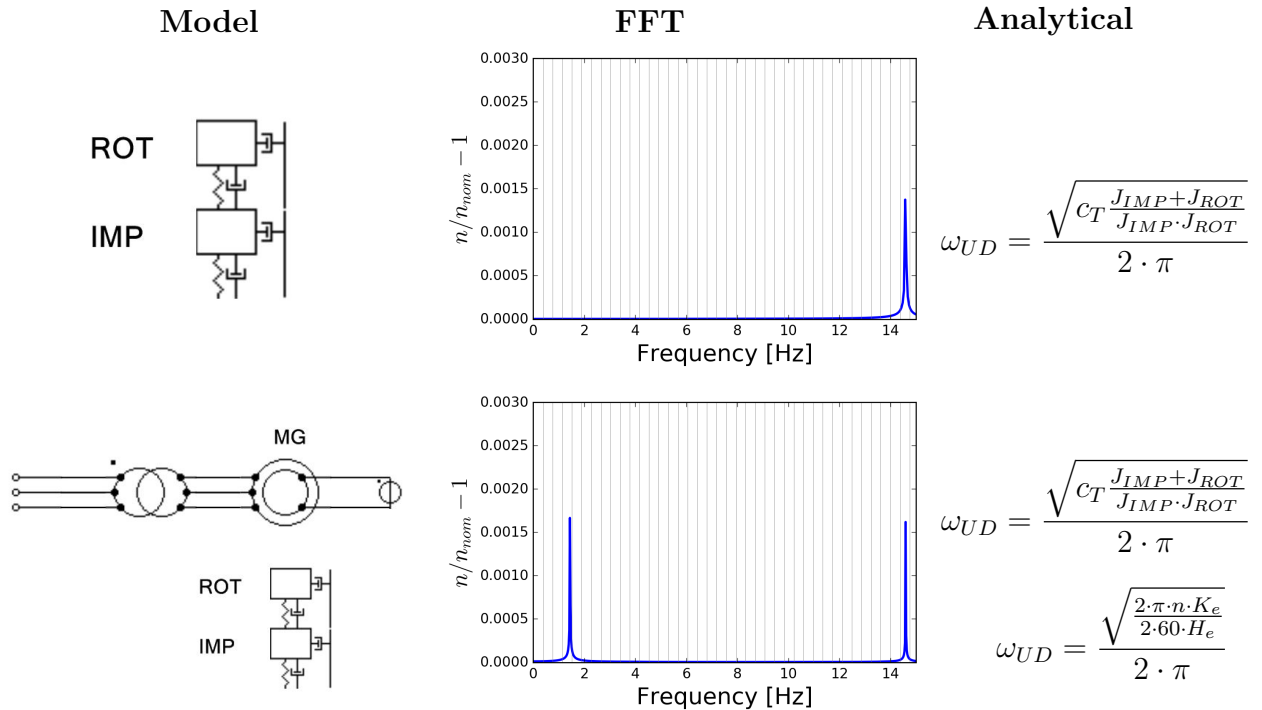

Figure 4.8.: Vibrations in the electromechanical equipment

Damping: The investigated vibrations do not take into account the damping. According to equation 4.1, the frequencies of the damped system are reduced by the factor $\sqrt{1 - 2D_F^2}$

[100]. Since the damping factor is always a positive factor, the damped frequencies are always lower than the undamped.

$$\omega_D = \omega_{UD} \cdot \sqrt{1 - 2D_F^2} \qquad (4.1)$$

Additional Vibrations: Beside the presented natural frequencies, there also exists the natural frequency of the rotor-stator interaction. This natural frequency appears in case a GV passes a vane of the impeller with little distance [101], [102]. For the investigation of this kind of natural frequency, it is required to simulate the flow through the GVs and the impeller. The one-dimensional structure of SIMSEN does not allow for such a kind of simulation, since the GVs and the impeller are reduced to one characteristic.

The vortex rope is another three-dimensional effect, which is not taken into account. The vortex rope causes a two-phase section downstream of the impeller (turbine mode). This gas-fluid mixture changes the wave propagation speed significantly. A changed wave propagation speed also changes the reflection time and thus the natural frequencies of the water hammer [103].

Partial reflections of the water hammer are considered neither. This type of reflection appears in case the water way consists of pipes of different inner diameters [104].

4.3.2. Connection to the Power System

Control structures, as presented in figures 4.1 to 4.4, may only be applied in continuous pump or turbine mode. However, PSPs have to switch between pump and turbine mode several times a day [105], [106], [42], [107]. Therefore, not only the pump and turbine starts are essential, but also the switchover from one mode to the other. Within this subsection, the coupling of the different plant schemes to the PS is investigated.

Turbine Mode

The coupling process of the PSP to the PS is illustrated for the turbine mode in figure 4.9. The FSTS and FSTS0 schemes are not included since they behave quite similar to the FSPT scheme in turbine mode. The figure shows reference values (red) and actual values for power, speed and GVO (blue). Additionally, the generated power (green) as well as the actual head values are included. The reference signal shows that each scheme gets the signal to change from standstill to the nominal power output at second ten. In order to do so, the GVs are opened for all schemes. The limited speed ranges of the FSPT and VSDFG schemes require them to accelerate, synchronize with the PS and connect to the PS. Thus, no synchronization of unit speed and PS frequency is necessary and power output can be generated much sooner. In terms of synchronization, the FSPT scheme has to synchronize the speed, phase and voltage amplitude. In the case of the VSDFG scheme, phase and voltage amplitude synchronization are sufficient, on the condition that the speed is within its speed limits. As visible in the third row of the FSPT and VSDFG schemes, the GVs are opened at around 20 % at the beginning of the synchronization, close to about ten percent and finally, if the synchronization conditions are sufficiently fulfilled, the connection to the PS is carried out. The lower speed needed for synchronization of the VSDFG scheme

has the advantage that the GVO is lower during the synchronization than in case of the FSPT scheme. Therefore, less amount of water is necessary for the synchronization. If the pump-turbine is connected to the PS, the GVs open and power output is generated. The acceleration is visible in the speed plots as well as in the power plots. Since there is generated power, but no power output is fed into the PS, it is absorbed in form of kinetic energy. This means the pump-turbine is accelerated. In the fourth row, the water hammer behaviour is illustrated. As described in subsection 4.1.1, a fast change of the GVO may lead to net head values exceeding their upper or lower limitation. It can clearly be seen that an opening of the GVs causes a reduction of the head value and vice versa. In terms of head value limits (table 4.1), it is visible that they are slightly breached. If the head value exceeds its limitations, the GVO is set constant until the head value returns to a value that is within the limitations. This control strategy ensures that in case the dynamic head breaks its limits, the head value can return within its limits.

It can be seen that the FSPT scheme requires about 50 second to be deliver power, while the VSDFG and VSFSC schemes require 40 and 20 seconds, respectively
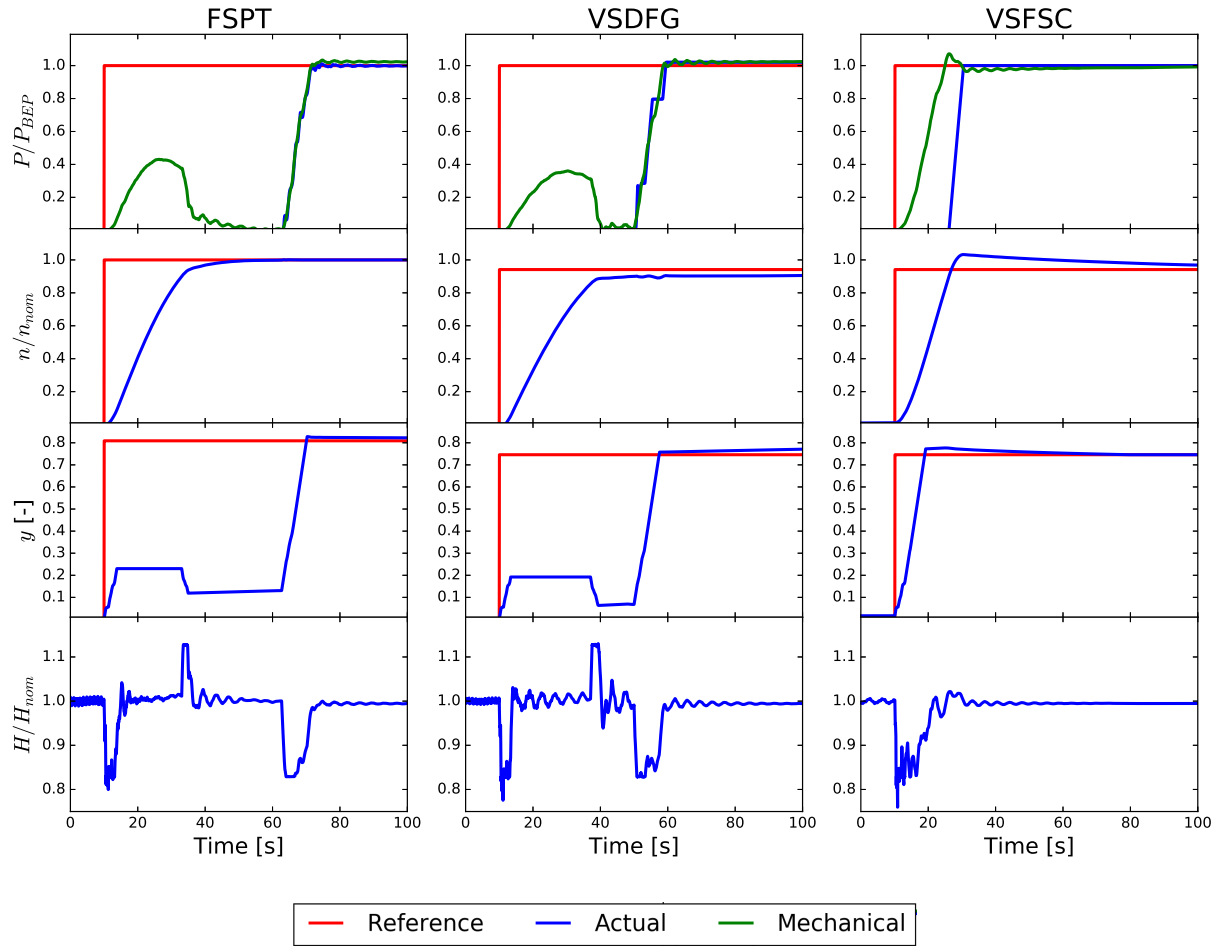

Figure 4.9.: Turbine start of different PSP schemes

Pump Mode

The pump start-up is more sophisticated than the turbine start-up. Since opening the GVs would accelerate the rotating assembly in the turbine direction, the rotating assembly has to be accelerated in a different way. The way of acceleration also depends on the plant scheme. The different start-up procedures are:

- **FSPT:** The motor-generator of this scheme is operated at synchronous speed and, therefore, additional equipment is required to accelerate the rotating assembly. Such equipment is an auxiliary motor, a start-up turbine or a start-up frequency converter. Since these types of start-up equipment usually provide a small amount of power, the impeller has to run in air. A start-up in water would require power magnitudes higher than in air.

- **VSDFG:** The start-up of this scheme is similar to the start-up of the FSPT scheme. Even if the speed range is variable, the motor-generator may not provide power output beyond its speed range. Nevertheless, the converter of the rotor circuit may be used to start-up the rotating assembly in case the impeller runs in air.

- **VSFSC:** In this scheme, the MG's power output is not restricted by any speed limits. Therefore, the impeller may be started-up filled with water.

- **FSTS/FSTS0:** One advantage of having separated pump and turbine units is to synchronize the pump to the already synchronized turbine and thereby to the PS. The pump impeller does not have to be blown out as the hydraulic torque converter [108] delivers sufficient power to start-up the rotating assembly even if the impeller is filled with water. In case the turbine is not connected to the PS, a synchronization as described in 4.3.2 has to be realized first.

4.3.3. Interaction of Two Units while connecting to the Power System

In this subsection, the interaction of two hydraulic units sharing mostly the same water way is investigated. As reference case, it is assumed that both units initially stand still and receive the order to connect to the PS at the same time. The results are illustrated in figure 4.10. The first ten seconds the units are at standstill, which means no power, no speed, GVs closed and a head value equal to the gross head value. As of second ten, power is required. This can be observed by the instantaneously changing reference signals of power, speed and GVO for both units. At the beginning of the start-up, the behaviour is analogous to the case of only one unit being placed in the water way (figure 4.9). At about second 35, where the GVs of the FSPT scheme close, a pressure peak occurs at the FSPT scheme. This peak propagates through the water way to the VSDFG scheme where the increased head also increases the generated power. Analogous behaviour occurs at second 50, where the GVO of the VSDFG scheme is reduced. Due to the successful synchronization of the VSDFG scheme about second 70 and the following opening of the GVs, the head value is reduced, propagates towards the FSPT scheme and at this point reduces the generated power. The synchronization of the FSPT scheme at about second 115 has the same influence on the VSDFG scheme. Since this scheme is already connected to the PS, a decrease of the generated power has to be accompanied by a decrease of the power output in case the kinetic energy buffer is insufficient to compensate the missing energy.

The start-up of the FSPT scheme requires about 85 % more time and the start-up of the VSDFG scheme requires 34 % more time to be successfully connected to the PS. Nevertheless, the higher amount of time is not only required by the interactions between the schemes, but also by the lowered net head value caused by a higher flow rate (two active hydraulic units).
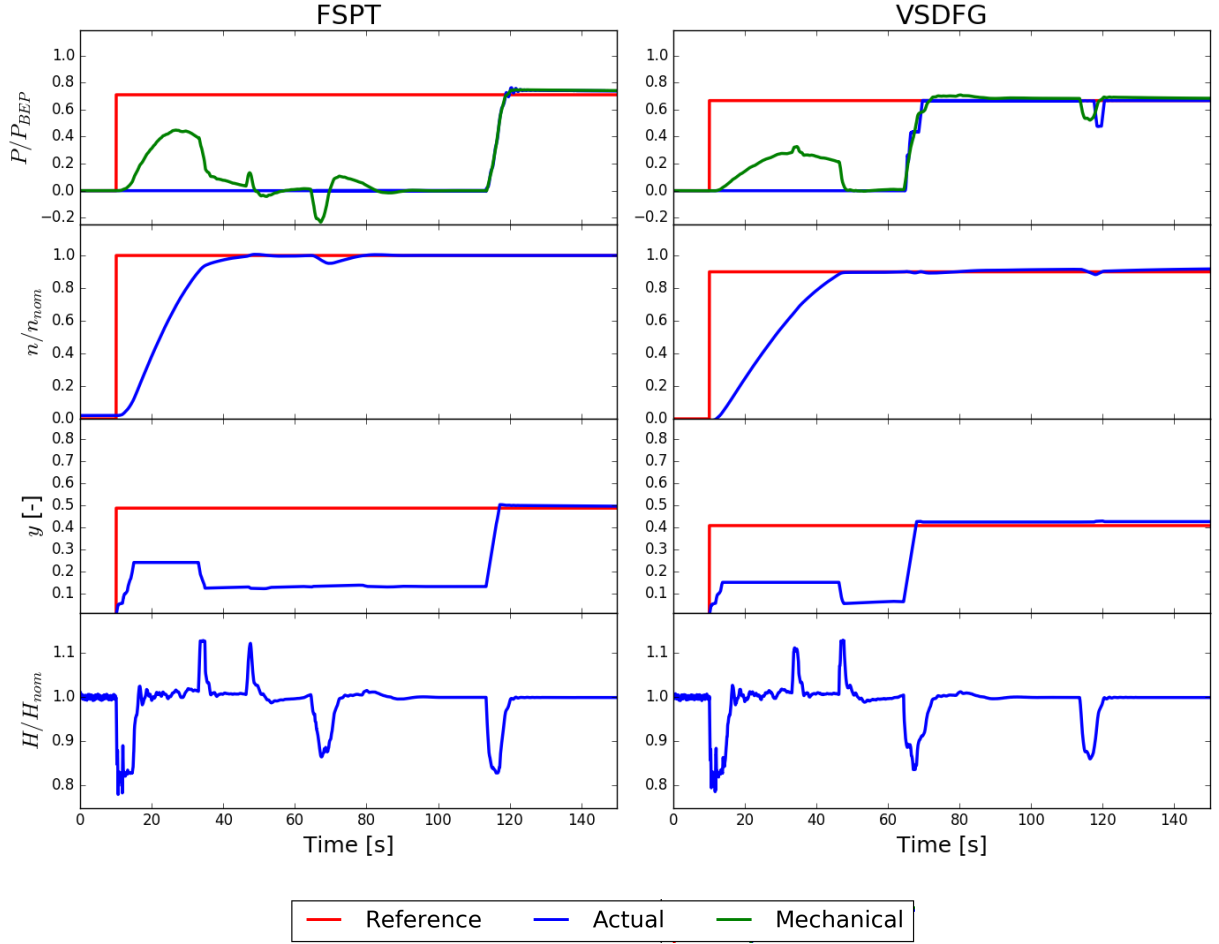
Figure 4.10.: Effect of one hydraulic unit on the other while synchronizing to the PS

4.3.4. Power Supply Accuracy

As mentioned at the beginning of this chapter, the quality of following a power reference signal as accurately as possible is essential for the income from the SCW market. In this subsection, the accuracy of the different PSPs is examined. In order to do so, the offered power of sections 3.2 and 3.3 is combined with the exact frequency trend to generate a power reference signal. A one-day time section of the four-year trend is used for the transient simulation.

Power System Frequency

The balance and stability of the PS is explained in section 1.2. The CEPS's actual frequency within June 4th 2015 and July 17th 2015 has been logged from [109]. Figure 4.11 shows the minimum and maximum frequency values with respect to time within the logged time frame.

The threshold of 49.8 Hz and 50.2 Hz, respectively, has never been reached. Furthermore, the CEPS has been quite stable as the frequency value has almost entirely stayed within the half frequency bandwidth. The reason why the increasing implementation of new renewable energies does not cause higher frequency deviations is that its volatility leads to power imbalances appearing relatively slowly compared to the agility of the balancing energy. This means that the imbalance of new renewable energies appears slowly enough to be absorbed by the balancing power [110]. Moreover, it is currently tried to avoid volatile power generation by installing system-friendly wind power [111]. It is characteristic that frequency leaps occur both at full hour and half hour. This behaviour is caused by day-ahead and intraday scheduling [110]. Considering the first three hours of a day, it can be assumed that the consumption declines. Therefore, power generation exceeds consumption which leads to a frequency increase. At full or half hour, power plants are shut down and the frequency value decreases. The opposite holds true for the hours between 6 and 10 am. Due to increasing consumption, plants are started at each full or half hour to meet this increase. The start-up of these plants increases the frequency.
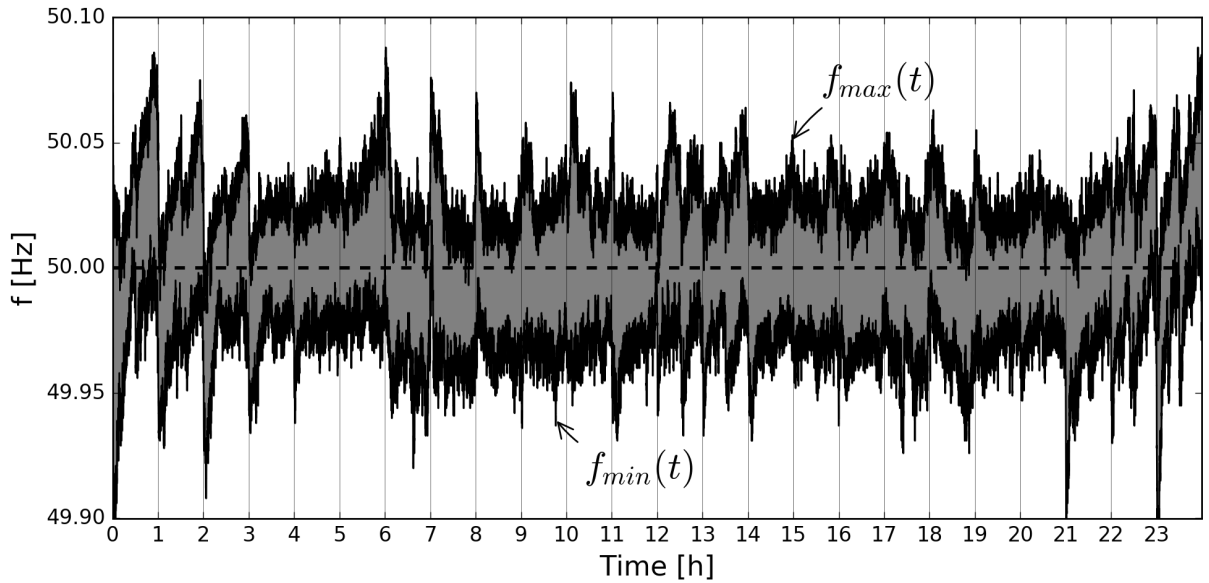
Figure 4.11.: Minimum and maximum CEPS frequency between June 4th 2015 and July 17th 2015 [109], [112]

Deviations during Operation

The deviations of the power reference signal and the power output during pump and turbine mode, respectively, are caused by limitations of the plants flexibility. Water hammer, speed limits and controller parameters influence this flexibility. For a fair comparison, the same power reference signal is used for all schemes. From those plant schemes which are able to generate balancing power, the VSDFG scheme is the most restricted one. Therefore, the maximized income operation of this scheme is used. As example day, June 24th 2015 is chosen randomly. Considering the upper graph of figure 4.12, the technically possible operating range of the VSDFG scheme (gray) can be seen. The green area represents the power range offered on the balancing energy market. The range of the offered power band is restricted by the minimum spread for pump, respectively turbine power. The bold blue

line symbolizes the power sold on the day-ahead market. As can be seen, the plant remains in pump mode at the early morning hours and switches to turbine mode at 6 am. The red trend represents the power reference signal. This signal is calculated by adding a frequency proportional power to the power sold on the day-ahead market.

The second graph shows the cumulative deviation between the power reference signal and the power output for the three schemes able to deliver balancing power. It can be seen that the deviation of the FSTS0 scheme is the highest with 8.05 %, followed by the VSDFG and VSFSC scheme with 0.24 % and 0.051, % respectively. Thereby, the VSDFG and VSFSC schemes only have a deviation of 3 and 0.63 %, respectively, of the FSTS0 scheme. The higher deviation of the VSDFG scheme is caused in turbine mode by its lower speed limit. In order to offer a kinetic energy buffer, the minimum steady speed value is set to have at least 0.5 % of the nominal speed distance to the lower speed limit. As already mentioned, while a higher distance to the lower speed limit offers a bigger kinetic energy buffer, a lower distance is tantamount to a higher efficiency value. The high speed required for a big kinetic energy buffer and the low speed required for a high efficiency value call for a design trade off.

While the deviations of the VSDFG and VSFSC schemes barely influence the SCW income of section 3.3, the 8.05 % lower income of the FSTS0 scheme's SCW reduces the entire income about 5.81 %. The lowered income also reduces the profit about 8.5 %.
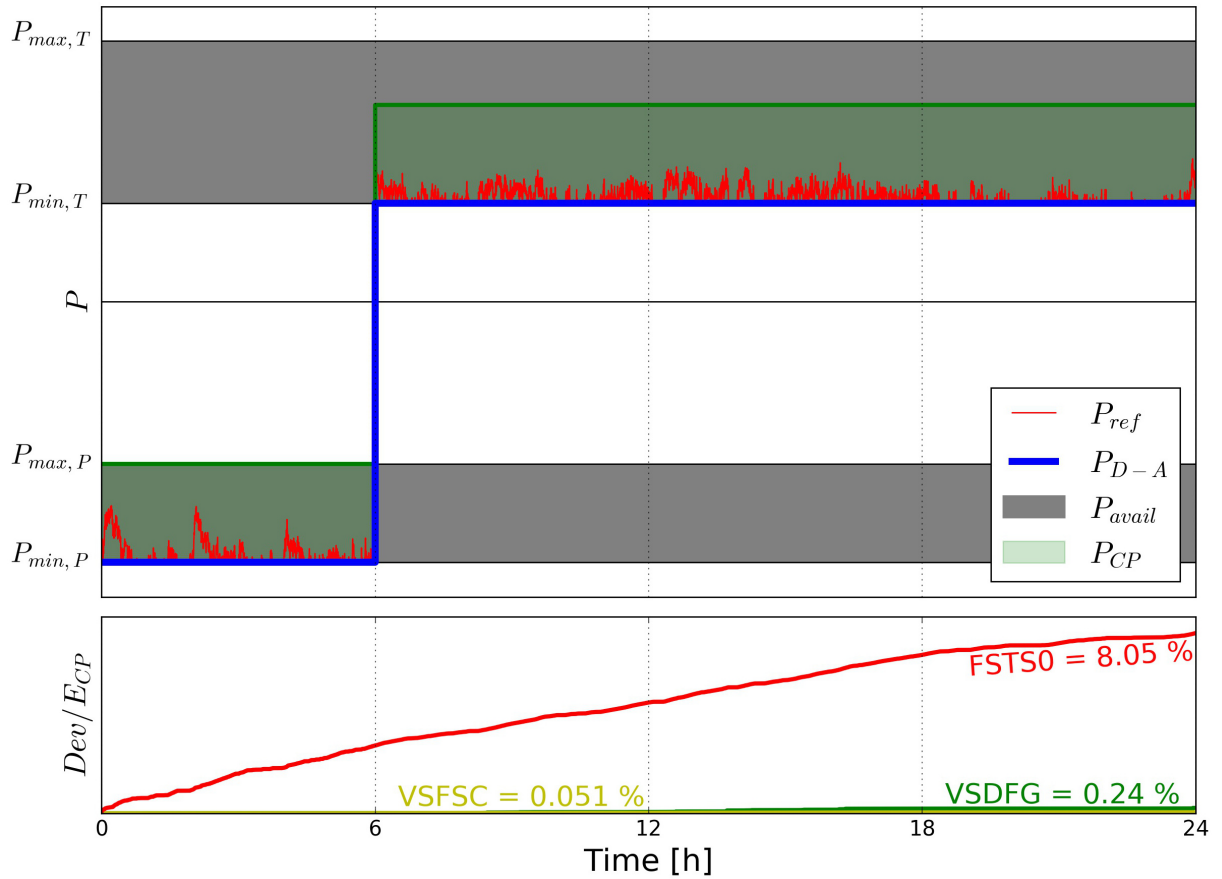

Figure 4.12.: VSDFG scheme's operating ranges, schedule and cumulative deviations of VSDFG, VSFSC and FSTS0 scheme for June 24th 2015

4.3.5. Ability of Power Leap Compensation

In this subsection, the ability of different PSP schemes in order to compensate PS faults is investigated. Faults may occur on the consumption side as well as on the generation side. A fault on the consumption side in further will hereinafter be referenced to as *Surplus*, while a fault on the generation side will be called *Outage*. For this kind of investigation, the fixed and variable speed models of section 4.1 are used. In the models, the *Power Reference Signal* block is replaced by a manually defined function. Thereby, the power reference signal, usually resulting from the *Power Reference Signal* block of the model, is substituted by a power trend staying at one value until a certain time, leaping to another value and staying constant until the end of the transient simulation. This power leap is to be followed as fast as possible by the different PSP schemes. Furthermore, the manually defined power leap is assumed to compensate a power imbalance in the PS. The resulting frequency deviation is determined by equation 1.1.

Modelling the Power System

The considered PS is the CEPS. As worst case, a fault of 3000 MW is defined as *Outage* or *Surplus* [8]. Each simulated case in this subsection represents a 3000 MW fault. Since the PSP is able to deliver only a share of the 3000 MW, it is assumed that the power leap compensated by the PSP is simultaneously compensated in exactly the same way by other power plants delivering balancing power in order to cover the 3000 MW fault.

According to data from [24], in 2015, the average inertia constant was 3.88 seconds resulting in an inertia value of 29.3 $\cdot 10^6 \cdot$kgm^2. The inertia constant as a result of the generation mix is presented in table 1.1 and figure 1.6.

Example Case

This subsection describes an example case of a simulated fault in the CEPS. The leap from minimum to nominal power output of the FSPT scheme is chosen as fault to be compensated. The same leap is also examined for the VSDFG and VSFSC schemes. Figures 4.13-4.15 show the transient behaviour of the different schemes in the unit speed-unit flow diagram. The colour coded areas represent the plant efficiency values in case of steady operation at nominal gross head. Red sections mark high efficiency values while blue sections indicate low ones. The operating ranges are limited by a minimum hydraulic efficiency value of 80 %, speed limits and maximum GVO. The black marks highlight the minimum ($\boxed{A}$) and nominal ($\boxed{B}$) turbine power of the FSPT. Even if the power output is the same for all points, $\boxed{A}$ and $\boxed{B}$, respectively, the operating point of all schemes is differently reasoned in their different operating ranges and BELs as presented in figure 2.1. Each mark is passed by three different types of lines. Dash-dotted lines represent lines of constant kinetic energy, dashed lines pass points of the same power output and solid lines represent the summation of operating points passed during the transient process ($\boxed{A} \Rightarrow \boxed{B}$ and $\boxed{B} \Rightarrow \boxed{A}$). While interrupted lines are created under steady conditions, solid lines refer to a constant gross head value, but dynamic net head. The dynamic behaviour of the net head is caused by the water hammer. Triangle markers are operating points passed in the case of an *Outage* ($\boxed{A} \Rightarrow \boxed{B}$) and are separated by three seconds. The same holds true for squared markers, except that they are operating

points passed in the *Surplus* case ($\boxed{\text{B}} \Rightarrow \boxed{\text{A}}$). It can be seen that the transient operating lines do leave the steady operating ranges. Net head oscillation excited by the water hammer can be mentioned as reason.

FSPT: In the *Outage* case ($\boxed{\text{A}} \Rightarrow \boxed{\text{B}}$), the PSP has to increase its power output. This means that the GVs open and the flow thereby increases. The increased flow through the turbine causes the net head to decrease and, subsequently, the unit speed increases (equation 2.1). Therefore, the operating line passes at the right hand side of the steady operating range. The *Surplus* case requires a reduction of the generated power ($\boxed{\text{B}} \Rightarrow \boxed{\text{A}}$). The GVs are closed, the flow thereby decelerates and the net head increases. The increased net head leads to lower unit speed values and an operating line at the left hand side of the steady operating range. Furthermore, the sharp change of direction in the operating line approximating the final operating point can be seen. The feed-forward part of the control structure causes the quickest possible change of the GVO to a value close to the final value. The feedback part of the structure adapts the value smoothly to the exact value. When the GVO value of the feed-forward part is reached, the change rate of the GVO decreases rapidly since it is only controlled by the slower feedback loop. This leads to a significantly reduced acceleration or deceleration of the flow. Thereby, the net head value is set back almost to its steady value and changes the unit speed, appearing in form of the mentioned changes of direction.

Figure 4.13.: Stationary operating range of the FSPT scheme inclusive operating lines (black-solid), lines of constant power (dashed), lines of constant GVO (magenta-solid) and constant kinetic energy lines (dash-dotted)

VSDFG: A variable speed scheme is able to distinguish the generated power and the power output. The deviation between power output and generated power is stored or extracted in form of kinetic energy causing speed changes. In the *Outage* case, extraction of kinetic

energy in order to stabilize the PS is desirable. As can be seen in figure 4.14, the scheme operates at its minimum speed, indicated by the mark on the left edge of the operating range, at the initial operating point $\boxed{\text{A}}$. Therefore, an extraction of kinetic energy and the accompanied reduction of the speed are permitted. Since the speed value at the final power output $\boxed{\text{B}}$ is higher than at the initial one $\boxed{\text{A}}$, the generated power has to exceed the power output for a certain amount of time in order to accelerate. This behaviour can be seen during the settling process.

In the *Surplus* case, a reduction of the power output faster than the one of the generated power is possible by buffering energy in form of kinetic energy. In order to avoid the turbine instability that occurs at low GVOs, a minimum GVO value is set. Reaching this value, the GVO stays constant, the net head value declines to its steady value and thereby, the unit speed increases. This is shown by the operating line break out towards the lower right corner. After the water hammer effects have mostly decayed, the power output higher than generated power stalls the turbine along the line of minimum GVO. The operating point $\boxed{\text{A}}$ on the edge of the operating range calls for enhanced regulation effort since no speed undershoot is allowed. It is essential that the steady speed value is above the lower speed limitation. Therefore, the reference values of the speed controller and the power output controller are different. While the speed controller tries to feedback the speed to its reference value, the power output controller reduces the power output in case the speed is stalled to the lower speed limit. In the case that the minimum steady speed value equals the lower speed limit, the spread between those values is zero. The result is that the same speed value affects power and speed controller, which makes the settling more difficult. Increasing spread between minimum steady speed and lower speed limit simplifies the settling process.
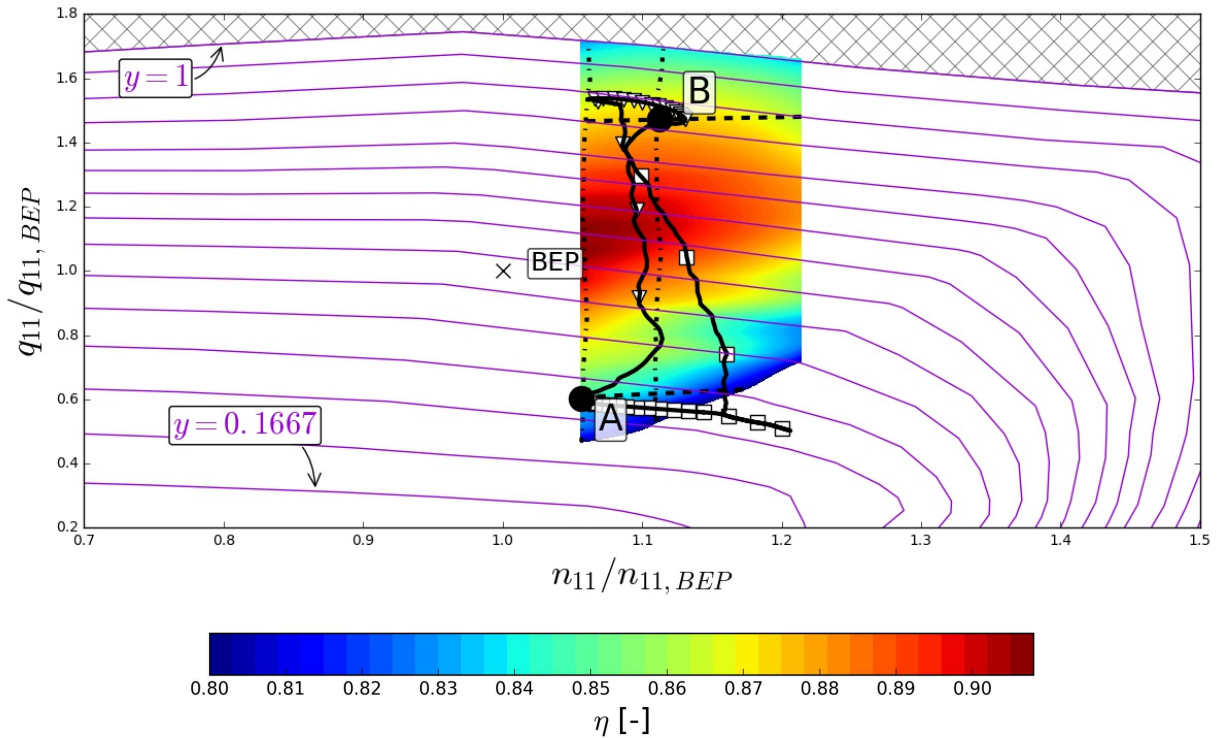

Figure 4.14.: Stationary operating range of the VSDFG scheme inclusive operating lines (black-solid), lines of constant power (dashed), lines of constant GVO (magenta-solid) and constant kinetic energy lines (dash-dotted)

VSFSC: In terms of speed limitations, the VSFSC scheme is the least restricted (figure 4.15. Since there is no lower speed limit, extraction of kinetic energy in order to allow for a fast power output increase is possible. However, another limitation appears. Switching from operating point $\boxed{A}$ to $\boxed{B}$ requires the operating line to cross the line of constant power output through operating point $\boxed{B}$ at some point in time. An acceleration is only possible above this line, since there the generated power exceeds the power output. Passing this section on the left hand side means that the power output exceeds the generated power at any time, thus, the rotating assembly is stalled. A further difference occurs during the switchover from point $\boxed{B}$ to $\boxed{A}$. Surplus energy is stored in form of kinetic energy, accelerating the rotating assembly. Acceleration in combination with a decreasing flow would move the operating point towards the lower right corner of the unit speed-unit flow characteristic. The S-shape instability in this section requires measures to avoid reaching this section. The S-shape means that there exist three possible operating points referring to one speed value and one GVO ([113], [114]). One measurement in order to avoid the S-shape is to define the lower limit of the GVO as function of the speed. The lower limit of the GVO increases for higher speed values in order to cut out the lower right corner and thereby avoid the S-shape instability. This cut out can be seen beyond the ninth second (fourth squared marker), since at this point the lower limit of the GVO value is reached, which can further only be reduced by decreasing the speed. This appears as an almost diagonal section of the operating line. At second 30, the controller reopens the GVO to settle at the steady operating point $\boxed{A}$.
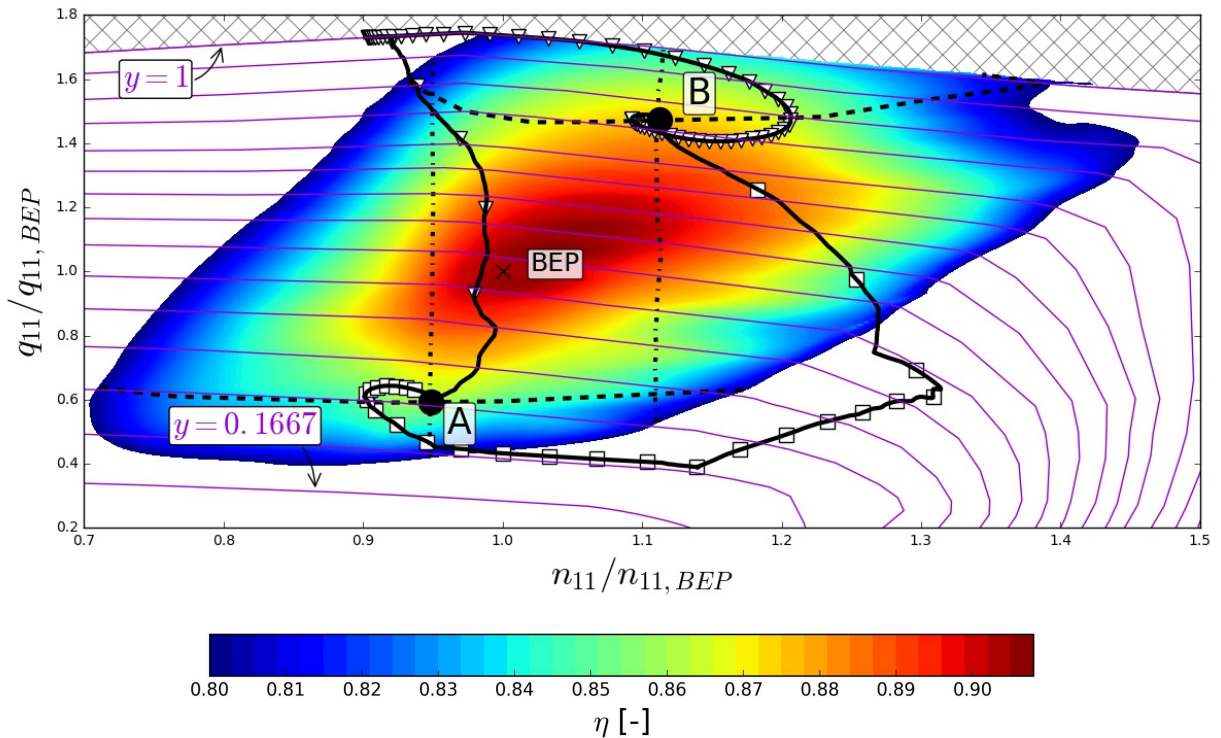

Figure 4.15.: Stationary operating range of the VSFSC scheme inclusive operating lines (black-solid), lines of constant power (dashed), lines of constant GVO (magenta-solid) and constant kinetic energy lines (dash-dotted)

The triangle and square markers of figures 4.13-4.15 mark time intervals of three seconds. To clarify the behaviour of essential parameters, their trends are pictured in dependence on time in figure 4.16. The vertical grid lines, indicating time frames of three seconds, match with

the markers of figures 4.13-4.15. Only the first 30 seconds of the transient simulation are pictured. Within these 30 seconds, not all schemes necessarily reach their steady operating conditions, but the main part of the transient process is finished. Plotted parameters are net head, speed, GVO, efficiency, generated power and power output.

Considering the FSPT scheme's *Outage* compensation, it can be seen that the speed remains constant and the GVs are opened. This opening increases the power output. Missing speed variability forces the FSPT scheme to feed-in the generated power, exclusive losses, into the PS. The reduction of the net head due to changes in the GVO is also visible. The efficiency trend shows low values at the beginning as well as at the end of the time line, interrupted by an convex behaviour. This trend is caused by the passage through the turbine characteristic (figure 4.13) from power output values below the BEP, to power output values above the BEP.

The compensation of the same outage by the VSDFG scheme is presented in the second row, left hand side. The behaviour does not diverge much from the FSPT scheme, even if few differences can be seen. One difference is the lower speed value compared to the FSPT scheme, which is required in order to generate power at higher efficiency values. Referring to the generated power and the power output, a similar behaviour to the FSPT scheme appears. The speed variability does not deliver advantages for the switch between these operating points, since the turbine already operates at minimum speed at the beginning and no kinetic energy extraction can therefore be realized. Different behaviour appears after second 15. At this point, the generated power exceeds the power output, which is accompanied by an acceleration as visible in the speed trend.

The VSFSC scheme operates at lower speed than the schemes discussed before, since this is advantageous in terms of high efficiency values. The generated power and power output trends diverge more than in previous schemes. By varying the power output, the operating line can be adjusted in such a way that it passes through the turbine characteristic in the most efficient way.

Surplus cases are pictured on the right hand side. The FSPT scheme's behaviour is analogous to the one in the *Outage* case. This refers to the almost constant speed value, which just changes with the PS's frequency. The increased head value due to the closing of the GVs and the almost congruent trend of generated power and power output are also analogous to the *Outage* case.

The VSDFG scheme exhibits an advantage of variable speed schemes. The power output declines much faster than the generated power. Thereby, the speed of the rotating assembly increases, but the PS is relieved. Passing second 13, the generated power is lower than the power output and therefore, the rotating assembly is decelerated in order to reach the final operating point. The amount of energy which may be stored in form of kinetic energy is limited by the upper speed limit.

This limitation is non-existent in the VSFSC scheme. As can be seen, the power output drops almost instantaneously. The gradient of the power output is only limited by the generators agility in order to change its power output. Furthermore, the minimum GVO related to the speed value can be seen. The GVO reaches its speed dependent lower limit around second ten. By permitting a further closure of the GVO, the flow deceleration stops, the net head drops and the generated power falls below the power output. Thereby, the speed decreases and its related lower limit of the GVO value too.
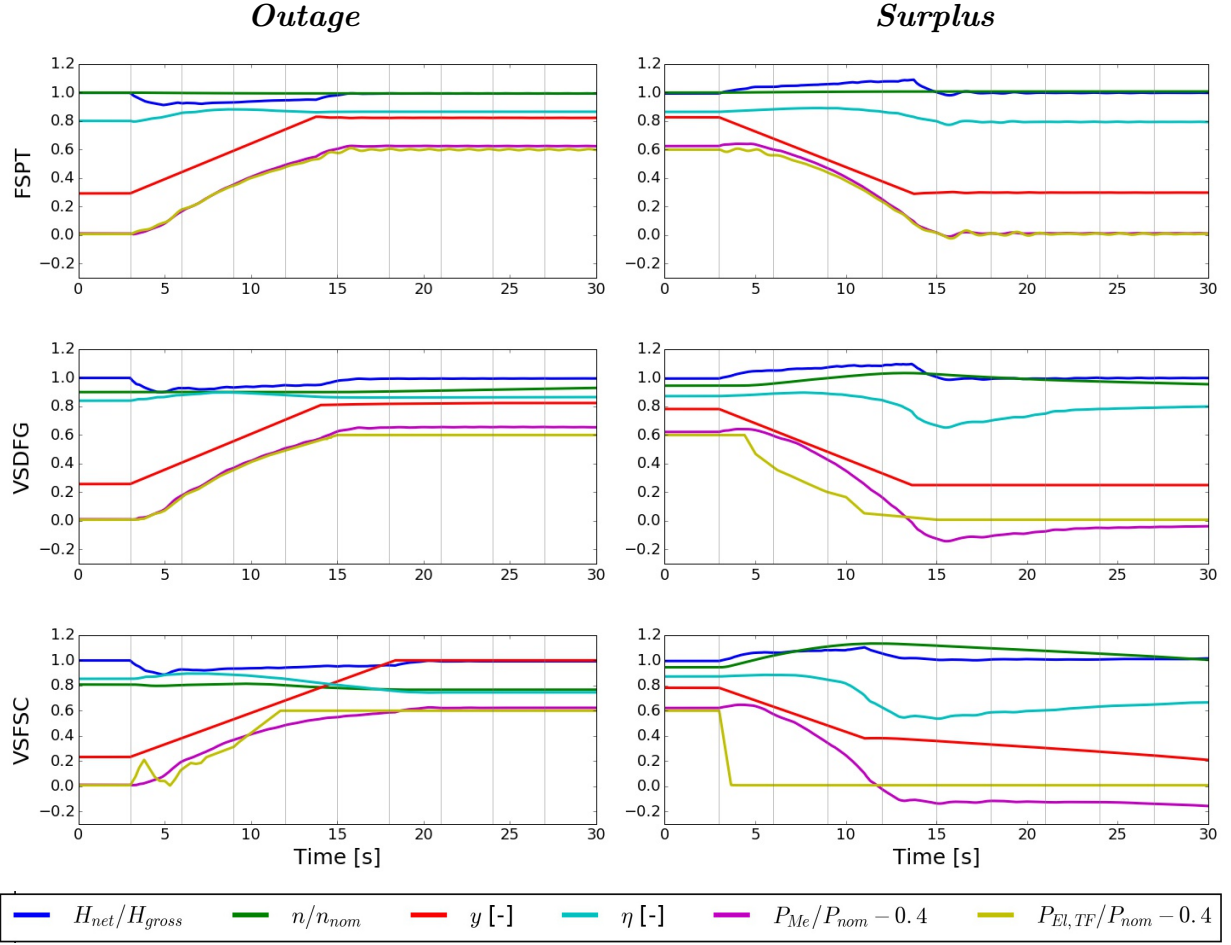
Figure 4.16.: Main plant parameters with respect to time while changing the operating point

As mentioned, the above examined transient behaviour is accompanied by a frequency deviation, which is tantamount to a power imbalance. For the frequency trend presented in figure 4.17, the imbalance is simplified to the difference between the 3000 MW power imbalance in the PS and power output of the PSP and the additional required plants. The response of a real PS is more complex since the consumption also depends on the frequency value and additional balancing energy is provided. However, presented trends are not to be seen as usual imbalance cases, but more as a possibility to compare the reactions of different PSP schemes to an imbalance.

The figure shows the frequency drops in the *Outage* case and the frequency surges in the *Surplus* case for the three investigated schemes. The response to the *Outage* is quite similar for all schemes, since their power output trends are very similar. With respect to the *Surplus* case, the responses vary widely. The FSPT scheme leads to the highest deviation from nominal frequency, followed by the VSDFG and the VSFSC schemes. This is caused by the ability of storing surplus energy in form of kinetic energy. As visible in the first row of figure 4.16, a linear change of the GVO is not tantamount to linear change of the generated power. The concave behaviour of the generated power causes different cumulative deviations in the *Outage* and *Surplus* case. Therefore, the frequency deviations, even for the FSPT scheme case, are different in the *Outage* and *Surplus* case.

The ability to compensate a power imbalance in the PS strongly depends on the chosen operating points A and B. Different efficiency trends, initial and final speed values and

section restrictions due to the line of constant power output can be named as reasons.
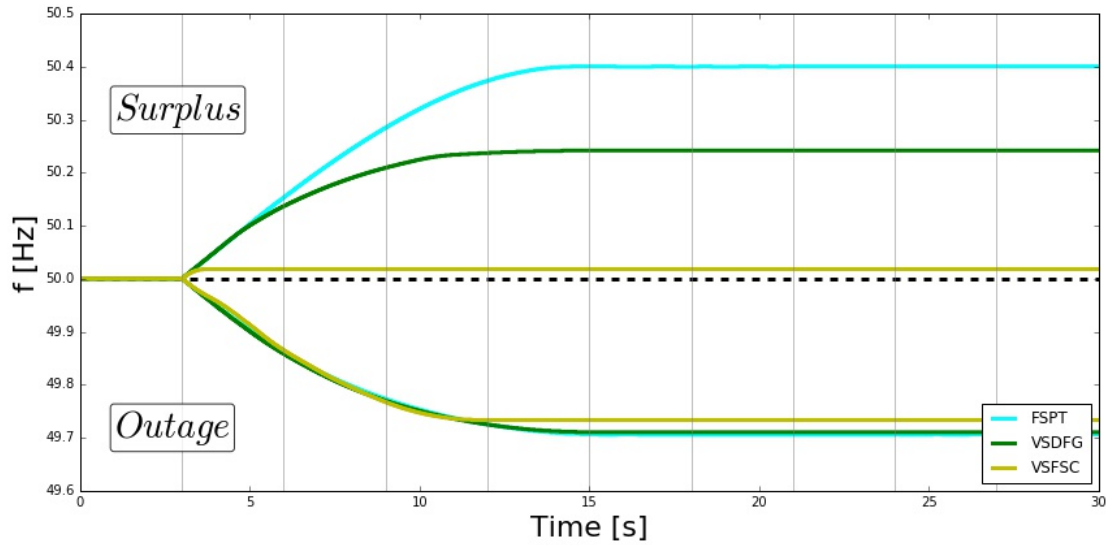

Figure 4.17.: Frequency deviation of *Outage* and *Surplus* cases for different schemes

Frequency Deviation Characteristic

Since simulation results of power imbalance compensation cases can be summed up in one value, namely the maximum frequency deviation, all combinations of initial and final power output values (P_I, P_F) can be simulated and merged in one figure. The merged simulation results of approximately 140,000 transient simulations are presented in figure 4.18. The frequency deviation is plotted depending on initial and final power output for the three investigated schemes. The diagonal magenta line indicates the same initial and final power output values and therefore, no imbalance and, subsequently, no frequency deviation. An increasing distance from this line is tantamount to an increased power leap to be compensated. Graphs include marks of the example case frequency deviations indicated by A $\Rightarrow$ B and B $\Rightarrow$ A, respectively. The size of the square indicates the operating range of the different schemes. It can be seen how the square size increases with increasing speed variability.

Primarily, the results of the *Outage* case are considered. For the FSPT scheme, a continuous rise of deviation can be seen for increasing power leaps. Better response behaviour occurs for low initial power output values, shown by the sharpening form of the colour coded plot towards higher initial and higher final power output values. The reason for this is the combination of the linear closure law with a non-linear relation between GVO and power output. The VSDFG scheme's *Outage* case shows a similar behaviour for low initial power output. In case of an initial power output value beyond 80 % of the nominal power output value, the speed belonging to the initial power value increases from minimum speed value towards higher speed values and thereby provides a kinetic energy buffer. With an increased buffer of kinetic energy, the change from initial to final power output is no longer restricted by the agility of the GVs. Kinetic energy can be extracted and, therefore, the change from an initial operating point of high power output towards a final operating point of even higher power output is only restricted by the generators agility. The imbalance-compensation performance of the VSFSC scheme is superior to the FSPT and VSDFG schemes in a large section. The non-existent lower speed limit enables extraction of kinetic energy at each

initial speed. However, the behaviour of high power leap compensation is the worst of all schemes. Since high power output may only be generated at high speed, but the turbine operates at low speed for low initial power output values, the rotating assembly has to be accelerated during the operating point change. This acceleration is tantamount to less power output than generated power (losses neglected), which causes higher frequency deviations as indicated in the upper left corner.

The *Surplus* case of the FSPT scheme shows more disadvantageous frequency deviations than in the *Outage* case. This asymmetry is due to the mentioned non-linear behaviour between the GVO and the power output and is shown by the red area of the FSPT scheme's graph in the lower right corner. The VSDFG scheme does have a favourable behaviour in the *Surplus* case. Surplus generated power can be stored in form of kinetic energy and the power output can therefore be adapted rapidly to the required value. Increasing speed values for an initial power output value beyond 0.8 reduce the available kinetic energy buffer. This means that the kinetic energy buffer is too small to buffer surplus energy entirely for great differences between initial and final power output. The resulting higher frequency deviations are visible in the lower right corner. Finally, the VSFSC scheme presents the ideal behaviour in order to compensate an imbalance in the *Surplus* case. Within the entire area, a minimal frequency deviation appears. This is because the entire surplus energy can be buffered in form of kinetic energy, unrestricted by any speed limitations.
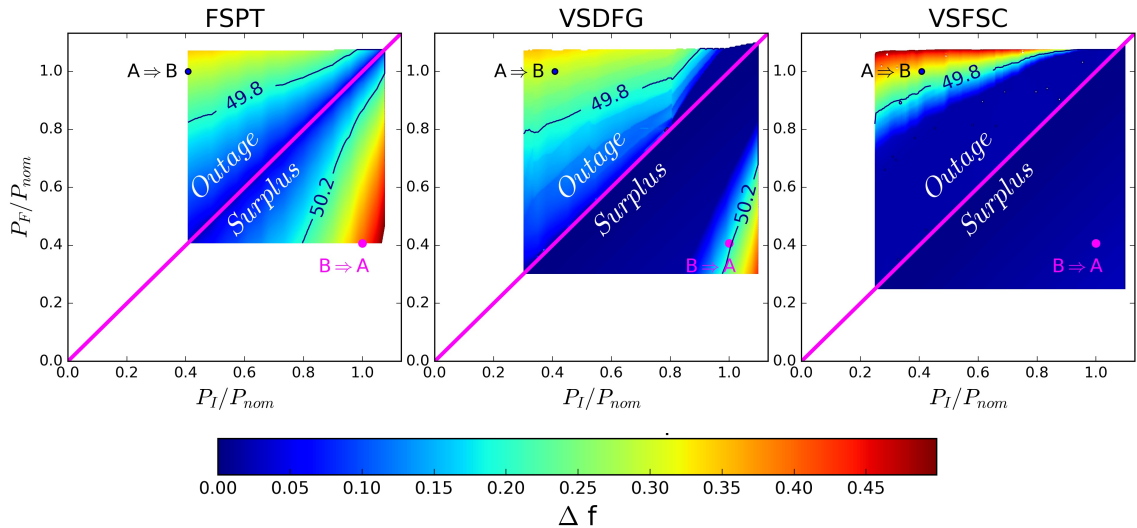

Figure 4.18.: Frequency deviation characteristics in turbine mode for different PSP schemes

Beside the turbine mode, the pump mode is investigated as well. The results are pictured in figure 4.19. This figure shows the FSTS0 and VSFSC schemes, since the FSPT and FSTS schemes do not allow for power regulation in pump mode and the characteristic of the VSDFG scheme is part of the VSFSC scheme's characteristic.

Taking a closer look at the FSTS0 scheme, the so far widest operating range, made possible by the HSC operation, can be observed. The shape of the FSPT scheme's characteristic in turbine mode and the FSTS0 scheme in pump mode are very similar, but with different ranges. This can be explained by the almost steady operation of the pump for all power output values and the power regulation by the turbine, which has a quite similar behaviour to the FSPT scheme in turbine mode.

The characteristic of the VSFSC scheme, which includes the characteristic of the VSDFG

scheme, shows an optimal behaviour. The homogeneous characteristic is made possible by the advantage that the GVs are opened and only the power has to be controlled. Since the power is controlled by the generator, steep gradients are possible. The natural stability in pump mode is another of its advantages. This means that in pump mode, the absolute values of power and speed are proportional, while in turbine mode, these parameters are indirectly proportional, e.g. from a steady initial operation in

- **Pump mode**:
  - **Increase of the pump power output:** In case the pump power output has to be increased, the generator transfers more power to the pump-turbine. Therefore, the rotating assembly accelerates, which causes a higher hydraulic power. The increased pump power output and the increased hydraulic power achieve an equilibrium and thereby a steady operation.

  - **Decrease of the pump power output:** In case the pump power output has to be decreased, the generator transfers less power to the pump-turbine. Therefore, the rotating assembly decelerates, which causes a lower hydraulic power. The decreased pump power output and the decreased hydraulic power achieve an equilibrium and thereby a steady operation.

- **Turbine mode**:
  - **Increase of the turbine power output:** In case the power output has to be increased, the generator extracts more power from the pump-turbine. Therefore, the rotating assembly decelerates, which causes a lower hydraulic power. The increased power output and the reduced hydraulic power achieve an imbalance and thereby an unsteady operation. Thus, an additional controlling (GVO) is necessary.

  - **Decrease of the turbine power output:** In case the power output has to be decreased, the generator extracts less power from the pump-turbine. Therefore, the rotating assembly accelerates towards the S-shape instability. In order to avoid operation close to the S-shape, an additional controlling (GVO) is necessary.
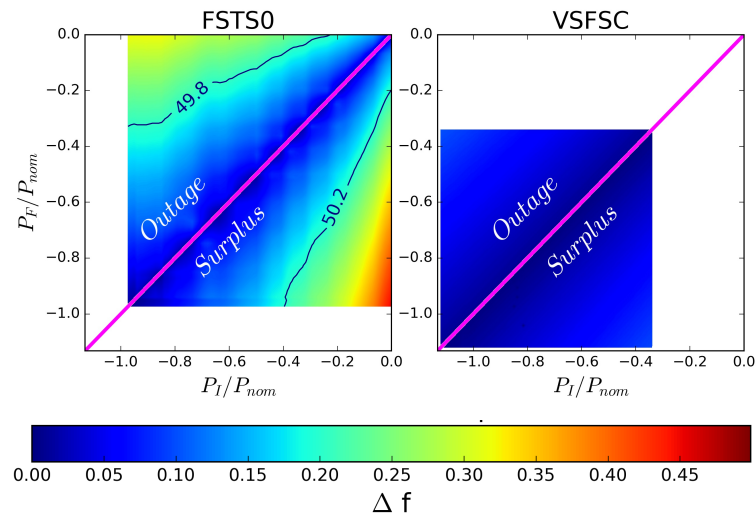

Figure 4.19.: Frequency deviation characteristic in pump mode for different PSP schemes

Influence of the Closure Law

The FSPT scheme in turbine mode (figure 4.18) and the FSTS0 scheme in pump mode (figure 4.19) show that the imbalance behaviour is not symmetrical with respect to the magenta lines. Furthermore, the behaviour worsens for high initial and final turbine power output and low initial and final pump power output, respectively. This is because of the application of a linear closure law. The difference between a linear and non-linear closure law is presented in figure 4.20. The red trend in the uppermost row represents the power reference signal in the *Outage* case and the *Surplus* case, respectively. Trends belonging to a linear closure law are printed solid, while trends showing the behaviour for a non-linear closure are plotted in dashed form. At first, the linear closure is considered. The asymmetrical behaviour of the FSPT and FSTS scheme's frequency is directly proportional to the filled area between power reference signal and the trend representing the power output of the linear closure case. It can be seen that this area is smaller in the *Outage* case than in the *Surplus* case. Since a linear closure law is applied, neither the flow variation nor the power are linear. The closure time is limited by the water hammer. In the third row, it can be seen that the extreme head values appear at low GVO values. A rapid change between two operating points requires the head trend to be as steady as possible and close to its extreme value during the transient process. Such a head trend would cause a linear increase or decrease of the output power and thereby, the *Outage* and *Surplus* case frequency deviation would be the same size. An approximation can be accomplished by changing the closure law in such a way that the GVs open faster at high GVO values. Thereby, the required time to switch between operating points is reduced and the head value approximates closer to its extreme value for high GVO values.

The changed closure law, allowing for higher change rates of the GVO at high GVO values, is presented by the dashed trends. Due to the non-linear closure of the GVs (second row), the change of the flow rate (fourth row) appears to be approximately constant for the time in which the GVO changes. The almost constant change of the flow rate is accompanied by an approximately constant head value trend during the phase of the GVO change. This becomes visible by comparing the linear closure head trends with the non-linear closure head trends. In terms of agility, it is visible that the feed-forward part of the GVO controlling, in the case of the linear closure law, is finished after second 13.5, while in the case of the non-linear closure law, it is already finished after second 11.5.
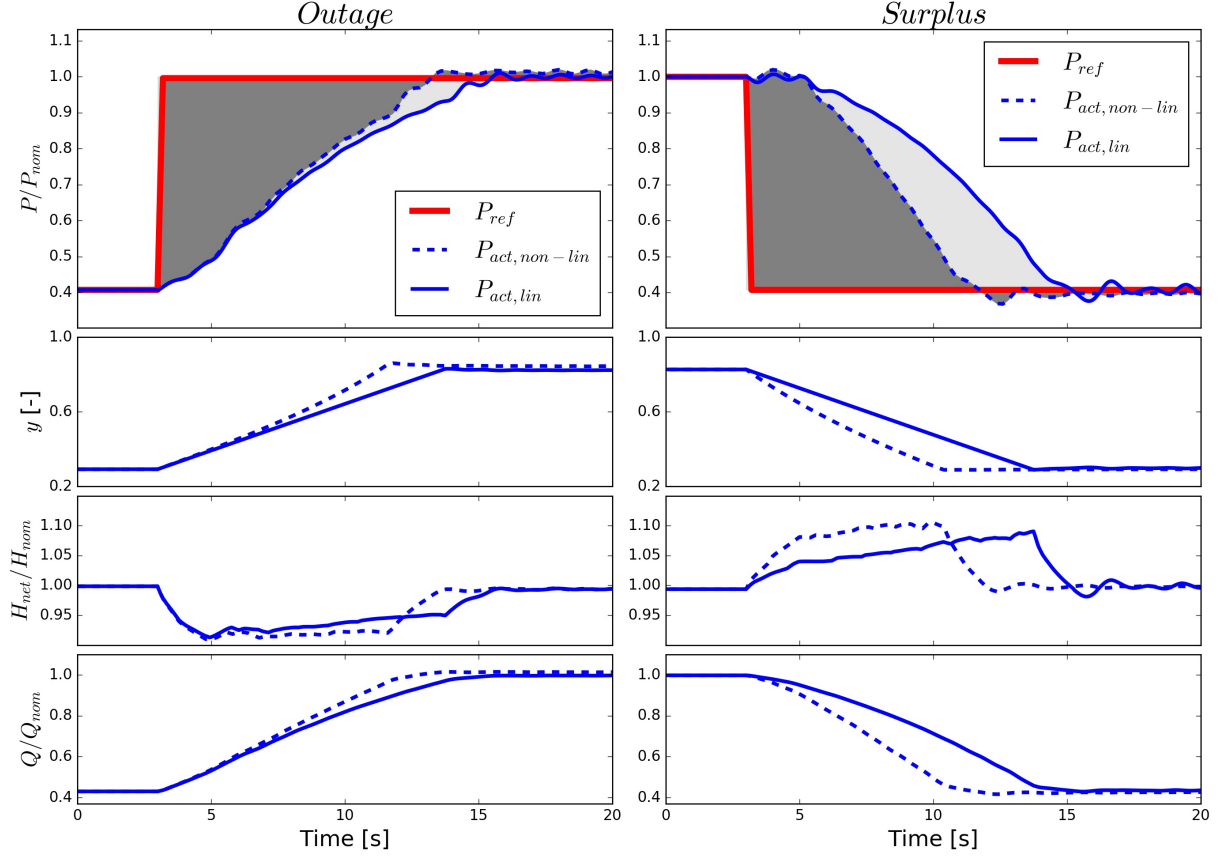
Figure 4.20.: Operating point change in turbine mode by applying a linear closure law (solid) and the non-linear closure law (dashed)

The frequency response in turbine mode as a result of a non-linear closure law can be seen in figure 4.21. Considering the *Outage* case, an improvement for all three schemes is achieved. The larger GVO gradient at high GVO values leads to a reduced opening time and thereby to marginal lower frequency deviations in the *Outage* case.

For the *Surplus* case, the FSPT and VSDFG schemes' behaviour is even more enhanced. Red areas in figure 4.18, indicating high frequency deviations, have entirely vanished in figure 4.21. Beside the above mentioned enhancements, the schemes also show a better behaviour at high initial and high final power output values. Since high power output values are accompanied by high GVO values and the non-linear closure law allows for higher GVO gradients, the plants are more agile at high power values than in the case of a linear closure law and the frequency deviations are thereby reduced.
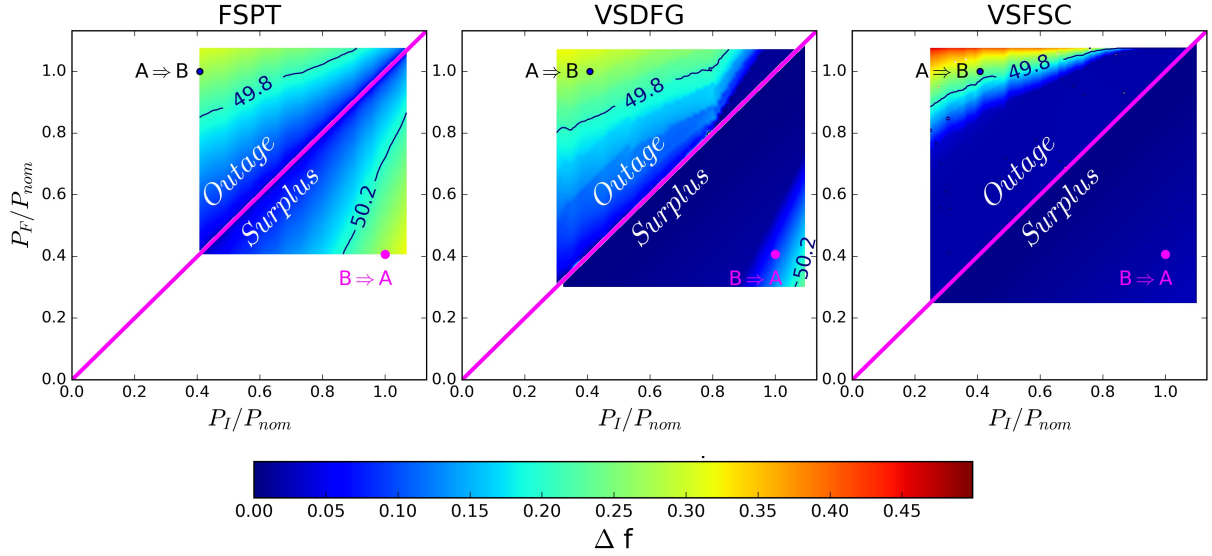
Figure 4.21.: Frequency deviation characteristic in turbine mode for different PSP schemes by applying a non-linear closure law

4.3.6. Transient Optimization

As mentioned in subsection 4.1.3, there exist two controllers for variable speed schemes: one acting on the turbine's GVO, the other acting on the generator's phase and line voltage. As the controllers influence one another, a superior control has to be applied in order to avoid the stall of the rotating assembly in turbine mode. This stall effect refers to the effect that the power output is higher than the generated power, losses neglected, and thereby, the rotating assembly is decelerated in such a way that the plant is not able to reach a steady operating point.

Stall Effect and Control Strategy of Variable Speed Plants

One critical point where such a stall effect may appear is in the *Outage* case if a fast switch from a low power output value towards a high power output value is required. If there is no interconnection between the two controllers, the generator controller increases the power output in time frames much shorter than the turbine controller opens the GVs. Thus, the increased power output reduces the kinetic energy by means of speed reduction. Since the generated power is, according to equation 4.2, proportional to the speed, the maximum generated power decreases in case the speed is reduced. The tipping point is a point where the GVs are completely open, but the speed is already so low that the generated power can not exceed the power output. In case the power output is higher than the generated power, the speed is further reduced until even the transient operating limits is breached. In order to avoid this behaviour for critical power leaps, the generator controller follows an optimized power reference signal instead of the required power reference signal. The optimized reference signal is determined in an optimization task and contains the power output values for the first 30 seconds of the transient process. An example for such an optimized power reference signal can be seen in figure 4.16 for the VSFSC scheme in the *Outage* case. The target function to be minimized in order to define such an optimum power reference signal is presented in

equation 4.3.

The bottleneck of the transient optimization is the net head variation caused by the water hammer. Even if not directly visible in equation 4.3, the net head influences the hydraulic power, which is linked to the generated power by the efficiency. To avoid the determination of the net head value within the optimization procedure, a systematic calculation sequence of different *Outage* cases is applied. Starting with equalling initial and final power output values, where the net head stays constant during the whole simulation, the final power output is slightly increased with each further case. The optimization script uses the net head trend of the previous transient simulation to determine the optimum power reference signal. The slightly changed final power output of each further case is accompanied by slightly different net head trends. After the optimization, the transient simulation is carried out in SIMSEN and the resulting head trend is used for the following optimization case. By reducing the leap steps from one case to the next, an arbitrary precise accordance between transient optimization and transient simulation can be achieved.

$$P_{Me} = 2 \cdot \pi \cdot T \cdot n \tag{4.2}$$

$$TF = \int_t (P_{imb}(t) - P_{Me}(t) - P_{kin}(t)) \cdot dt \tag{4.3}$$

Wherein the power output is defined as in equation 4.4.

$$P_{El,TF} = P_{Me} + P_{kin} \tag{4.4}$$

As visible in equation 2.3, the generated power output depends on the net head. The worst case is the change from a low initial power output value, generated at low speed values, towards high speed requiring high final power output values. This issue will be explained in the following three paragraphs.

Unproblematic Power Leap (figure 4.22): For a relatively small step between initial and final power output no superior control is required. On the left hand side, the switch without a superior control is pictured, while the right hand side shows the switch with a superior control. The magenta coloured line represents the operating line as result of the optimization process. The lowest graphs show the trend of the power output ($P_{El,TF}$) and the generated power (P_{Me}). It can be seen that the power output changes with a steep gradient for the not-optimized and the optimized case, respectively. While the power output changes to its final value within less than a second, it is visible in the uppermost graph that the generated power exceeds the final power output at around second seven (shown by the operating line intersecting the line of constant power output through operating point $\boxed{B}$). This means that for the first seven seconds after the incident, the power output is higher than the generated power. Thereby, kinetic energy is extracted, leading to lower speed values as visible in the speed plots. In case the operating line is within the parabola through point $\boxed{B}$, the generated power exceeds the power output and thereby, the rotating assembly is accelerated.
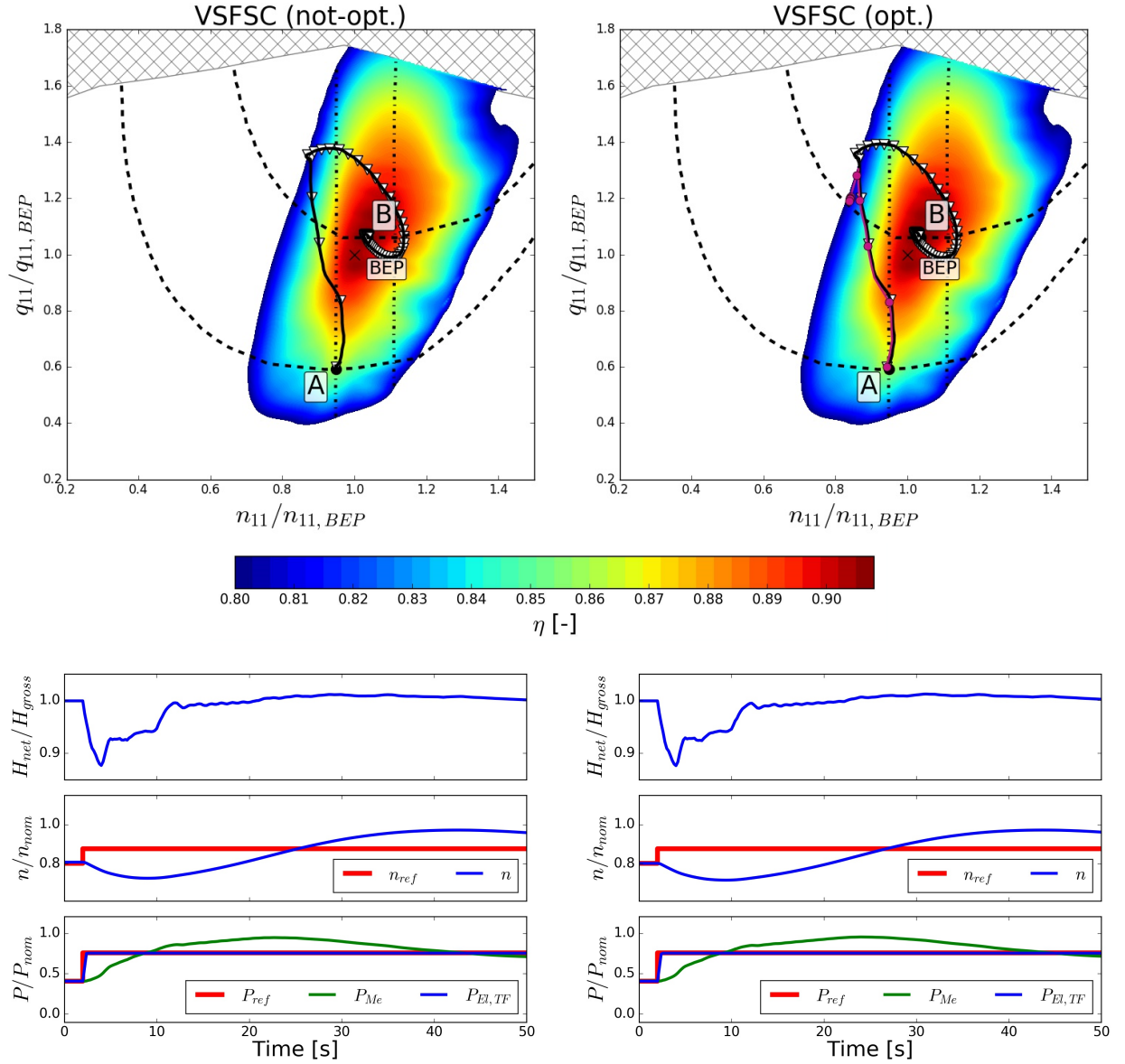
Figure 4.22.: Not-optimized vs. optimized change from 0.41 0.75 power output

Power Leap towards a Point requiring superior Control (figure 4.23): In case a higher final power output is required, the operating point B and, both the operating point and the parabola of constant power through the former move upwards to higher unit flow values. This comes along with higher minimum unit speed values required for the operating line to intersect the parabola through operating point B. Considering the not-optimized case, it can be seen in the lowermost graph that the power output is increased in the fastest way possible to its final value. Since the power output exceeds the generated power, the speed declines. As visible in the uppermost graph, the speed decline forces the operating line to pass by the parabola through operating point B without intersection. Without operation within the parabola, no acceleration is achieved and the rotating assembly stalls as visible in the speed graph. The stalling continues until even the transient operating limits are breached. At this point, the power output is reduced (second 23 in power graph). The opened GVs in combination with zero power output lead to an acceleration of the rotating

assembly. As soon as the speed is within the transient operation limits, the power output is increased. The power output increase leads to a deceleration, a breach of the transient limits and a reduction of the power output. This is an infinite loop shown by the oscillation of the power output trend.

In comparison with the optimized power reference signal, the optimized case varies the power output directly after the incident in order to intersect the parabola of constant power through operating point $\boxed{B}$. The non-obvious form of the power reference signal is better visible and therefore, explained in the following case.
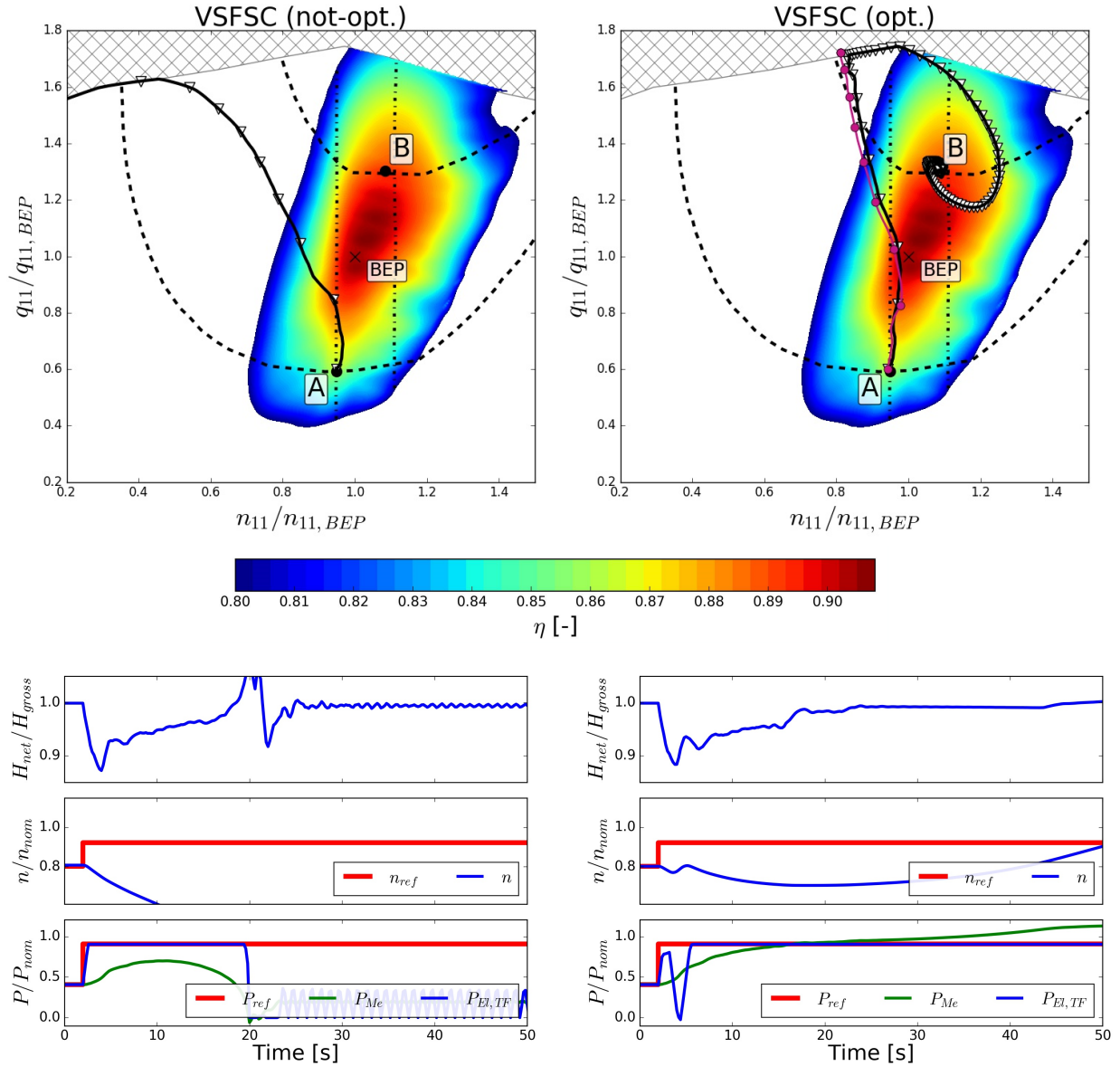

Figure 4.23.: Not-optimized vs. optimized change from 0.41 to 0.91 power output

Switching to the highest possible Power Output Value (figure 4.24): The last case illustrates the switch from a low initial to the highest possible final power output value. The not-optimized case behaves the same way as in the case presented before. The power output ramp follows the steep ramp of the power reference signal, stays at its required power

81

output value but thereby stalls the rotating assembly. In the optimized case, the optimized power reference signal adapts the operating line in such a way that it is able to intersect the parabola of constant power through operating point $\boxed{\text{B}}$. The resulting operating line can be subdivided into two parts. The first is to follow the BEL in order to generate maximum possible power output for each GV opening, the second is to extract as much kinetic energy as possible while still allowing the operating line to intersect the required parabola. The almost congruent trend of operating line and BEL is visualized by the plot of the BEL (green).
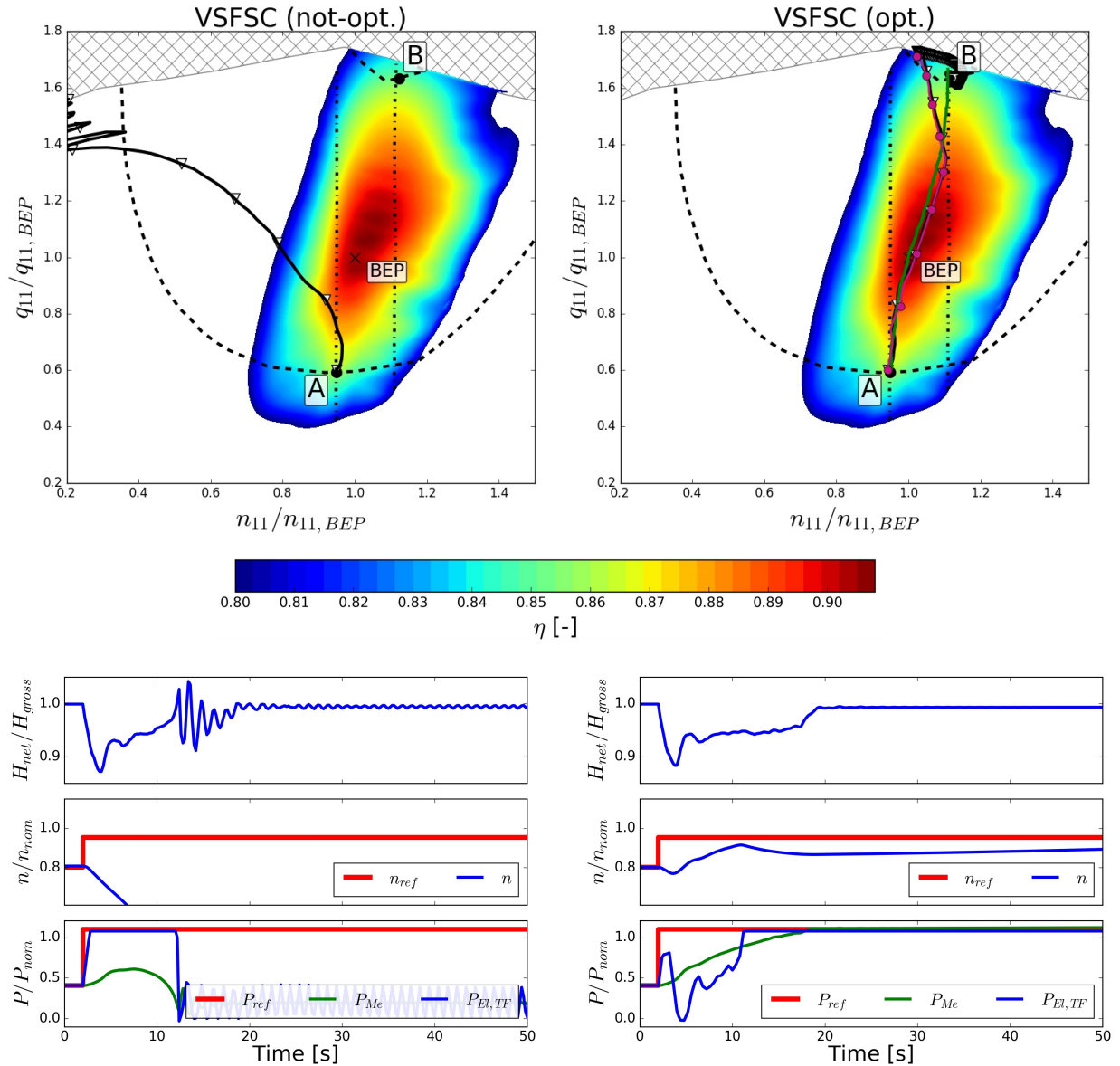

Figure 4.24.: Not-optimized vs. optimized change from 0.41 to 1.08 power output

Following the BEL during a transient operation requires the power output for compensating water hammer effects as can be seen by comparing the head and the power output trends. This means, that the net head decrease also calls for a speed decrease in order to keep the unit speed constant (equation 2.1), as it is required for the beginning of the transient process. This can be accomplished by a power output exceeding the generated power as visible in the

power graph. After the almost vertical increase of the operating line, an almost continuous increase of the unit speed and unit flow occurs. The increase of the unit speed is realized by an increasing speed. This is enabled by the power output being lower than the generated power. The final part is the extraction of kinetic energy during a time span, in which the power output is above the generated power. At the end of this section, the operating line has already crossed the parabola through the operating point $\boxed{\text{B}}$ and the settling process for the stationary operating point $\boxed{\text{B}}$ takes place.

4.4. Discussion of the Transient Simulations

Within chapter 4 sensitive cases appearing during transient operation are examined. Such cases are the connection to the PS, the influence of one generating unit on the other, the ability to follow a power reference signal as accurate as possible and the ability to stabilize the power system if an imbalance occurs.

The analysis of PSP connecting to the PS shows that with increasing flexibility the connection time decreases. This result does not align with [45]. The difference may conclude from the fact that most PSPs are fixed speed schemes and therefore, there exist plenty experience while the variable speed schemes' controlling may still be improved.

The impact one unit may have on another is demonstrated by connecting two units sharing one water way simultaneously to the PS. The water hammer, caused by the opening of one pump-turbine's GVs, propagates towards the other pump-turbine and the following head variation delays the connection about 50 seconds.

The ability to follow a power reference signal is of high interest in the event that balancing energy is delivered, since deviations to the reference signal are not paid. The three schemes capable of delivering balancing energy showed that the variable speed schemes' deviations are at least 30 times smaller than the deviations of schemes with fixed speed. This is caused by the advantage of controlling the power from the generator side instead of the GVO. The VSDFG scheme's deviation is about four times higher than the VSFSC scheme's deviation. This difference is due to the speed restriction of the VSDFG scheme.

For the as soon as possible compensation of an imbalance in the PS it is essential that PSPs may change their operating point as fast as possible. The flexibility of PSPs vary widely since variable speed schemes may make use of their rotating assemblies' kinetic energy. In order to provide a fair comparison of all schemes, all possible imbalance compensations are simulated. The resulting PS frequencies are combined to one characteristic for each scheme, respectively. The advantage of increasing speed variability is clearly visible. Nevertheless, in the mentioned characteristics exist sections where fixed speed schemes outperform variable speed schemes. Furthermore, in order to operate the VSFSC scheme in this section, a superior control is required. This control is realized by a transient optimization.

The transient optimization's purpose is to find the best possible compromise between compensating an imbalance in the PS and stalling the pump-turbine. The rotating assembly may be stalled in case an imbalance in the PS requires the VSFSC scheme to change its operating point from a low power output to an operating point delivering a high power output. The transient optimization predefines a power output signal, which the generator has to follow.

5. Conclusion

In the presented work, common pumped-storage schemes have been investigated and compared to each other. The investigated schemes include fixed and variable speed schemes as well as binary and ternary sets. The main points investigated are losses, economics and the transient behaviour of the different schemes.

In the losses-chapter (2), the operating ranges of the different pumped-storage plant (PSP) schemes have been elaborated and the plant efficiency values have been determined in dependency on the power output as well as on the gross head value. It has been shown that plants which are able to be operated in the hydraulic short circuit mode have the biggest operating range, but that these operating ranges result in a lower efficiency.

Based on the operating ranges and efficiency values of the losses-chapter, an economic investigation has been carried out (chapter 3). The profitability of the different power plants has been calculated by comparing the possible income with the investment costs. For the possible income, an optimization task has been applied. The task takes into account the day-ahead market, primary control market, secondary control market, power respectively head dependent efficiency and storage management. It shows that the income on the day-ahead market is much smaller than on the balancing energy market. The operating range is the parameter with the most influence on the balancing energy market income. Considering the investment costs, it has been shown that all PSP schemes are within a narrow price range. Whether binary set, ternary set, fixed speed or variable speed scheme, the investment costs vary by less than 15 %. The reason for such a small variation is that the majority of the costs are widely independent of the scheme. Such cost elements are the costs for the engineering, head water, waterway, cavern and motor-generator. The profits show that the FSTS0 scheme is the most profitable, followed by the VSFSC and VSDFG schemes. The FSPT and FSTS schemes do not generate profits under the current circumstances and are thereby uneconomically. Beside the PSP schemes, the economic investigation has also considered the possibility of a battery storage. It has turned out that this type of storage does generate the most income, but due to its high investment costs, this storage technology is not profitable for the investigated case either.

In the transient chapter (4), models of different PSP schemes are established in order to investigate their transient behaviour. For one scheme a validation has been carried out, which shows that the transient model, in terms of following a power reference signal, is more accurate than the real plant. Afterwards, the transient model's behaviour regarding vibrations has been examined, showing possible interactions of the generator's natural frequency and the natural frequencies of the waterway. The calculated income and profitability of the second chapter assumed a perfect accuracy in terms of following a power reference signal. Nevertheless, switchover processes and limitations of the power control speed have led to inaccuracies. Therefore, the start-up and the accuracy with respect to follow a power reference signal have been investigated. The start-up has shown clear advantages of variable

speed schemes. The VSDFG scheme needs 20 % less start-up time than the FSPT scheme. The VSFSC scheme even cuts down the start-up time by another 50 %. The control speed investigation of the VSDFG, VSFSC and FSTS0 schemes has been realized by following a power reference signal which depends on the power system frequency. It has turned out that the different control strategy for the FSTS0 scheme leads to an eight percent deviation of the generated and required balancing energy, while the VSDFG and VSFSC schemes' deviation is only 0.24 and 0.051 %, respectively. Referring to the VSDFG scheme's accuracy, a trade-off between efficiency and flexibility has to be found. High efficiency values for low power output values call for low speed, while high flexibility requires high speed values. In order to evaluate the technical limits of compensating power system faults, all combinations of two power output values have been simulated. The results of these calculations have been used to generate characteristics, showing that variable speed schemes are not necessarily better for all fault cases than fixed speed schemes. It has also turned out that for some fault cases, a superior control is required. A transient optimization task has been applied as such a control. This optimization predefines an optimized power reference signal in such a way that fault cases which are not compensable without this optimization, become compensable.

Conclusively, it can be said that all relevant aspects of a plant operation have been addressed in this work. Operating ranges, losses, income, costs, profitability, vibrations, start-up and fault compensation have been investigated with a partly validated model. The developed model structure and the interaction between the individual models is a new approach which allows for a variety of investigations. It has been shown that the FSTS0 scheme is the most profitable scheme as it possesses the widest operating range, while the variable speed schemes are preferable in terms of generation accuracy. The combination of a transient optimization with a transient simulation was proven to be useful. The developed models address the majority of operator issues and can be used for a preliminary design of new projects or as virtual plant in order to compare simulated and real plants for the purpose of parameter adjustments.

6. Outlook

In this work, pumped-storage plant schemes have been investigated with regard to their losses, profitability and transient behaviour. Suggested work to continue this work is:

In the losses-chapter, it is assumed that the operating range is limited by a minimum hydraulic efficiency value of 80 %. This is only an approximated value and should be specified more accurately in terms of cavitation, vortices and vibrations.

The economic chapter takes into account the day-ahead and balancing energy market. For storage applications with small capacity, the intraday market may be a useful supplement and should therefore be taken into account as well. In terms of storage capacity, a one-week storage and two-days storage are investigated. It has turned out that the income of both storages is almost the same. The economical investigation can be used in order to examine the lowest required storage capacity, which does not significantly reducing the income. This result is of importance, since at a certain capacity-power ratio of the storage, battery storages become more profitable.

The model validation within the transient chapter only consists of an accuracy comparison between power reference signal and power output. Beside the accuracy of following a power reference signal, simulated parameters like net head, speed, guide vane opening, flow and mechanical power should be compared with real plant values as well. The start-up in turbine mode is completely simulated in SIMSEN. However, the start-up in pump mode could be enhanced. The blow out process and the ancillary motor could be reproduced more accurately. A more accurate start-up model would allow for estimating the influence of the start-ups on the possible accuracy of following a power reference signal.

For specific cases, the generated frequency characteristics are presented. A completion of the other schemes has not been performed due to the high required computational time (several weeks per scheme).

A high potential is ascribed to the transient optimization. Only used for the switch between two steady operating points, a possible application would be for more complex power reference signals. An implementation of an optimizer to a transient simulation software would allow for several additional applications, but its accomplishment is assumed to be time-expensive.

The presented work has dealt with losses, economics and transient behaviour. These topics are of interest for plant operators and therefore, a cooperation with operators is recommended for further work. Validated economic models allow for the development of operating strategies in order to maximize the income. The developed transient models make it possible to estimate the loss of income caused by an inaccurate generation. An additional application could be to estimate the profitability of a new plant. Since the entire technical and economical behaviour can be simulated, a very accurate estimation of a real plant can be made. Beside the mentioned applications, the models enable to operate plants entirely virtually. Thereby, control parameters can be varied to enhance the dynamic behaviour of a real plant.

A. High head Ternary-set

The majority of pumped-storage plants fall into the category of pump-turbines or Francis-turbines in combination with a pump. Nevertheless, high head applications are usually executed with a Pelton-turbine in combination with a multi-stage pump. Therefore, an additional model has been developed in order to investigate analogous behaviour for this kind of plants. In this chapter, the model is presented and different control strategies are investigated. Figure A.1 shows the SIMSEN model of the high head PSP. The model consists of a head water, tail water, water way, surge tank, fixed speed Pelton-turbine (FSPTT), fixed speed pump (FSP), mechanical masses of pump, turbine and generator rotor and the electrical equipment including MG, circuit breaker, TF, electric line losses and the PS. Furthermore, the model contains the following control and controlled elements, respectively:

- **Input:** The input elements read in the power reference signal.

- **Green framed block:** The green framed block contains elements calculating nozzle values, state and action of the gear coupling, speed values for the start-up converter, value and action of the valve and predefined nozzle values associated with the current power reference signal value. The two leftmost elements of this block check the current state of the power plant and determine which state is required.

- **FSPTT:** The elements upstream the arrow indicating the opening of each nozzle (y), respectively, determine the required nozzle position in dependence on predefined values and the control strategy.

- **Loss Coefficient:** The HSC requires a valve in order to stop the flow through the pump in case the pump has to be shut down. This element calculates the loss coefficient (K), which is set on the valve. This coefficient has to be minimal if the pump is operational and maximal if not. The loss coefficient simulates the state of the valve (opened, closed, partially closed).

- **External torque:** The external torque is required, similar as in the pump-turbine model, in case the pump has to be accelerated for the purpose of connection. This external torque simulates the hydraulic torque converter. If the speed matches with the speed of the generator, the gear coupling ([50], [115]) is closed and the external torque is set zero, which means that its value has to be provided by the generator.
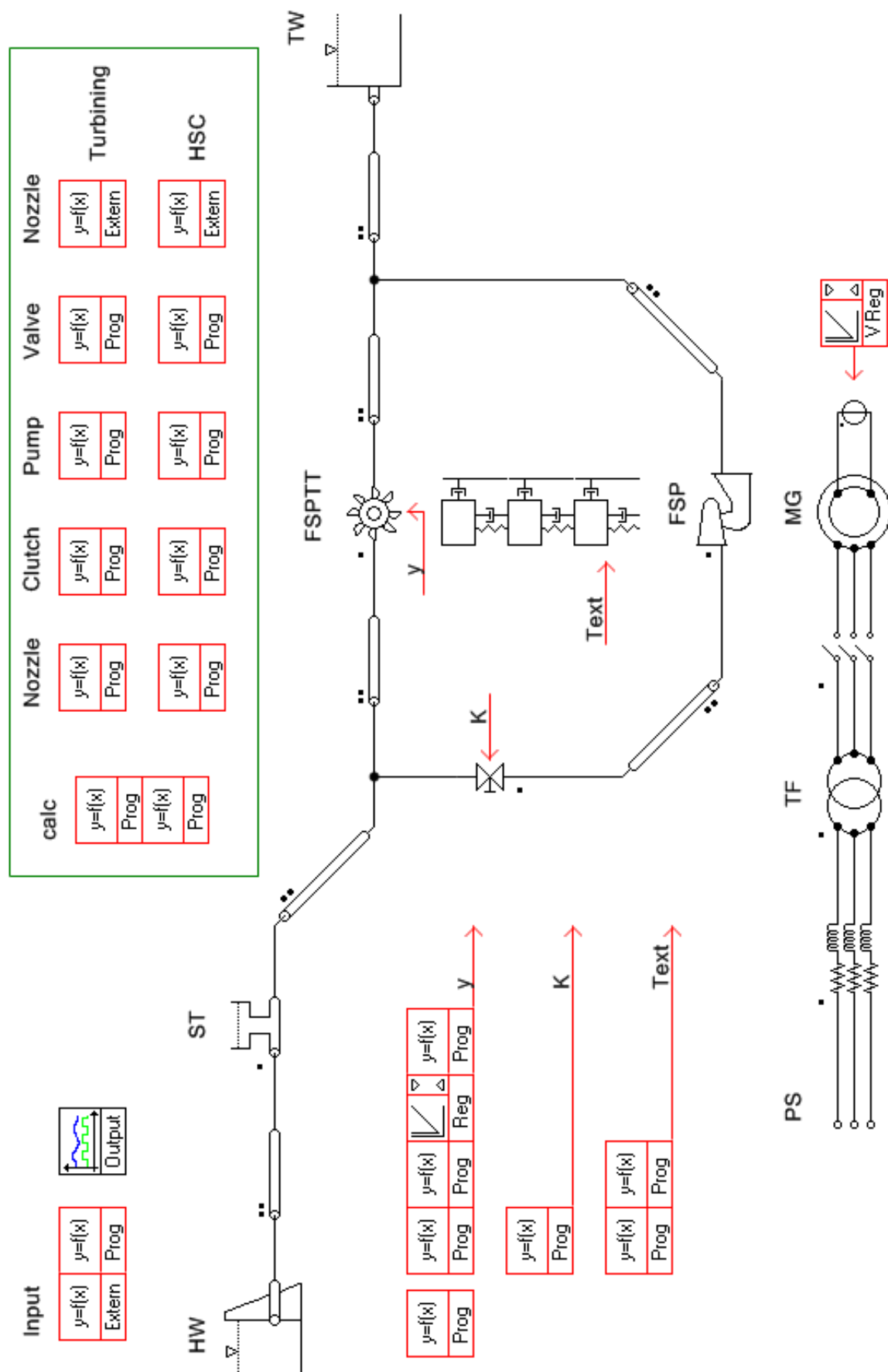
Figure A.1.: High head ternary set scheme

A.1. Characteristics of Pelton-Turbines

A ternary set consisting of a Pelton-turbine and a (multi-stage) pump distinguishes in several points from a ternary set with a Francis-turbine and pump. Pelton-turbines allow for a higher accuracy regarding power generation than Francis-turbines. The higher accuracy is reached due to power regulation by the more flexible nozzles instead of the GVs. An additional advantage of nozzles is a higher efficiency across a wide power range by varying the number of active nozzles [47]. Pelton-turbines are action turbines, which means that they operate in air. Francis-turbines, in contrast, operate in water at overpressure. In case of a ternary set including a Francis-turbine, the pump as well as the Francis-turbine are at risk of cavitation, which can be reduced by mounting them at lower head values. The requirement of air surroundings for the Pelton-turbine prevents a deep mounting of this turbine and therefore, the connected pump can not be placed arbitrarily deep either.

A.2. Pelton-Turbine Control Strategy

The nozzle number of Pelton-turbines varies between one and six ([116], [117], [118]). The number of the required nozzles depends on the amount of the desired flow. In this section, a configuration with six nozzles is chosen, since on the one hand, it is a common configuration and on the other hand, it allows for a variety of control strategies on the other hand. Figure A.2 shows eight different control strategies, their cumulative deviation to a power reference signal and the steady efficiency values for different numbers of active nozzles. Positive power values indicate turbine mode, while negative power values indicate pump mode. The power reference signal starts at a power reference signal equal zero, changes to pump mode, turbine mode, pump mode and ends in turbine mode. The eight graphs in the first two columns show the power reference signal and the trend of the power output for the different control strategies. The eight applied strategies are:

- **Feed-forward:** Each nozzle operates independently from the others. The nozzle opening values are obtained in the same way as the guide vane opening in the *BEL* block of subsection 4.1.2. The nozzle opening values are applied by a feed-forward strategy without any feedback loop.

- **Feedback:** The same strategy as in the case above, with the only difference that one nozzle is feedback controlled in order to eliminate steady deviations between power reference signal and power output.

- **Linearised:** In the feedback case, a stepped form of the power reference signal is assumed. The power reference signal for balancing energy generation depends on the frequency and therefore, no significant gaps are expected. The stepped shift from one value of the power reference signal to the next is changed to a linear interpolated trend between those power reference signal values.

- **Variable control parameters:** Towards the end of the linearised case, an instability of the feedback controller can be observed. This instability is caused by the non-linear relation between nozzle opening and flow. In order to avoid this instability, the control parameters are changed for low nozzle openings.

- **Same nozzle openings:** The number of operating nozzles is variable and depends

on the current value of the power reference signal. For this case, it is assumed that all active nozzles operate at the same opening. Therefore, not only one nozzle is feedback controlled, but all.

- **Even number of operating nozzles:** Only an even number of active nozzles is permitted and all active nozzles operate at the same opening. This is a common kind of operation, since an even number of active nozzles with the same opening allows for an advantageous load for the turbine shaft. By combining two opposite nozzles, the bending stress on the shaft can be eliminated and only the torsional stress remains.

- **Even number of nozzles operate (offset of limits):** The same approach as in the point above, but with different limits for the activation of an additional pair of nozzles.

- **All nozzles operate:** At each value of the power reference signal, all nozzles are operating with the same opening. This strategy allows for maximum flexibility of the plant.
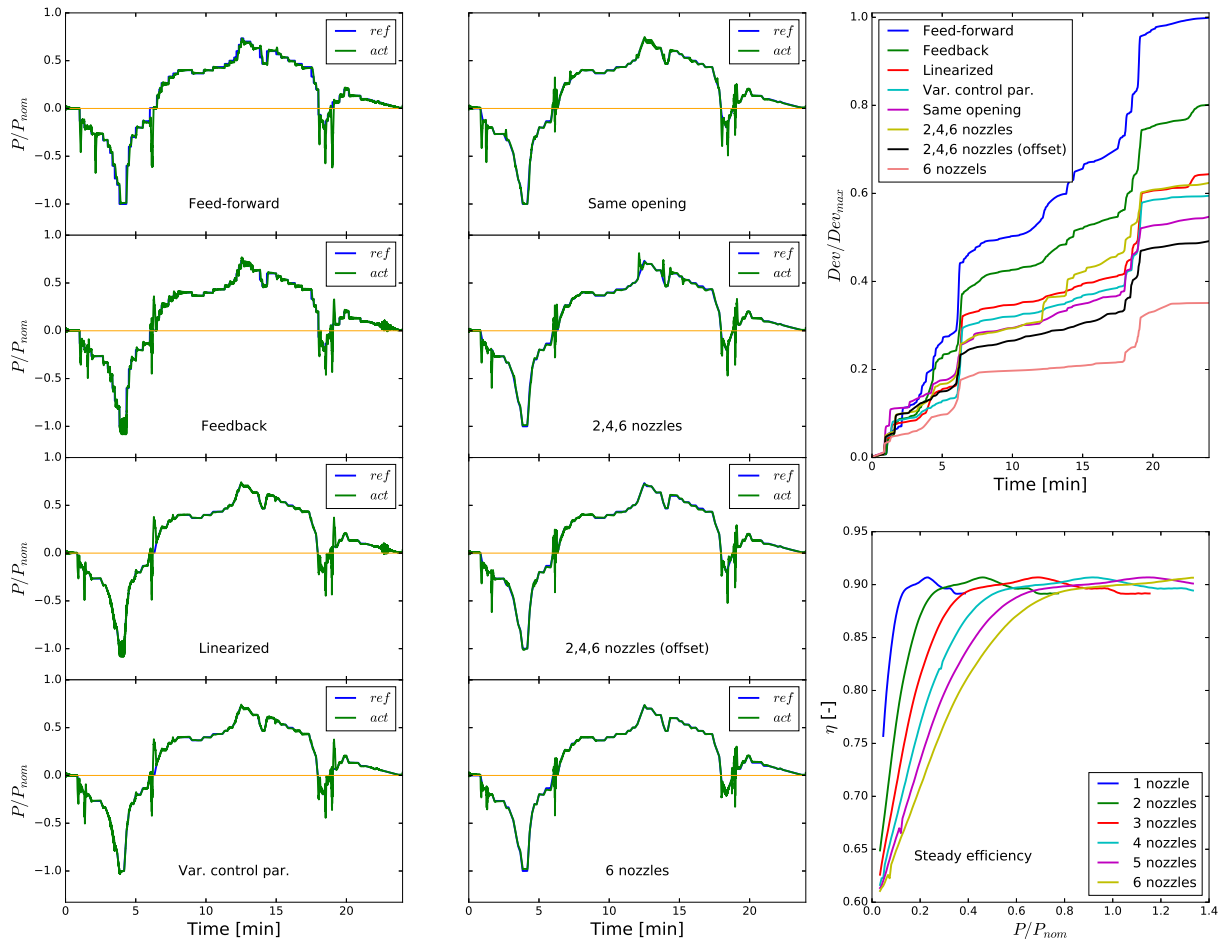

Figure A.2.: Accuracy of different control strategies

Considering the uppermost graph of the first column, two peaks for the beginning of the pump mode can be seen. These peaks are caused by the stepwise start-up of the pump. The filling of the hydraulic torque converter and the accompanying acceleration of the pump lead to a swift increase of the pump power, which causes the first peak. After synchronous speed is reached and the gear coupling is engaged, the valve, which inhibits the flow passing

the pump, is opened. The flow increases relatively fast, which leads to another pump power peak. While the pump power increases in form of the two described steps, the turbine state passes two phases as well. At the beginning of the simulation, all nozzles are closed. When pump power is required, the nozzles are feed-forward controlled to the value compensating the pump power appearing while pumping against a closed valve. Additionally to this power value, the current value of the power reference signal is added in order to converge the power output to the power reference signal. In case the gear coupling is closed, the nozzles are feed-forward controlled to the power value belonging to pump operation against an opened valve. For the reversed case, the deactivation of the pump, the nozzles are closed more or less in the same time as the valve. Afterwards, the hydraulic torque converter is filled, the gear coupling is disengaged and the hydraulic torque converter is emptied. During the disengagement and emptying, the pump still requires power, causing the peak visible in the graph where the power switches from pump to turbine power. For the feedback controlled simulations, the behaviour for the pump shut down is different. The feed-forward closure of the nozzles is partly compensated by the feedback loop. Therefore, the pump power does not reach a peak as high as in the feed-forward only case. Nevertheless, an additional peak in turbine direction appears, since the feedback loop can not compensate the steep power gradient caused by the draining of the hydraulic torque converter.

The cumulative deviation shows that the activation and deactivation of the pump causes the highest deviations. Due to the missing feedback loop, the feed-forward case possesses the highest deviation. By applying a feedback loop for one nozzle, the deviation is already reduced by about 20 %. The assumption of a gapless power reference signal reduces the deviation by approximately a further 18 %. The feedback case as well as the linearised case contain an instability in the feedback loop. This instability, which can be seen around minute 23, leads at this time to increased deviations for these two cases while remaining mostly constant for all other cases. By applying graded control parameters (Var. control par. case), the final deviation has been reduced to a value of about 40 % of the feed-forward final value. As common control strategy, the deviations are also determined for the case that all nozzles operate, if active, at the same opening. Since for this case, all active nozzles are driven by a feedback control, the accuracy further increases. The case of only even numbers of operating nozzles is, as mentioned above, of practical importance. Nevertheless, the activation and deactivation of two additional nozzles cause additional deviations. The effect of the activation and deactivation of two additional nozzles can be seen by comparing the 2,4,6 nozzles case with the 2,4,6 nozzle (offset) case. In the latter case, the activation is offset out of the simulated power reference signal. Therefore, the deviation increase, caused by the additional activation and deactivation of two nozzles, can be eliminated for the considered case. This reduces the deviation at minute 12 and 14. As last case, the behaviour of six permanently active nozzles is investigated. The feedback control of all nozzles delivers highest possible flexibility. Furthermore, deviations caused by activation and deactivation of nozzles are avoided. The flexibility along with the missing activation and deactivation, respectively, are the reasons why this control strategy allows for the lowest cumulative deviation (less than 40 percent of the initial value).

The lower graph in the third column shows the steady efficiency values of the turbine with respect to power output and number of active nozzles. It can be seen that for low power output values, one nozzle would be the most efficient choice. By an increase of the power output value, the number of active nozzles should increase as well in order to operate at highest possible efficiency. Furthermore, the power output per nozzle is limited and thereby,

higher power output values call for more active nozzles.

To summarize, it can be said that there is no optimal operation strategy. The three layout criteria stress, deviation and efficiency require different operation strategies. Lowest stress calls for an even number of active nozzles operating on opposite sides of the Pelton-turbine, lowest deviation requires all nozzles to operate permanently and highest efficiency requires the activation of one nozzle after another. Therefore, the plant operator has to find a design trade-off between efficiency, flexibility and stress similar to the speed value of the VSDFG scheme.

B. Relation between Power Imbalance and Power System Frequency

In case there is a power imbalance ($P_{imb}(t)$), the generated power ($\sum_i P_{G,i}(t)$) does not equal the consumed power ($\sum_i P_{C,i}(t)$) (equation B.1).

$$\underbrace{\sum_i P_{G,i}(t) - \sum_i P_{C,i}(t)}_{P_{imb}(t)} \neq 0 \tag{B.1}$$

By taking into account the correlation between the power system frequency ($f(t)$) and the generator's angular speed ($\omega_i(t)$) (equation B.2),

$$\omega_i(t) = 2 \cdot \pi \cdot \frac{f(t)}{p_{e,i}} \tag{B.2}$$

the kinetic energy ($E_{kin}(t)$) (equation B.3),

$$E_{kin,i}(t) = \frac{1}{2} \cdot J_i \cdot \omega_i^2(t) \tag{B.3}$$

the power imbalance (equation B.4),

$$P_{imb}(t) = \sum_i T_i(t) \cdot \omega_i(t) \tag{B.4}$$

and, subsequently, the frequency trend can be determined.

Since the power imbalance is compensated by the derivation of the kinetic energy (equation B.5)

$$\sum_i \dot{E}_{kin,i}(t) = P_{imb}(t) \tag{B.5}$$

and the derivation of the kinetic energy equals equation B.6,

$$\dot{E}_{kin,i}(t) = J_i \cdot \omega_i(t) \cdot \dot{\omega}_i(t) \tag{B.6}$$

equations B.4, B.5 and B.6 can be merged to form equation B.7.

$$\sum_i J_i \cdot \omega_i(t) \cdot \dot{\omega}_i(t) = \sum_i T_i(t) \cdot \omega_i(t) \tag{B.7}$$

Equation B.7 can be reformed to equation B.8.

$$\sum_i \dot{\omega}_i(t) = \sum_i \frac{T_i(t)}{J_i} \tag{B.8}$$

By inserting the derivation of equation B.2, equation B.8 changes to:

$$\dot{f}(t) = \sum_i \frac{T_i(t) \cdot p_{e,i}}{2 \cdot \pi \cdot J_i} \tag{B.9}$$

The frequency at a certain point in time can be calculated by its initial value and its integrated variation:

$$f(t) = f_{t=0} + \int_t \dot{f}(t)dt \tag{B.10}$$

In equation B.10, equation B.9 can be inserted, resulting in the equation for the frequency deviation.

$$f(t) = f_{t=0} + \int_t \sum_i \frac{T_i(t) \cdot p_{e,i}}{2 \cdot \pi \cdot J_i} dt \tag{B.11}$$

C. Maximum Gradients of New Renewable Energies within a Quarter Hour

Extreme values of load and generation have been presented in subsection 1.3.1. For the sake of completeness, the extreme gradients of wind and solar power are illustrated in this chapter. The partial solar eclipse on March 20th, 2015 and the day with the widest spread of generated wind power are illustrated in figure C.1. These situations are crucial since generation gradients of new renewable energies have to be compensated by indirect proportional gradients of conventional generation. This means that with increasing capacity of new renewable energies, the conventional generating units have to become more flexible as well. In case of the partial solar eclipse, sun power generation has a gradient of 5.5 GW within a quarter of an hour, while the gradient of wind power does not exceed 2.56 GW within a quarter of an hour. Fortunately, the solar power gradient can be predicted quite precisely and appropriate operation schedules can be developed on time. Nevertheless, it can be seen that even if hard coal and pumped-storage ramp-up their generation, the generation decrease caused by the partial solar eclipse can not be compensated only within Germany. In terms of the generation gradient, the wind generation seems more unproblematic, since the highest gradient was 2.56 GW within a quarter of an hour. However, unpredictability of these gradients make theme more complicated to handle.
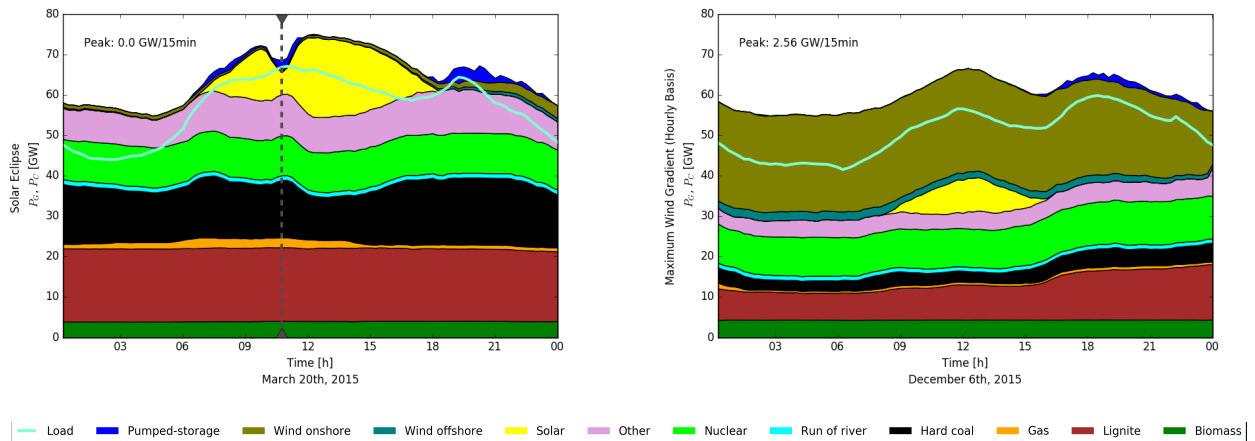

Figure C.1.: Partial solar eclipse and biggest deviation of wind power within one day

Bibliography

[1] [Online]. Available: http://www.iiasa.ac.at/web/home/resources/publications/ options/Sustainable.en.html

[2] N. Nakicenovic, "Energieökonomie," 2012, university lecture.

[3] S. Nakada, D. Saygin, and D. Gielen, "Global bioenergy- supply and demand projections," International Renewable Energy Agency, Tech. Rep., 2014. [Online]. Available: http://www.irena.org/remap/irena_REmap_2030_Biomass_paper_2014.pdf

[4] "Bp statistical review of world energy June 2016," BP, Tech. Rep., 2016. [Online]. Available: http://www.bp.com/en/global/corporate/energy-economics/ statistical-review-of-world-energy.html

[5] "Key world energy statistics," International Energy Agency, Tech. Rep., 2015.

[6] K. Neuhoff, "Rolle der Regionalmärkte in der gesamten Versorgungsgemeinschaft," 2017. [Online]. Available: http://eeg.tuwien.ac.at/eeg.tuwien.ac.at_pages/events/ iewt/iewt2017/html//files/extra/Pr_Neuhoff_Karsten.pdf

[7] B. Schmidt, "Empowering Austria - Der Beitrag der österreichischen E-Wirtschaft," 2017. [Online]. Available: http://eeg.tuwien.ac.at/eeg.tuwien.ac.at_pages/events/ iewt/iewt2017/html//files/extra/Pr_Schmidt_Barbara.pdf

[8] *Frequency Stability Evaluation Criteria for the Synchronous Zone of Continental Europe.* [Online]. Available: https://www.entsoe.eu/Documents/SOC%20documents/ RGCE_SPD_frequency_stability_criteria_v10.pdf

[9] "Technology roadmap energy storage," International Energy Agency, Tech. Rep., 2014. [Online]. Available: https://www.iea.org/publications/freepublications/publication/ TechnologyRoadmapEnergystorage.pdf

[10] "Electrical energy storage," International Electrotechnical Commission, Tech. Rep., 2011. [Online]. Available: http://www.iec.ch/whitepaper/pdf/iecWP-energystorage-LR-en.pdf

[11] *Geschäftsbericht 2015*, Austrian Power Grid.

[12] *Continental Europe Operation Handbook: Load-Frequency Control and Performance*, 2009. [Online]. Available: https://www.entsoe.eu/publications/system-operations-reports/operation-handbook/Pages/default.aspx

[13] *Network Code on Operational Planning and Scheduling*, ENTSO-E. [Online]. Available: https://www.entsoe.eu/fileadmin/user_upload/_library/resources/OPS_ NC/130924-AS_NC_OPS_2nd_Edition_final.pdf

[14] F. Andersen, H. Larsen, and T. Boomsma, "Long-term forecasting of hourly electricity load: Identification of consumption profiles and segmentation of customers," *Energy*

Conversion and Management, vol. 68, pp. 244 – 252, 2013. [Online]. Available: http://www.sciencedirect.com/science/article/pii/S0196890413000381

[15] *dena-Studie Systemdienstleistungen 2030. Sicherheit und Zuverlässigkeit einer Stromversorgung mit hohem Anteil erneuerbarer Energien.* [Online]. Available: http://www.dena.de/fileadmin/user_upload/Projekte/Energiesysteme/ Dokumente/dena-Studie_Systemdienstleistungen_2030.pdf

[16] R. Schürhuber, A. Lechner, and W. Gawlik, "Bereitstellung synthetischer Schwungmasse durch Wasserkraftwerke," *e & i Elektrotechnik und Informationstechnik*, vol. 133, no. 8, pp. 388–394, Dec. 2016. [Online]. Available: http://dx.doi.org/10. 1007/s00502-016-0445-3

[17] A. Renganathan and R. Dunn, "The evolving landscape of der's and energy storage," Tech. Rep., 2016.

[18] "Global ev outlook," Interantional Energy Agency, Tech. Rep., 2016.

[19] *Electromobility in Germany: Vision 2020 and Beyond*, Germany Trade & Invest, 2015.

[20] [Online]. Available: https://transparency.entsoe.eu/

[21] K. Atsonios, I. Violidakis, K. Sfetsioris, D. Rakopoulos, P. Grammelis, and E. Kakaras, "Pre-dried lignite technology implementation in partial load/low demand cases for flexibility enhancement," *Energy*, vol. 96, pp. 427 – 436, 2016. [Online]. Available: http://www.sciencedirect.com/science/article/pii/S0360544215017211

[22] H. D. Piriz, A. R. Cannatella, E. Guerra, and D. A. Porcari, "Inertia of hydro generators. Influence on the dimensioning, cost, efficiency and performance of the units," in *cigre*, 2012.

[23] E. Ørum, M. Kuivaniemi, M. Laasonen, A. I. Bruseth, E. A. Jansson, A. Danell, K. Elkington, and N. Modig, "Future system inertia," entso-e, Tech. Rep., 2015.

[24] *Net installed generating capacity.* [Online]. Available: https://www.entsoe.eu/db-query/miscellaneous/net-generating-capacity

[25] [Online]. Available: https://www.tesla.com/blog/addressing-peak-energy-demand-tesla-powerpack

[26] S. M. Knupfer, R. Hensley, P. Hertzke, P. Schaufuss, N. Laverty, and N. Kramer, "Electrifying insights: How automakers can drive electrified vehicle sales and profitability," McKinsey&Company, Tech. Rep., 2017.

[27] D. A. Notter, M. Gauch, R. Widmer, P. Wäger, A. Stamp, R. Zah, and H.-J. Althaus, "Contribution of li-ion batteries to the environmental impact of electric vehicles," *Environmental Science & Technology*, vol. 44, no. 17, pp. 6550–6556, 2010, pMID: 20695466. [Online]. Available: http://dx.doi.org/10.1021/es903729a

[28] C. Grosjean, P. H. Miranda, M. Perrin, and P. Poggi, "Assessment of world lithium resources and consequences of their geographic distribution on the expected development of the electric vehicle industry," *Renewable and Sustainable Energy Reviews*, vol. 16, no. 3, pp. 1735 – 1744, 2012. [Online]. Available: http://www.sciencedirect.com/science/article/pii/S1364032111005594

[29] E. Rahimzei, K. Sann, and M. Vogel, "Kompendium: Li-ionen-batterien; grundlagen,

bewertungskriterien, gesetze und normen," VDE Verband der Elektrotechnik, Tech. Rep., 2015. [Online]. Available: https://www.dke.de/resource/blob/933404/fa7a24099c84ef613d8e7afd2c860a39/kompendium-li-ionen-batterien-data.pdf

[30] J. M. Allwood, J. M. Cullen, and R. L. Milford, "Options for achieving a 50% cut in industrial carbon emissions by 2050," *Environmental Science & Technology*, vol. 44, no. 6, pp. 1888–1894, Mar. 2010. [Online]. Available: http://dx.doi.org/10.1021/es902909k

[31] J. A. P. Lopes, F. J. Soares, and P. M. R. Almeida, "Integration of electric vehicles in the electric power system," *Proceedings of the IEEE*, vol. 99, no. 1, pp. 168–183, Jan. 2011. [Online]. Available: http://dx.doi.org/10.1109/JPROC.2010.2066250

[32] "Pc world vehicles in use," oica, Tech. Rep. [Online]. Available: http://www.oica.net/wp-content/uploads//pc-inuse-2014.pdf

[33] M. Z. Jacobson and M. A. Delucchi, "Providing all global energy with wind, water, and solar power, part I: Technologies, energy resources, quantities and areas of infrastructure, and materials," *Energy Policy*, vol. 39, no. 3, pp. 1154 – 1169, 2011. [Online]. Available: http://www.sciencedirect.com/science/article/pii/S0301421510008645

[34] X. Lu, M. McElroy, and J. Kiviluoma, "Global potential for wind-generated electricity," *Proceedings of the National Academy of Sciences*, vol. 106, no. 27, pp. 10 933–10 938, Jun 2009. [Online]. Available: http://dx.doi.org/10.1073/pnas.0904101106

[35] *Electricity Energy Storage Technology Options: A White Paper Primer on Applications, Costs, and Benefits.* [Online]. Available: http://large.stanford.edu/courses/2012/ph240/doshay1/docs/EPRI.pdf

[36] X. Luo, J. Wang, M. Dooner, and J. Clarke, "Overview of current development in electrical energy storage technologies and the application potential in power system operation," *Applied Energy*, vol. 137, pp. 511 – 536, 2015. [Online]. Available: http://www.sciencedirect.com/science/article/pii/S0306261914010290

[37] N. Hartmann, L. Eltrop, N. Bauer, J. Salzer, S. Schwarz, and M. Schmidt, "Stromspeicherpotenziale für Deutschland," Universität Stuttgart, Tech. Rep., Juli 2012.

[38] M. Boxleitner and C. Groiß, "Speicherbedarf für eine Vollversorgung Österreichs mit regenerativem Strom," in *12. Symposium Energieinnovation*, 2012. [Online]. Available: http://www.ea.tuwien.ac.at/fileadmin/t/ea/projekte/super-4-micro-grid/Boxleitner_M._Groiss_Chr._-_Speicherbedarf_fuer_eine_Vollversorgung_OEsterreichs_mit_regenerativem_Strom.pdf

[39] A. Moser, "Unterstützung der Energiewende in Deutschland durch einen Pumpspeicherausbau," Institut für Elektrische Anlagen und Energiewirtschaft, Tech. Rep., 2014.

[40] J. Mayrhuber and P. Stering, "Pressure shaft steel lining for pumped storage plants material and installation at the Limberg 2 and Reißeck 2 projects," *Hydropower & Dams (Hg.) 2013 − HYDRO 2013*, 2013.

[41] T. Beyer, "Goldisthal Pumped-Storage Plant: More than Power Production," *Hydro Review Worldwide Magazine (HRW)*, 2007. [Online]. Available: http://www.hydroworld.com/articles/print/volume-15/issue-1/articles/

goldisthal-pumped-storage-plant-more-than-power-production.html

[42] H. Schlunegger and A. Thöni, "100 MW full-size converter in the Grimsel 2 pumped-storage plant." Hydro 2013, 2013. [Online]. Available: www.grimselstrom. ch/home/download/1291

[43] P. Meusburger and L. Werle, "Pumped storage power plant Obervermuntwerk II - the hydraulic machinery." 18th International Seminar on Hydropower Plants, 2014.

[44] E. Puerer and G. Goeckler, "The power plant Kops II - basic conditions, design and details of construction," *Hydropower & Dams (Hg.) 2005 − HYDRO 2005*, 2005.

[45] J. Koutnik, "Hydro power plant," in *AGCS, Munich*, 2013. [Online]. Available: http://www.changanath.de/assets/Global%20offices%20assets/Germany/ Expert%20Days%202013/03%20Koutnik_Hydro%20Power%20Plants.pdf

[46] C. Bauer, "Hydraulische Maschinen und Anlagen I & II," 2016, university lecture.

[47] J. Giesecke and E. Mosonyi, *Wasserkraftanlagen*. Springer Science + Business Media, 2009. [Online]. Available: http://dx.doi.org/10.1007/978-3-540-88989-2

[48] F. Geth, T. Brijs, J. Kathan, J. Driesen, and R. Belmans, "An overview of large-scale stationary electricity storage plants in Europe: Current status and new developments," *Renewable and Sustainable Energy Reviews*, vol. 52, pp. 1212–1227, Dec. 2015. [Online]. Available: http://dx.doi.org/10.1016/j.rser.2015.07.145

[49] J. Raabe, *HYDRO POWER; The design, use and function of hydromechanical, hydraulic and electrical equipment*. VDI-Verlag GmbH, 1985.

[50] A. Mitteregger and G. Penninger, "Austrian pumped storage power stations supply peak demands," *World Pumps*, vol. 2008, no. 500, pp. 16–21, May 2008. [Online]. Available: http://dx.doi.org/10.1016/S0262-1762(08)70147-0

[51] A. Bergant, A. Simpson, and A. Tijsseling, "Water hammer with column separation: A historical review," *Journal of Fluids and Structures*, vol. 22, no. 2, pp. 135–171, Feb. 2006. [Online]. Available: http://dx.doi.org/10.1016/j.jfluidstructs.2005.08.008

[52] M. Afshar and M. Rohani, "Water hammer simulation by implicit method of characteristic," *International Journal of Pressure Vessels and Piping*, vol. 85, no. 12, pp. 851 – 859, 2008. [Online]. Available: http://www.sciencedirect.com/science/ article/pii/S0308016108001075

[53] V. Hasmatuchi, S. Roth, F. Botero, F. Avellan, and M. Farhat, "High-speed flow visualization in a pump-turbine under off-design operating conditions," *IOP Conference Series: Earth and Environmental Science*, vol. 12, p. 012059, Aug. 2010. [Online]. Available: http://dx.doi.org/10.1088/1755-1315/12/1/012059

[54] D. A. Katsaprakakis, D. G. Christakis, K. Pavlopoylos, S. Stamataki, I. Dimitrelou, I. Stefanakis, and P. Spanos, "Introduction of a wind powered pumped storage system in the isolated insular power system of karpathos-kasos," *Applied Energy*, vol. 97, pp. 38– 48, Sept. 2012. [Online]. Available: http://dx.doi.org/10.1016/j.apenergy.2011.11.069

[55] J. Krenn, H. Keck, and M. Sallaberger, "Concept of small and mid-size pump-turbines." 17th International Seminar on Hydropower Plants, 2012.

[56] V. Hasmatuchi, M. Farhat, S. Roth, F. Botero, and F. Avellan, "Experimental

evidence of rotating stall in a pump-turbine at off-design conditions in generating mode," *Journal of Fluids Engineering*, vol. 133, no. 5, p. 051104, 2011. [Online]. Available: http://dx.doi.org/10.1115/1.4004088

[57] J. Kathan, T. Esterl, F. Leimgruber, and B. Helfried, *Pumpspeicher Römerland*, Austrian Institute of Technology, Nov. 2012. [Online]. Available: http://www.energiepark. at/fileadmin/user_upload/Dokumente/INREN/Pumpspeicher_Roemerland.pdf

[58] C. Pfleiderer and H. Petermann, *Strömungsmaschinen.* Springer Nature, 1991. [Online]. Available: http://dx.doi.org/10.1007/978-3-662-10101-8

[59] U. Jese, R. Fortes-Patella, and S. Antheaume, "High head pump-turbine: Pumping mode numerical simulations with a cavitation model for off-design conditions," 2014.

[60] P. Matt, "The plant "Obervermuntwerk II" and its flexibility," in *VGB-Kongress "Kraftwerke 2015"*, 2015. [Online]. Available: https://www.vgb.org/kurzfassung_b03. html#prettyPhoto

[61] *HydroNews-Magazin der Andriz Hydro*, no. 26, 2014.

[62] *Gutachten zur Rentabilität von Pumpspeicherkraftwerken*, 2014. [Online]. Available: http://www.stmwi.bayern.de/fileadmin/user_upload/stmwivt/Themen/Energie_und_ Rohstoffe/Dokumente_und_Cover/2014-Pumpspeicher-Rentabilitaetsanalyse.pdf

[63] P. Brown, J. Peas Lopes, and M. Matos, "Optimization of pumped storage capacity in an isolated power system with large renewable penetration," *IEEE Transactions on Power Systems*, vol. 23, no. 2, pp. 523–531, May 2008. [Online]. Available: http://dx.doi.org/10.1109/TPWRS.2008.919419

[64] A. Ruprecht, "Pump storage-requirements and comparison with other storage technologies," *VGB PowerTech*, 2015.

[65] "Renewables 2015 global status report," Renewable Energy Policy Network for the 21st Century, Tech. Rep., 2015.

[66] [Online]. Available: https://www.eex.com/en/products/power/power-derivatives-market

[67] D. Connolly, H. Lund, P. Finn, B. Mathiesen, and M. Leahy, "Practical operation strategies for pumped hydroelectric energy storage (phes) utilising electricity price arbitrage," *Energy Policy*, vol. 39, no. 7, pp. 4189 – 4196, 2011, special Section: Renewable energy policy and development. [Online]. Available: http://www.sciencedirect.com/science/article/pii/S0301421511003156

[68] L. Hirth, "The market value of variable renewables," *Energy Economics*, vol. 38, pp. 218–236, Jul. 2013. [Online]. Available: http://dx.doi.org/10.1016/j.eneco.2013.02.004

[69] J. Xiao, J. Y. Chung, J. Li, R. Boutaba, and J. Won-Ki Hong, "Near optimal demand-side energy management under real-time demand-response pricing," *2010 International Conference on Network and Service Management*, Oct 2010. [Online]. Available: http://dx.doi.org/10.1109/CNSM.2010.5691349

[70] M. Hartner and A. Permoser, "Ist die Talsole erreicht? - Die Auswirkungen des PV Ausbaus auf die Preisvarianz und Wirtschaftlichkeit von Speichern im Stromsystem," 2017. [Online]. Available: http://eeg.tuwien.ac.at/eeg.tuwien.ac.at_ pages/events/iewt/iewt2017/html//files/presentations/PR_216_Hartner_Michael.pdf

[71] [Online]. Available: http://www.exaa.at/de/marktdaten/historische-daten

[72] M. Pfleger, "Strommärkte Deutschland-Österreich," 2013, university lecture.

[73] K. H. Gruber, "Entwicklungen in der Wasserkraft als Bausteine der Stromwende," Verbund. Praktikerkonferenz Wasserkraft, 2015.

[74] "Statistical review of world energy 2016 - data," BP, Oct. 2016. [Online]. Available: http://www.bp.com/en/global/corporate/energy-economics/statistical-review-of-world-energy.html

[75] [Online]. Available: http://appsso.eurostat.ec.europa.eu/nui/submitViewTableAction.do

[76] J. Cludius, H. Hermann, F. C. Matthes, and V. Graichen, "The merit order effect of wind and photovoltaic electricity generation in germany 2008-2016: Estimation and distributional implications," *Energy Economics*, vol. 44, pp. 302 – 313, 2014. [Online]. Available: http://www.sciencedirect.com/science/article/pii/S0140988314001042

[77] [Online]. Available: http://www.epexspot.com/en/

[78] [Online]. Available: https://www.apg.at/emwebapgrem/startApp.do

[79] *Austrian Power Grid AG (APG) opens the balancing energy market for international partners.* [Online]. Available: https://www.apg.at/~/media/5ED9458E22EF4A7396596590D6F1A734.pdf

[80] *Verordnung der Regulierungskommission der E-Control, mit der die Entgelte für die Systemnutzung bestimmt werden (Systemnutzungsentgelte-Verordnung 2012 in der Fassung der Novelle 2016, SNE-VO 2012 idF Novelle 2016).*

[81] F. Senn and S. Thurner, "Pumped storage power in Austria - experience, new projects, economic situation."

[82] F. Diaz-Gonzalez, A. Sumper, O. Gomis-Bellmunt, and R. Villafafila-Robles, "A review of energy storage technologies for wind power applications," *Renewable and Sustainable Energy Reviews*, vol. 16, no. 4, pp. 2154–2171, May 2012. [Online]. Available: http://dx.doi.org/10.1016/j.rser.2012.01.029

[83] B. Dunn, H. Kamath, and J.-M. Tarascon, "Electrical energy storage for the grid: A battery of choices," *Science*, vol. 334, no. 6058, pp. 928–935, Nov. 2011. [Online]. Available: http://dx.doi.org/10.1126/science.1212741

[84] V. Crastan, *Elektrische Energieversorgung 2*, Springer, Ed. Springer Nature, 2008. [Online]. Available: http://dx.doi.org/10.1007/978-3-540-70882-7

[85] "Renewable energy technologies: Cost analysis series - hydropower," IRENA, Tech. Rep., 2012. [Online]. Available: https://www.irena.org/documentdownloads/publications/re_technologies_cost_analysis-hydropower.pdf

[86] H. Qian, J. Zhang, J.-S. Lai, and W. Yu, "A high-efficiency grid-tie battery energy storage system," *IEEE Transactions on Power Electronics*, vol. 26, no. 3, pp. 886–896, Mar 2011. [Online]. Available: http://dx.doi.org/10.1109/TPEL.2010.2096562

[87] E. Mahnke, J. Mühlenhoff, and L. Lieblang, "Renews Spezial: Strom Speichern," Agentur für erneuerbare Energien, Tech. Rep., 2014.

[88] [Online]. Available: https://www.tesla.com/powerpack/design#/

[89] G. Fuchs, B. Lunz, M. Leuthold, and D. U. Sauer, "Technology overview on electricity storage," iSEA, Tech. Rep., 2012. [Online]. Available: http://www.sefep.eu/activities/projects-studies/120628_Technology_Overview_Electricity_Storage_SEFEP_ISEA.pdf

[90] *EXAA: Quarter Hour trading at exaa.* [Online]. Available: http://www.exaa.at/exaa/docs/factsheet-quarter-hours-english-v4.pdf

[91] "Beschreibung von Regelleistungskonzepten und Regelleistungsmarkt," Consentec GmbH, Tech. Rep., 2014.

[92] C. Maier, W. Gawlik, and L. Ruppert, "Combined electrical and hydraulic model for dynamic long-term operation of pumped-storage in SIMSEN," in *Flexible Operation of Hydropower Plants in the Energy System*, 2016.

[93] C. Maier, W. Gawlik, and L. Ruppert, "Vergleich von drehzahlvariablen Pumpspeichertechnologien in einem dynamischen Modell für Langzeitbetrachtungen," in *Klimaziele 2050: Chance für einen Paradigmenwechsel?*, 2017.

[94] E. Kopf, S. Brausewetter, M. Giese, and F. Moser, "Optimized control strategies for variable speed machines," 2004.

[95] C. NICOLET, "Hydroacoustic modelling and numerical simulation of unsteady operation of hydroelectric systems," Ph.D. dissertation, ÉCOLE POLYTECHNIQUE FÉDÉRALE DE LAUSANNE, 2007.

[96] [Online]. Available: http://simsen.epfl.ch/

[97] F. Gao, D. Xu, and Y. Lv, "Pitch-control for large-scale wind turbines based on feed forward fuzzy-pi," *2008 7th World Congress on Intelligent Control and Automation*, 2008. [Online]. Available: http://dx.doi.org/10.1109/WCICA.2008.4593277

[98] P. Zeller, Ed., *Handbuch Fahrzeugakustik: Grundlagen, Auslegung, Berechnung, Versuch.* Vieweg+Teubner Verlag, 2009.

[99] M. K. Pal, "Lecture notes on power system stability."

[100] M. Kaltenbacher, H. Ecker, J. Metzger, C. Junger, and D. Ruckser, *Skriptum zur Vorlesung Mess- und Schwingungstechnik*, Technische Universität Wien, 2016, university lecture.

[101] H. Joslyn, L. Hardin, and J. Wagner, "Turbine rotor-stator interaction," *Journal of Engineering for Power*, vol. 104, p. 729, Oct. 1982.

[102] C. G. Rodriguez, E. Egusquiza, and I. F. Santos, "Frequencies in the vibration induced by the rotor stator interaction in a centrifugal pump turbine," *Journal of Fluids Engineering*, vol. 129, no. 11, p. 1428, 2007. [Online]. Available: http://dx.doi.org/10.1115/1.2786489

[103] C. Nicolet, J.-J. Herou, B. Greiveldinger, P. Allenbach, J.-J. Simond, and F. Avellan, "Methodology for risk assessment of part load resonance in francis turbine power plant," *IAHR Int. Meeting of WG on Cavitation and Dynamic Problems in Hydraulic Machinery and Systems*, 2006. [Online]. Available: https://infoscience.epfl.ch/record/129889/files/IAHRtransient.pdf

[104] R. Logar, "Druckstoss bei plötzlichem Abschluss einer gestuften Rohrleitung,"

Österreichische Zeitschrift für Elektrizitätswirtschaft, 1991. [Online]. Available: http://cat.inist.fr/?aModele=afficheN&cpsidt=5071386

[105] W. Stroppa, "Ausbau der Wasserkraft in Tirol," TIWAG. RENEXPO, 2015.

[106] P. Meusburger, "Obervermuntwerk I." Praktikerkonferenz Wasserkraft, 2015.

[107] H. Mennel, "Der Strommarkt - ein Auslaufmodell?" Illwerke vkw. Praktikerkonferenz Wasserkraft, 2013.

[108] S. Xiangzhong, L. Bo, and Z. Zheng, "Measures of internal flow calculation accuracy improvement on hydraulic torque converter," *Procedia Engineering*, vol. 28, pp. 235 – 240, 2012. [Online]. Available: http://www.sciencedirect.com/science/article/pii/S1877705812007229

[109] [Online]. Available: http://www.netzfrequenzmessung.de/

[110] T. Gobmaier, "Netzfrequenz als Indikator für die Stabilität des Verbundnetzes," 2017. [Online]. Available: http://eeg.tuwien.ac.at/eeg.tuwien.ac.at_pages/events/iewt/iewt2017/html//files/fullpapers/25_Gobmaier_fullpaper_2017-02-14_10-54.pdf

[111] P. Buck, "Ökonomische Bewertung systemfreundlich optimierter Windenergieanlagen," 2017. [Online]. Available: http://eeg.tuwien.ac.at/eeg.tuwien.ac.at_pages/events/iewt/iewt2017/html//files/presentations/Pr_72_Tafarte_Philip.pdf

[112] [Online]. Available: http://www.netzfrequenz.info/

[113] C. Nicolet, S. Alligne, B. Kawkabani, J.-J. Simond, and F. Avellan, "Unstable operation of francis pump-turbine at runaway: Rigid and elastic water column oscillation modes," *International Journal of Fluid Machinery and Systems*, vol. 2, no. 4, pp. 324–333, Dec. 2009. [Online]. Available: http://dx.doi.org/10.5293/IJFMS.2009.2.4.324

[114] C. Nicolet, S. Alligne, A. Bergant, and F. Avellan, "Simulation of water column separation in francis pump-turbine draft tube," *IOP Conference Series: Earth and Environmental Science*, vol. 15, no. 2, p. 022002, 2012. [Online]. Available: http://stacks.iop.org/1755-1315/15/i=2/a=022002

[115] H. Happoldt, O. Hartmann, and E. Wiedemann, "The present state of pumped storage in europe," *IEEE Transactions on Power Apparatus and Systems*, vol. 82, no. 68, pp. 618–631, Oct. 1963. [Online]. Available: http://dx.doi.org/10.1109/TPAS.1963.291376

[116] T. Staubli, A. Abgottspon, P. Weibel, C. Bissel, E. Parkinson, J. Leduc, and F. Leboeuf, "Jet quality and pelton efficiency," *Proceeding of Hydro-2009, Lyon, France*, 2009. [Online]. Available: https://www.researchgate.net/profile/Thomas_Staubli/publication/290989838_Jet_quality_and_Pelton_efficiency/links/56aa230508aeaeb4cefae8e8.pdf

[117] Y. Xiao, Z. Wang, J. Zhang, C. Zeng, and Z. Yan, "Numerical and experimental analysis of the hydraulic performance of a prototype pelton turbine," *Proceedings of the Institution of Mechanical Engineers, Part A: Journal of Power and Energy*, vol. 228, no. 1, pp. 46–55, 2014. [Online]. Available: http://journals.sagepub.com/doi/abs/10.1177/0957650913506711

[118] K. Hirtenlehner, "Real efficiency of a pelton turbine in back pressure operation," 2006. [Online]. Available: http://www.zt-hirtenlehner.at/wp-content/uploads/2013/04/Real-Efficiency-of-Pelton-Turbine-in-Back-Pressure-Operation1.pdf
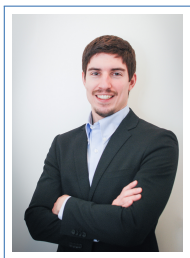
Leopold Ruppert

Tel.: +43-1-58801-302410
E-mail: leopold.ruppert@tuwien.ac.at

Personal Data

Birth	August 9th, 1985, Vienna (AUT)
Citizenship	Austria
E-mail	leopold.ruppert@tuwien.ac.at

Education

2013–actual	**PhD**, *Vienna University of Technology*. Institute for Energy Systems and Thermodynamics
2009–2010	*Universidade de Vigo*. Ingeniería Industrial
2005–2013	**MSc**, *Vienna University of Technology*. Mechanical Engineering
2004–2005	*Jagdkommando Ausbildungskompanie*. Military Service
1999–2004	*Higher Technical Education Institute Hollabrunn*. Mechanical Engineering

PhD Thesis

Title	*Pumped-Storage Implementation in Order to Balance Volatile Renewable Energy Generation*
Supervisors	Dipl.-Ing. Dr.Ing. Christian Bauer, Dipl.-Ing. Dr. Klaus Käfer
Description	Energy market based operation of common pumped storage schemes delivering system services such as control power for the purpose of frequency stabilization

MSc Thesis

Title	*Hydraulic System Study for Variable Speed Pumped Storage Applications*
Supervisors	Dipl.-Ing. Dr.Ing. Christian Bauer, Dipl.-Ing. Dr. Klaus Käfer
Description	Investigation of the possibility to minimize water hammer phenomena in pumped storage plants by speed variation

Publications

[1] L. Ruppert, R. Schürhuber, B. List, A. Lechner, and C. Bauer. An analysis of different pumped storage schemes from a technological and economic perspective. *Energy*, 2017 (under Review).

[2] L. Ruppert, R. Schürhuber, and C. Bauer. Technisch-wirtschaftliche Untersuchung verschiedener Großspeicherlösungen. 2017.

[3] L. Ruppert, C. Maier, and C. Bauer. Service of different pumped-storage schemes for an electrical grid with increased renewable energy generation. In *19th International Seminar on Hydropower Plants*, 2016.

[4] C. Maier, W. Gawlik, and L. Ruppert. Combined electrical and hydraulic model for dynamic long-term operation of pumped-storage in SIMSEN. In *19th International Seminar on Hydropower Plants*, 2016.

[5] L. Ruppert, K. Käfer, and C. Bauer. *Optimizing Steady Operating Points of Several Generating unit Systems for Transient Applications*. Wasserwirtschaft, 105 edition, 2015.

[6] L. Ruppert, K. Käfer, and C. Bauer. Steady efficiency optimization of several hydraulic generating unit systems. In *18th International Seminar on Hydropower Plants*, 2014.